ENDOPLASMIC RETICULUM STRESS-MEDIATED SIGNALING IN PANCREATIC CANCER

A DOCTORAL DISSERTATION
SUBMITTED TO THE FACULTY OF THE
UNIVERSITY OF MINNESOTA
BY

Patricia Dauer

IN PARTIAL FULFILLMENT OF THE REQUIREMENTS
FOR THE DEGREE OF
DOCTOR OF PHILOSOPHY

Advisor: Ashok K. Saluja, Ph.D

APRIL 2018

ACKNOWLEDGEMENTS

As I was preparing my graduate school applications, I recall having conversations with acquaintances and colleagues about the pros and cons to joining a Ph.D. program. One of my colleagues reflected on his Ph.D. experience as one that he was glad he did but would never want to repeat again. I did not understand his perspective at the time because I was excited about going back to school. However, I never once expected getting a Ph.D. to be easy. If it were easy, everyone would do it. It did not take very long before I began to understand what he meant.

Despite my early enthusiasm and genuine thirst for knowledge, I struggled to find rhythm in graduate school. I constantly doubted myself, if my results were not as expected. I struggled with my perfectionist tendencies, often repeating an experiment because I just wanted to be sure, (but really, it was just a little messy, and I thought it could be better). I felt more isolated than I did living on a mountain in Tanzania. I faced cultural walls, impenetrable regardless of trying for years. I cried more tears than I would like to admit. I felt broken.

I would like to think that I persevered, though. I have learned how to be strong, how to stand up for what is right, even if that means standing alone. I have learned to defend my opinion with facts, and to ask as many questions as necessary, in order to understand. My experience has made me a better scientist, and it has made me a better person. I would not want to do it again, but it was necessary for me to reach the point where I am now, and necessary for where I want to be in the future.

I would like to thank Dr. Ashok Saluja, for welcoming me into his lab. His high expectations for his graduate students provided me with lofty goals to set and achieve. I would be remiss if I did not also thank Dr. Sulagna Banerjee. Dr. Banerjee has played an integral role in my doctoral education, and I cannot begin to list all the ways in which she has helped. She has provided technical training, taught me how to carefully plan and execute experiments, proofread my manuscript drafts, as well as participated in

thoughtful scientific discussions. I am also forever grateful for the few beautiful souls who helped me along my path. Your words of encouragement and advice, hugs, high fives, and happy hours have been indispensable. Thank you.

DEDICATION

I would like to dedicate my work to my mother, who is the most wonderful and kind-hearted person that I know. She has been a constant supporter and cheerleader of my academic pursuits, and I am eternally grateful to her for that.

ABSTRACT

Pancreatic ductal adenocarcinoma (PDAC) ranks among the poorest prognoses for cancer patients, with an estimated 5-year survival of just 8%. The stagnant survival rates are a result of late detection, chemoresistance, and an aggressive tumor phenotype. Too few patients are eligible for surgery, which results in an urgent need for more effective chemotherapeutic treatment options.

One promising pharmacological advancement is currently undergoing a Phase II clinical trial and has been studied by our laboratory. Triptolide is a Chinese herb, which has shown to be very effective in eliminating pancreatic cancer cells *in vitro* and *in vivo*. In conjunction with the Medicinal Chemistry Department at the University of Minnesota, a prodrug of triptolide, named Minnelide™, has been synthesized. Our laboratory has since studied triptolide and Minnelide™ extensively, in order to determine the mechanisms of action.

The initial study in this dissertation precipitated based on an earlier finding in the Saluja laboratory that triptolide not only downregulates heat shock protein 70 (HSP70) and specificity protein 1 (SP1), but also causes chronic endoplasmic reticulum (ER) stress and cell death. Our study shows that downregulating SP1, a transcription factor that is overexpressed in pancreatic cancer, activates the unfolded protein response (UPR) and results in chronic ER stress. We further show that inhibition of SP1, as well as inducing ER stress, leads to lysosomal membrane permeabilization (LMP), a sustained accumulation of cytosolic calcium, and eventually cell death in pancreatic cancer.

Even though ER stress can result in cell death, it is initially a homeostatic mechanism, which aims to protect cells. This led us to ask what role acute ER stress and UPR plays in pancreatic cancer. We show that modulating glucose regulatory protein 78 (GRP78), the master regulator of the UPR, can have a profound effect on multiple pathways that mediate chemoresistance. Our study showed for the first time that knockdown of GRP78 can diminish efflux activity of ATP-binding cassette (ABC) transporters, and it can decrease the antioxidant response resulting in an accumulation of reactive oxygen species (ROS). We also show that these effects can be mediated by the activity of SP1.

Our investigation into acute ER stress led to further studies to characterize the UPR signaling in pancreatic cancer. We show that shGRP78 dysregulates multiple transcriptomic and proteomic pathways important in cancer (proliferation, survival, fatty acid metabolism). GRP78 downregulation decreases stemness and self-renewal properties *in vitro. In vivo* studies demonstrate that GRP78 knockdown results in delayed tumor initiation, and decreased tumor growth. Further, downregulation of GRP78 results in fatty acid metabolism dysregulation.

The last study in this dissertation focuses on the tumor microenvironment and SP1 oncogenic signaling. We evaluated the transcriptomic profiling conducted after treatment with triptolide revealed deregulation of the transforming growth factor beta (TGF-β) signaling pathway in cancer-associate fibroblasts (CAFs), resulting in an apparent reversal of their activated state to a quiescent, non-proliferative state. The neighboring epithelial cells exhibited a decrease in oncogenic signaling as manifested by downregulation of SP1. Our findings suggest that approaches to inactivate CAFs and prevent tumor-stromal crosstalk may offer a viable strategy to treat pancreatic cancer.

These studies underscore the importance of ER stress and understanding the complex balance of adaptation versus cell death in pancreatic cancer. We have identified SP1 and GRP78 as potential targets for future PDAC therapies. These findings have clinical relevance as both SP1 and GRP78 are overexpressed in pancreatic cancer patients and increased expression of these proteins are indicative of poor prognosis.

Table of Contents

LIST OF TABLES

Supplementary Table

LIST OF FIGURES

Supplementary Figures

LIST OF ABBREVIATIONS

ABC: ATP-binding cassette

AML: Acute Myeloid Leukemia

ARE: Antioxidant Response Elements

ATF6: Activating Transcription Factor 6

BAPTA: Glycine, N,N'-(1,2-ethanediylbis(oxy-2,1-phenylene))bis(N-(carboxymethyl))-, tetrapotassium salt

BFA: Brefeldin A

CAF: Cancer Associated Fibroblast

CHAPS: 3-[(3-Cholamidopropyl) dimethylammonio]-1-propanesulfonate

ChIP: Chromatin Immunoprecipitation

CM: Conditioned Media

CSC: Cancer Stem Cell

DAB: 3,3′-Diaminobenzidine

DAPI: 4',6-diamidino-2-phenylindole

DCFDA: 2',7' –dichlorofluorescin diacetate

DEG: Differentially Expressed Gene

DMEM: Dulbecco's Modified Eagle Medium

DMSO: Dimethyl sulfoxide

DTT: Dithiothreitol

ECIS: Electric Cell-substrate Impedance Sensing

ECM: Extracellular Matrix

EDTA: Ethylenediaminetetraacetic acid

EGF: Epidermal Growth Factor

ELISA: Enzyme-linked Immunosorbent Assay

ER: Endoplasmic Reticulum

ERSE: ER Stress Response Elements

FBS: Fetal Bovine Serum

FDR: False Discovery Rate

FGF: Fibroblast Growth Factor

FCCP: Carbonyl cyanide 4-(trifluoromethoxy)phenylhydrazone

FOLFIRINOX: Therapy consisting of 5-fluoruracil, oxaliplatin, irinotecan, and leucovorin

GEM: gemcitabine

GI: Gastrointestinal

GRP78: Glucose Regulatory Protein 78

GSEA: Gene Set Enrichment Analysis

GSH: Glutathione

H&E: Hematoxylin and Eosin

HA: Hyaluronan

HEPES: 4-(2-hydroxyethyl)-1-piperazineethanesulfonic acid

HGF: Hepatocyte Growth Factor

HRP: Horseradish peroxidase

IACUC: Institutional Animal Care and Use Committee

IHC: Immunohistochemistry

IPA: Ingenuity Pathway Analysis

KPC: LSLKrasG12D; LSL-Trp53R172H; Pdx-1-Cre

LMP: Lysosomal Membrane Permeabilization

MDR: Multi-drug Resistance

MMP: Mitochondrial Membrane Potential

MOMP: Mitochondrial Outer Membrane Permeabilization

MTH: Mithramycin, Sp1 Inhibitor

NAC: N-acetyl-cysteine

NS: Non-silencing siRNA

O-GlcNAc: O-linked N-acetylglucosamine

PAC: Paclitaxel

PARP: Poly (ADP-ribose) polymerase

PBS: Phosphate Buffered Saline

PD-1: Programmed Cell Death-1

PDAC: Pancreatic Ductal Adenocarcinoma

PSC: Pancreatic Stellate Cell

RARE: Retinoic Acid Response Elements

RBP: Retinol Binding Protein

RDH: Retinol Dehydrogenase

RLU: Relative Luciferase Units

ROS: Reactive Oxygen Species

RPMI: Roswell Park Memorial Institute

SERCA: Sarcoplasmic Endoplasmic Reticulum Calcium ATPase

SFA: Saturated Fatty Acid

SP1: Specificity Protein 1

TAE: Tris-acetate-EDTA

TEC: Tumor Epithelial Cell

TG: Thapsigargin

TM: Tunicamycin

TUNEL: Terminal Deoxynucleotidyl Transferase dUTP Nick End Labeling

UFA: Unsaturated Fatty Acid

UPR: Unfolded Protein Response

VEGF: Vascular Endothelial Growth Factor

5-FU: 5-fluorouracil

INTRODUCTION

Challenges in treating pancreatic ductal adenocarcinoma

Pancreatic ductal adenocarcinoma (PDAC) ranks among the poorest prognoses for cancer patients, with an overall estimated 5-year survival of just 8%. The estimated 5-year survival rate for local disease is 32%, whereas regional metastasis is 12%, and distant metastasis is 3%[1]. In 2018, it is estimated that 55,440 people will be diagnosed with pancreatic cancer, and 44,330 people will succumb to the disease[1]. These survival statistics have remained relatively unchanged for over 50 years.

Symptoms of pancreatic cancer are general (weight loss, abdominal discomfort, nausea), and there are no reliable biomarkers, which often makes an early diagnosis difficult. Fewer than 20% of patients diagnosed with pancreatic cancer are eligible for surgery. Unfortunately, the majority of new cases are diagnosed with distant metastasis (52%), making them ineligible for surgical resection (SEER)[1]. Chemoresistance presents an ongoing challenge to researchers and clinicians, and is responsible for greater than 90% of therapeutic failures[2, 3]. There are multiple proposed mechanisms of resistance, including reduced drug uptake or increased drug efflux, alteration of the drug target, and reduced sensitivity to cell death[2-4]. Thus, the stagnant survival rates are a result of late detection, an aggressive tumor phenotype, and chemoresistance.

The approved chemotherapeutics are nucleoside analogs, DNA-crosslinking agents, and microtubule inhibitors; all targeting rapidly proliferating cells. Gemcitabine (a nucleoside analog) monotherapy was approved as a first-line treatment for patients with locally advanced or metastatic pancreatic cancer in 1996, showing a median survival of 5.65 months[5]. The current standard of care consists of gemcitabine in combination with Abraxane/nab-paclitaxel (albumin-bound microtubule poison, paclitaxel). Abraxane and gemcitabine combination extends survival to 8.5 months[6]. The chemotherapeutic cocktail, named FOLFIRINOX, consists of 5-Fluorouracil (5-FU), leucovorin, irinotecan, and oxaliplatin. FOLFIRINOX extends the median survival to 11 months, but is recommended for only a small subset of patients in good performance status[7]. There

have been other drugs combined with gemcitabine, but the survival benefit was comparable to gemcitabine alone. Overall, the chemotherapeutic agents that are currently approved for pancreatic cancer are largely ineffective.

There are a variety of chemotherapeutics in development and clinical trials, as well as a variety of therapeutic combinations and techniques. Recently, ficlatuzumab, a hepatocyte growth factor (HGF) inhibitory monoclonal antibody completed a Phase I clinical trial for advanced solid tumors and liver metastases (Clinicaltrials.gov; NCT00969410). However, none of the enrolled patients had a reduction in tumor size, but rather, achieved "stable" disease[8]. Ficlatuzumab will now be tested in combination with gemcitabine and nab-paclitaxel in a Phase I study for pancreatic cancer (Clinicaltrials.gov; NCT03316599). Preclinical studies using programmed death receptor 1 (PD1) blockade show an increase in survival in the KPC murine model. α-PD1 in combination with gemcitabine and nab-paclitaxel is undergoing a Phase II clinical trial in pancreatic cancer (Clinicaltrials.gov; NCT03214250).

One promising pharmacological advancement, Minnelide™, is currently undergoing a Phase II clinical trial for GI cancers. Minnelide™ is a prodrug of a compound called triptolide, derived from the Chinese herb *Tripterygium wilfordii*. Preclinical studies conducted by our laboratory have shown significant reduction in tumor size, metastasis, and tumor-initiating cells[9-21]. The following studies detailed in this dissertation precipitated based on an earlier finding in the Saluja laboratory that triptolide not only downregulates heat shock protein 70 (HSP70) and specificity protein 1 (SP1), but also causes chronic endoplasmic reticulum (ER) stress leading to pancreatic cancer cell death[15, 20, 22, 23].

SP1 in Pancreatic Ductal Adenocarcinoma

SP1 is a zinc-finger transcription factor, with a GC-rich binding sequence[24-27]. It regulates multiple biological functions, including cell growth, differentiation, angiogenesis, and survival; its dysregulation, therefore, can aid in several hallmarks of cancer, leading to tumor progression and metastasis[15, 24, 28]. *SP1* is essential for embryological development of the pancreas, and *SP1*$^{-/-}$ murine models die 10 days post-gestation[26, 29].

As cells become terminally differentiated, SP1 is SUMOylated and ubiquitinated, which inactivates the transcription factor in adult pancreata[26]. SP1 becomes overexpressed in PDAC, but the mechanism as to how is unclear. Further, studies from our laboratory have shown that SP1 is not expressed in acute or chronic pancreatitis, or endothelial cells, suggesting that SP1 overexpression is unique to cancer cells, and may offer a protective role in cancer**.** It has been shown from patient tumors, that higher levels of SP1 expression correlate with poor prognosis (Figure 1) and metastasis[26].

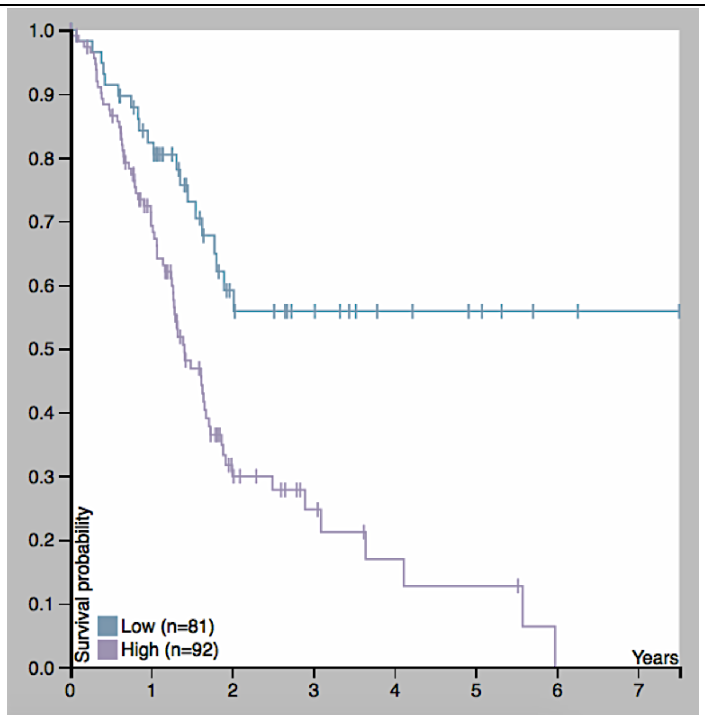

Figure 1: SP1 overexpression correlates with poor survival in patients with pancreatic cancer
5-year survival for high expression is 13%, whereas low expression is 56%. Data is from Human Protein Atlas.

ER stress and the Unfolded Protein Response

ER stress is a well-characterized homeostatic mechanism, but arguably underappreciated considering its role in cells. The ER is fundamental in maintaining secretory protein biosynthesis, a site for sterol and phospholipid synthesis, as well as a major calcium storage site[4, 7, 30-33].

Newly synthesized secretory and surface proteins enter the ER where chaperone proteins aid in folding into their tertiary structures[4, 31, 32]. Only properly folded proteins are exported from the ER to their respective destinations, and misfolded proteins get retained and/or degraded[30-33]. When misfolded or unfolded proteins accumulate inside the ER, it initiates the unfolded protein response (UPR). The UPR is the homeostatic mechanism that is often referred to as ER stress. UPR activation is initially an adaptive response to stressful stimuli[7, 30-33]. UPR intracellular signaling is activated through three transmembrane sensors: inositol-requiring enzyme 1 (IRE1-α), protein kinase RNA-like ER kinase (PERK), and activating transcription factor 6 (ATF6)[7, 30-33]. Without stress, these sensors are kept inactive by binding to glucose regulatory protein 78 (GRP78), an ER-resident folding chaperone protein. Upon stress, misfolded or unfolded proteins sequester GRP78 from the sensors, allowing for UPR signaling to commence[4, 7, 32, 33].

IRE1 activation is immediate and leads to X box protein 1 (XBP1) mRNA cleavage, resulting in a 26 base pair excision and a transcription factor, XBP1s. IRE1-XBP1s increases protein folding and trafficking[7, 32, 33]. Downstream of PERK activation, eukaryotic initiation factor 2α (eIF2α) is phosphorylated and global translation is attenuated[7, 30, 32, 33]. This global stop allows for only UPR genes to be transcribed and translated, allowing for more folding chaperones to be made to alleviate the unfolded protein burden[7, 32, 33]. Nuclear factor erythroid 2-related factor 2 (NRF2) is also activated upon PERK activation, which is necessary for the antioxidant response. Finally, ATF6α gets trafficked to the Golgi apparatus, where two proteases (S1P and S2P) cleave ATF6α into an active transcription factor, ATF6α-fragment[7, 32, 33]. Multiple studies have sought to understand the individual signaling cascades of the UPR, by using knockout mouse models. Knockout models of *IRE1α* and its downstream transcription factor, *XBP1s*, as well as *GRP78* have shown to be embryonic lethal, suggesting that a functional UPR is essential for growth and cell survival[7, 31, 34-41].

In addition to activating the UPR under stress, the ER actually dilates in size, in order to accommodate more unfolded proteins. As a result, part of the UPR transcribed genes are involved in membrane lipid biogenesis[31].

Not surprisingly, ER stress and the UPR are involved in many diseases, including

cancer. Cancers generally promote a hostile tumor microenvironment, which can result in hypoxia and nutrient deprivation, and ultimately activate the UPR. Because the UPR is an adaptive mechanism, cancer utilizes it to its advantage for cancer cell survival. UPR-related proteins have been described in multiple cancers. For example, in breast cancer, GRP78 is more highly expressed in estrogen receptor negative cancers than positive[32]. In colon cancer, GRP78 expression is correlated with malignant cells and a higher tumor stage[32]. GRP78 is also correlated with shorter survival and castration-resistant subtypes of prostate cancer[32].

Chemoresistance can occur through activating parts of the UPR. For example, elevated levels of glutathione, which is involved in drug metabolism and downstream of NRF2 activation, has been associated with platinum-resistance[3]. Additionally, thiol glutathione (GSH) can conjugate drugs, making them ideal substrates for ABC-transporters[2]. Hypoxia-induced UPR has been shown to reduce the number of rapidly proliferating cells, causing G_0 arrest, as well has inducing pro-survival signaling[3].

The UPR has been described to play a role in metastasis, cell dormancy, angiogenesis, immune tolerance, metabolic status, and chemoresistance[2, 3, 33]. However, as many advantages the UPR can provide to cancer cell growth and survival, cancer cells are still susceptible to chronic or prolonged UPR signaling, which can activate cell death pathways[7, 32].

PDAC tumor microenvironment

There are multiple cellular and acellular components, which make up the tumor microenvironment in pancreatic cancer. There are the epithelial cells, which diverge into non-tumor initiating cells and tumor initiating cells; there is a dense stroma, consisting of pancreatic stellate cells (PSCs), cancer- associated fibroblasts (CAFs), and extracellular matrix (ECM) that develop with the tumor; there are also the infiltrating immune cells (tumor associated macrophages and neutrophils)[42]. Due to the bulk of rapidly proliferating cells and the surrounding dense stroma, the centers of pancreatic tumors tend to be hypoxic in nature[42, 43]. Hypoxia is one of the extrinsic driving forces of activating the UPR and chemoresistance. Further, hypoxia-inducible factor 1 (HIF1)

expression has been reported to act as a cofactor with XBP1s for transcription.

The role of the stroma is a controversial component in the pancreatic tumor microenvironment. As the stroma develops, the interstitial pressure constricts blood vessels, thereby not only reducing flow of oxygen and nutrients but also chemotherapeutic compounds[44, 45]. However, only targeting the stroma has not yielded significant benefit it terms of the survival in pancreatic cancer patients[46, 47]. A study by Rhim *et al*. has demonstrated that the role of stroma in pancreatic cancer may be restraining, and thus, inhibiting it would likely be detrimental for survival and this would result in extensive metastasis of the cancer[48]. However, a study by Banerjee *et al.* has found that Minnelide™ targets the stroma and the epithelial tumor cells. As a result, they found reduced stromal components hyaluronan and collagen, improved vasculature function, and increased intra-tumoral drug delivery[12].

In clinical practice, combination therapy is generally preferred over monotherapy, in order to manage dose-limiting toxicities and to reduce the onset of drug resistance. The ideal treatment option will incorporate a therapy that targets rapidly proliferating cells, quiescent tumor-initiating cells, as well as the dense desmoplastic stroma that surrounds the tumor.

In this dissertation, I will present four studies that centralize around ER stress, UPR signaling, and SP1-mediated oncogenic signaling. Chapter 1 discusses how SP1 downregulation can result in chronic ER stress and cell death. Chapter 2 covers how acute ER stress and UPR signaling can result in chemoresistance, and targeting the master regulator GRP78, or GRP78 through SP1 downregulation can re-sensitize resistant cells to chemotherapeutics. In Chapter 3, we further investigate the implications of GRP78 in the aggressive phenotype of pancreatic cancer, through the use of a stable shGRP78 cell line. Lastly, in Chapter 4, we explore the mechanism of action of triptolide/Minnelide™ on the crosstalk between tumor epithelial cells and stromal cells, and how triptolide can be used to inactivate stromal cells, thereby decreasing the oncogenic signaling of SP1.

CHAPTER 1: CHRONIC ER STRESS IN CANCER BIOLOGY

Inhibition of SP1 prevents ER homeostasis and causes cell death by lysosomal membrane permeabilization in pancreatic cancer

Patricia Dauer[1], Vineet K. Gupta[2], Olivia McGinn[1], Alice Nomura[1,2], Nikita S. Sharma[2], Nivedita Arora[1], Bhuwan Giri[2], Vikas Dudeja[2], Ashok K Saluja[1,2], Sulagna Banerjee[2]

1 Department of Pharmacology, University of Minnesota, Minneapolis, MN 55455, USA
2 Department of Surgery, University of Miami, Miami, FL 33136, USA

Previously published in *Scientific Reports*. 2017 MAY 8;7(1):1564.
DOI: 10.1038/s41598-017-01696-2

SUMMARY

Background: Endoplasmic reticulum (ER) stress initiates an important mechanism for cell adaptation and survival, named the unfolded protein response (UPR). Severe or chronic/prolonged UPR can breach the threshold for survival and lead to cell death. There is a fundamental gap in knowledge on the molecular mechanism of how chronic ER stress is stimulated and leads to cell death in pancreatic ductal adenocarcinoma (PDAC).

Methods: MIA PaCa-2, S2-VP10, and S2-013 cells were treated with pharmacological inhibitors or genetically silenced using ON-TARGETplus SMARTpool siRNA. ChIP and an ERSE reporter assay were used to determine the loss of ER stress response by downregulation of glucose regulatory protein 78 (GRP78). Lysosomal activity was measured with a cathepsin B activity assay. Intracellular calcium was measured by staining with calcium orange dye and measured with a spectrophotometer. MIA PaCa-2 cells were injected into athymic nude mice subcutaneously and treated with two doses of mithramycin [specificity protein 1 (SP1) inhibitor] for four weeks.

Results: Our study shows that downregulating SP1, a transcription factor that is overexpressed in pancreatic cancer, activates UPR and results in chronic ER stress. In addition, downregulation of SP1 results in its decreased binding to the ER stress response element present in the promoter region of *GRP78*, the master regulator of ER stress, thereby preventing homeostasis. We further show that inhibition of SP1, as well as induction of ER stress, leads to lysosomal membrane permeabilization (LMP), a sustained accumulation of cytosolic calcium, and eventually cell death in pancreatic cancer.

Conclusion: This study underscores the importance of ER stress and understanding the complex balance of adaptation versus cell death in pancreatic cancer. The current study

identified SP1 and GRP78 as potential targets for future therapeutics in PDAC; discovered a protective role of SP1 in cancer; as well as further detailed ER stress response in cell death mechanisms.

INTRODUCTION

Pancreatic cancer is the fourth leading cause of cancer deaths in the United States. It was estimated that in 2016, 53,070 people would be diagnosed with pancreatic cancer and nearly 42,000 would die from it in the United States alone[49]. There is currently no effective treatment approved for pancreatic cancer. Gemcitabine has been the standard of care for pancreatic cancer for 19 years; however, it adds a survival advantage of only 6.8 months[50]. The most widely used treatment algorithms employing gemcitabine in combination with nanoparticle bound albumin (nab-paclitaxel) or the chemo-intensive regimen of FOLFIRINOX (5-fluoruracil, oxaliplatin, and folate supplementation), offer a meager survival benefit of a few weeks over traditional gemcitabine alone regimens[6]. Preclinical studies from our laboratory have shown that triptolide, a diterpene triepoxide from a Chinese herb, is cytotoxic in a number of cancers, including pancreatic ductal adenocarcinoma (PDAC)[9]. Our laboratory has synthesized Minnelide™, a water-soluble prodrug of triptolide, which just completed Phase I clinical trials[9]. Though the exact mechanism of triptolide induced cell death remains unknown, our previous studies have indicated that triptolide-induced cell death is caused by chronic Endoplasmic Reticulum (ER) stress[23]. However, there remains a gap in knowledge on the molecular mechanism of how ER stress is stimulated and how chronic ER stress causes cell death in pancreatic cancer.

The ER is a site for calcium storage, protein folding, and modifications[29, 51-54]. ER stress is a well-characterized condition that plays a role in multiple pathologies, including neuro-degeneration, rheumatoid arthritis, atherosclerosis, and many types of cancer[54, 55]. A variety of cellular insults can result in ER stress, including hypoxia, calcium fluctuations, oxidative stress, and nutrient deprivation[52-54]. When ER function is impaired during stress, the cell initiates the evolutionarily conserved unfolded protein response (UPR), which helps to adapt and survive stressful conditions. Three transmembrane

sensors mediate the UPR: inositol-requiring enzyme 1 (IRE1), activating transcription factor 6 (ATF6), and protein kinase-like ER kinase (PERK). During normal conditions, these three sensors are kept silent by associating with glucose regulatory protein 78 (GRP78), a protein chaperone. Upon experiencing stress, GRP78 will disassociate from the sensors to activate the UPR. In cases of severe or chronic/prolonged ER stress, the UPR is overwhelmed, and the cell will initiate cell death pathways[52]. In some diseases like neuro-degeneration or type II diabetes, recent studies show promise in inhibiting ER stress, resulting in cell survival[55]. However, in cancer, treatment strategies aim to prevent ER homeostasis to cause cell death[55].

Multiple studies have underscored the importance of specificity protein 1 (SP1), a transcription factor, in malignant tissues. In fact, SP1 has recently been described as a non-oncogene addiction gene in cancer[56]. SP1 has been reported to regulate many biological functions, including cell growth, differentiation, survival, tumor progression, and metastasis[15, 24, 26, 28, 56-58]. It has also been reported in colon, gastric, pancreatic, and breast cancers that SP1 is overexpressed, whereas minimal to no SP1 expression is detected in normal differentiated cells[15, 24, 26, 28, 56, 57]. Owing to its binding sites present in a large number of genes, downregulation of SP1 is likely to have a profound effect on cancer cell survival. Further, in the context of ER stress, it has been reported by Safe *et al*, that SP1 binding is necessary for the UPR[59]. However, it has not been determined whether chronic ER stress as a result of SP1 downregulation leads to cell death in pancreatic cancer.

One of the hallmarks of cancer cells is their resistance to apoptosis. Thus, a number of studies have been focused on overcoming this resistance by targeting pathways leading to apoptosis. Lysosomal membrane permeabilization (LMP) often precedes apoptosis in response to cytotoxic compounds in cancer cells[60, 61]. Lysosomes contain a number of hydrolytic enzymes, and are essential in autophagy-mediated recycling and cell survival[60, 61]. Due to the contents of lysosomes, they have been described as “suicide bags”, and when permeabilized, the contents can be released into the cytosol, leading to unregulated proteolysis and cell death[60].

Calcium regulation is also an important component of cell survival and thus, cell death[29,

[51, 62]. Calcium is also a second messenger to a variety of cellular processes, including protein synthesis and folding, proliferation, and apoptosis[51, 63]. The ER and mitochondria provide the major storages sites of calcium for the cell, and a dysregulation of calcium can not only cause ER stress, but also can also be a consequence of ER stress, and lead to cell death[29, 62, 64].

Previous studies from our laboratory have shown that triptolide results in chronic ER stress by downregulating GRP78, leading to cell death in pancreatic cancer[23]. In addition to these effects, triptolide downregulates the activity of SP1[15], thereby starting a cascade of events that lead to downregulation of several pro-survival genes. In this study, we show that SP1 downregulation in pancreatic cancer results in chronic ER stress, which in turn leads to a sustained increase in cytosolic calcium, LMP, and cell death.

RESULTS

SP1 downregulation causes ER stress and tumor regression

We have previously shown that SP1 downregulation with mithramycin (MTH) results in pancreatic cancer cell death[15]. In the current study, we showed that both 0.3 and 0.6 mg/kg MTH decreased tumor burden in a subcutaneous model with MIA PaCa-2 cells in athymic nude mice (Figure 1.1A), which is consistent with our previous work. Table 1.1 below outlines the study design.

Table 1.1: *In vivo* study design

Group	Treatment and Dosage	No. of Mice
Control	Saline	7
MTH 0.3	0.3 mg/kg, 3x weekly	7
MTH 0.6	0.6 mg/kg, 3x weekly	7

After four weeks, the average tumor volume in saline treated mice was 876 mm^3, whereas mice treated with 0.3 mg/kg MTH and 0.6 mg/kg of MTH was 632 mm^3 and 447 mm^3 respectively (Figure 1.1B). The average tumor weights in the MTH treated mice were also decreased (0.56 g in 0.3 mg/kg; 0.34 g in 0.6 mg/kg) compared to saline treated mice (0.76 g) (Figure 1.1C). Inhibition of SP1 also led to an increase in PARP cleavage (Figure 1.1D) and increased cleaved caspase 3 staining (Figure 1.1E), indicating apoptotic cell death in these tumors.

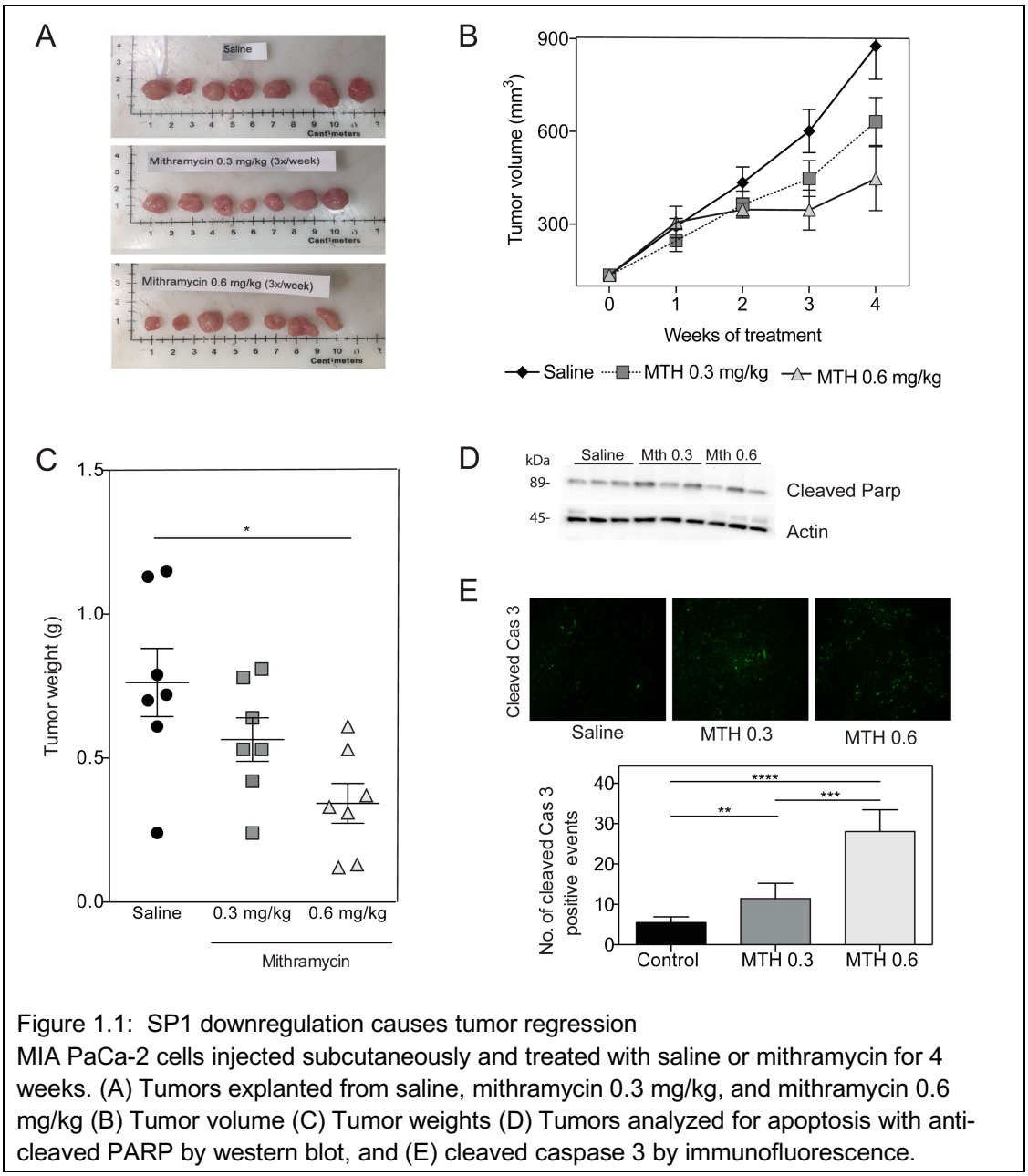

Figure 1.1: SP1 downregulation causes tumor regression
MIA PaCa-2 cells injected subcutaneously and treated with saline or mithramycin for 4 weeks. (A) Tumors explanted from saline, mithramycin 0.3 mg/kg, and mithramycin 0.6 mg/kg (B) Tumor volume (C) Tumor weights (D) Tumors analyzed for apoptosis with anti-cleaved PARP by western blot, and (E) cleaved caspase 3 by immunofluorescence.

Consistent with our findings *in vivo*, treatment with MTH also caused UPR in pancreatic cancer cell lines MIA PaCa-2, S2-VP10, and S2-013 (Supplementary Figure 1.1A-D). Notably, using a UPR gene expression array, multiple genes were found to be dysregulated in MIA PaCa-2 cells treated with MTH for 1-6 hours (Supplementary Figure 1.1A). In S2-VP10 and S2-013 cells, mRNA expression for the UPR regulator, GRP78, was upregulated in 1-3 hours, indicating the UPR was activated (Supplementary Figure 1.1B). Additionally, protein expression from the UPR sensor, IRE1-α, and directly

downstream of a second UPR sensor, PERK, phosphorylated-eukaryotic initiation factor 2α (p-EIF2α) were upregulated in a time-dependent manner (Supplementary Figure 1.1C). Lastly, Downstream of IRE1-α activation, x box binding protein 1 (XBP1) has endoribonuclease activity, which splices 26 base pairs from the gene to create an active transcription factor, XBP-1s. MIA PaCa-2 cells demonstrate RNA splicing of the XBP1 gene when treated with MTH from 1-24 hours (Supplementary Figure 1.1D). We further observed that while a short treatment (6 hours) with MTH elicited an “acute” response by triggering the UPR in the cancer cells, a longer treatment (24 hours) with MTH caused a complete breakdown of the ER stress machinery resulting in downregulation of UPR genes and causing “chronic” ER stress (Supplementary Figure 1.1B,C).

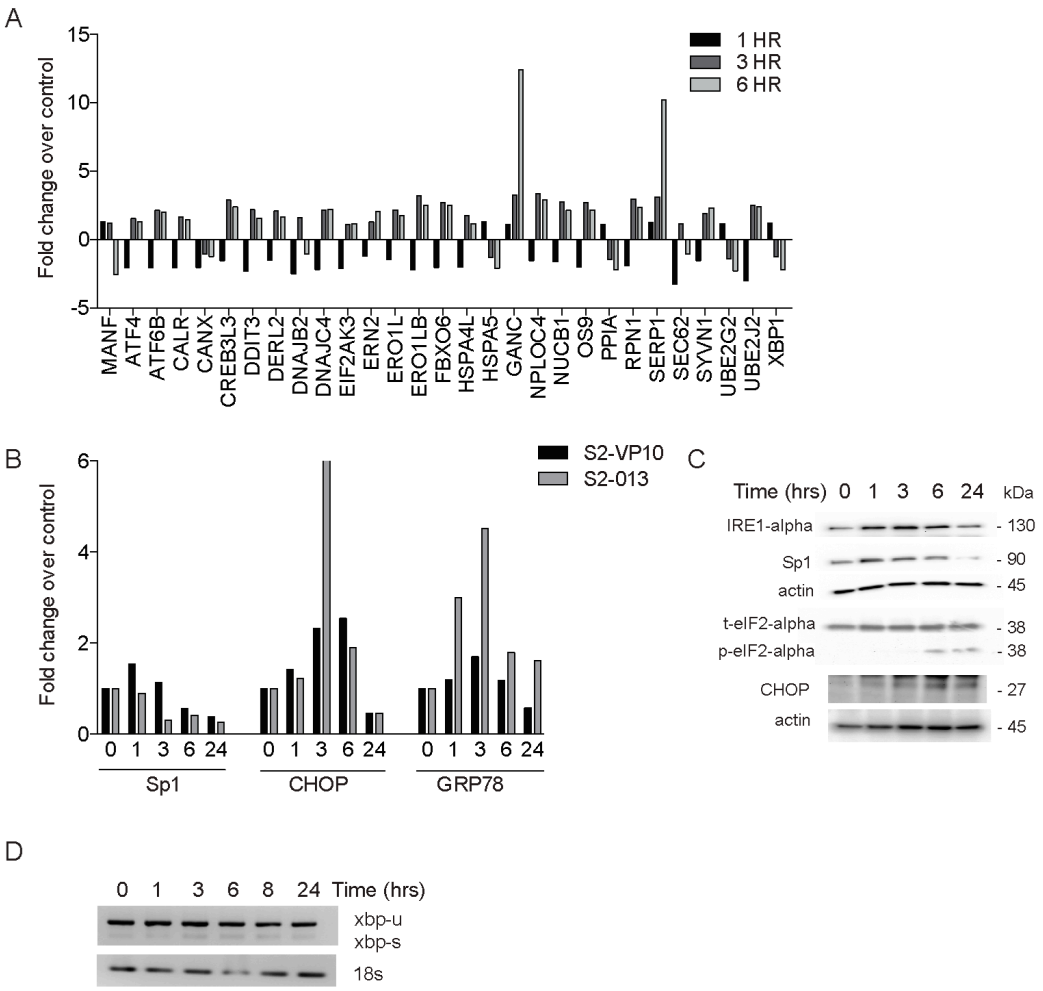

Supplementary Figure 1.1: Mithramycin treatment activates the unfolded protein response (A) MIA PaCa-2 cells treated with 100 nM mithramycin for 1-6 hours. (B) S2-VP10 and S2-013 cells treated with 100 nM mithramycin for 0-24 hours. (C) Protein expression of UPR-related genes in MIA PaCa-2 cells treated with 100 nM mithramycin for 0-24 hours. (D) RNA splicing of XBP gene in MIA PaCa-2 cells treated with 100 nM mithramycin for 0-24 hours, compared to 18s.

Further, upon silencing SP1 in these cells using siRNA, we observed a similar induction of chronic ER stress in 24-48 hours (Supplementary Figure 1.2A-B).

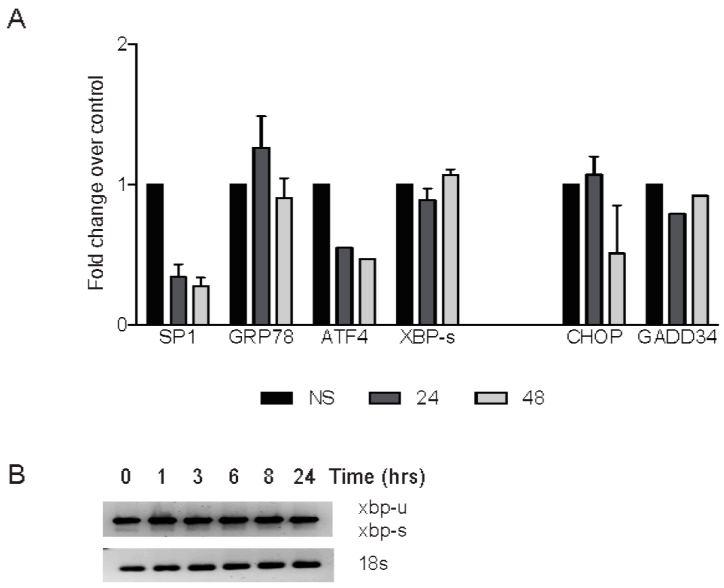

Supplementary Figure 1.2: siSP1 results in chronic ER stress MIA PaCa-2 cells transfected with siSP1 (A) RNA expression of UPR related genes at 24-48 hours. (B) Results in RNA splicing of XBP gene compared to 18s.

SP1 downregulation leads to chronic ER stress via homeostatic disruption

In order to elucidate how MTH causes chronic ER stress, we focused on the "master regulator" of UPR, GRP78. We first performed an activity assay of ER Stress Response Elements (ERSE), using a Cignal reporter assay (Qiagen). ERSE are the binding motifs that transcriptionally regulate UPR-induced genes. It has been reported that NF-Y, YY1, and Sp-family proteins, along with multiple ER stress-associated transcription factors all bind to the ERSE during a stress response[59]. Upon treatment with 100 nM MTH, the ERSE activity decreased to 0.771 RLU (relative luciferase units) compared to untreated cells (normalized to 1.0) in 8 hours (Figure 1.2A). After 24 hours of treatment, MTH treated cells showed a further decreased activity of 0.344 RLU compared to untreated cells (normalized to 1.0). Tunicamycin, a known ER stress inducer, was used as a positive control, and showed a robust increase in ERSE activity compared to untreated cells in 8 and 24 hours (2.500 and 4.861 RLU, respectively).

To study if the decrease in ERSE activity was owing to decreased binding of SP1 to the

GRP78 promoter elements, we performed chromatin immunoprecipitation of SP1 on the *GRP78* promoter. MIA PaCa-2 cells treated with 100 nM MTH showed a decrease in the % input of SP1 on the *GRP78* promoter. Untreated cells had a % input of 3.177, whereas 6 hours of MTH treatment decreased to 1.348% and 0.239% in 24 hours (Figure 1.2B).

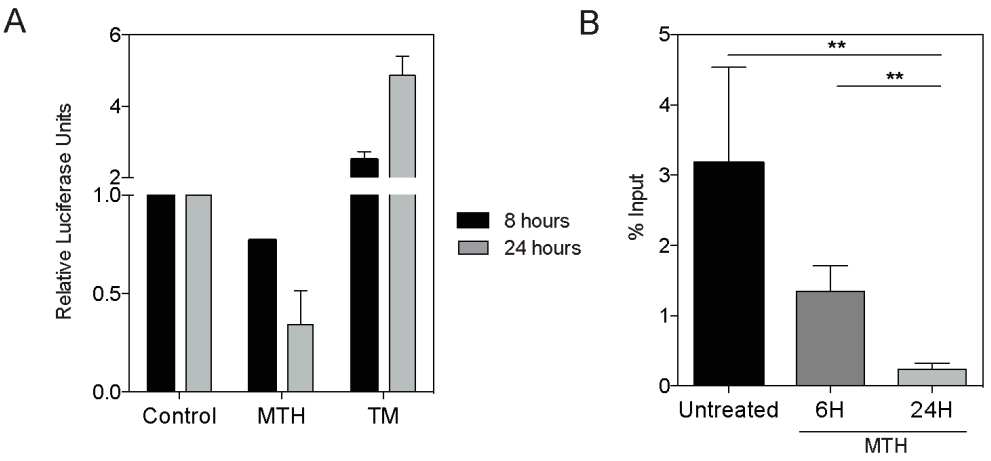

Figure 1.2: SP1 downregulation leads to chronic ER stress by deregulating the homeostatic mechanism
Mithramycin treated MIA PaCa-2 cells analyzed for (A) ERSE dual-luciferase activity assay from 0-24 hours, and (B) ChIP of SP1 on the *GRP78* promoter, from 0-24 hours.

Tunicamycin treatment did not affect the SP1 binding on the *GRP78* promoter after 6 hours (Supplementary Figure 1.3A).

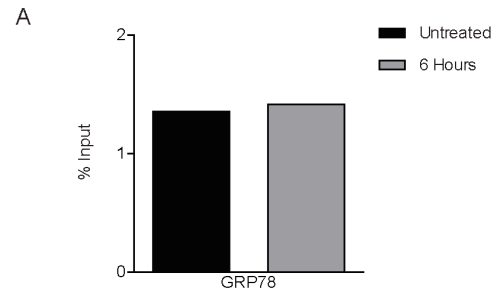

Supplementary Figure 1.3: Tunicamycin does not affect SP1 binding on the *GRP78* promoter
(A) MIA PaCa-2 cells analyzed for ChIP of SP1 on the *GRP78* promoter, after 6 hours of treatment with tunicamycin compared to untreated cells.

ER stress initiates cell death via LMP

To characterize how chronic ER stress, mediated by downregulation of SP1, results in cell death, we examined two common processes associated with apoptosis: permeabilization of lysosomal and mitochondrial membranes. We first studied the effect of chronic ER stress on lysosomal integrity.

LMP leads to a release of cathepsins (lysosomal enzymes) into the cytosol. Treatment for 1 hour with 1 μM tunicamycin, a known ER stress inducer, resulted in a 5.92-fold increase in cathepsin B cytosolic activity in MIA PaCa-2 cells compared to untreated cells (Figure 1.3A). By downregulating SP1 with MTH for 1 hour, cathepsin B activity was 3.36-fold greater than untreated MIA PaCa-2 cells (Figure 1.3C).

Additionally, using immunofluorescence detection, we saw a release of cathepsin B from the lysosomes upon treatment with TM (Figure 1.3B), and MTH (Figure 1.3D) for 6 hours, as well as with other known ER stress inducers thapsigargin (TG) (Supplementary Figure 1.4A), and brefeldin A (BFA) (Supplementary Figure 1.4B).

These findings unequivocally show that induction of chronic ER stress leads to LMP, indicated by a release of cathepsin B into the cytosol. Further, pre-treatment with a cathepsin B inhibitor, Ca074me, results in a rescue of viability after 24 hours (Figure 1.3E). MIA PaCa-2 cells were also treated for 6 hours with tunicamycin and a cathepsin B inhibitor, which resulted in a reduction of cathepsin B release from the lysosomes compared to tunicamycin alone, as detected using immunofluorescence (Figure 1.3F).

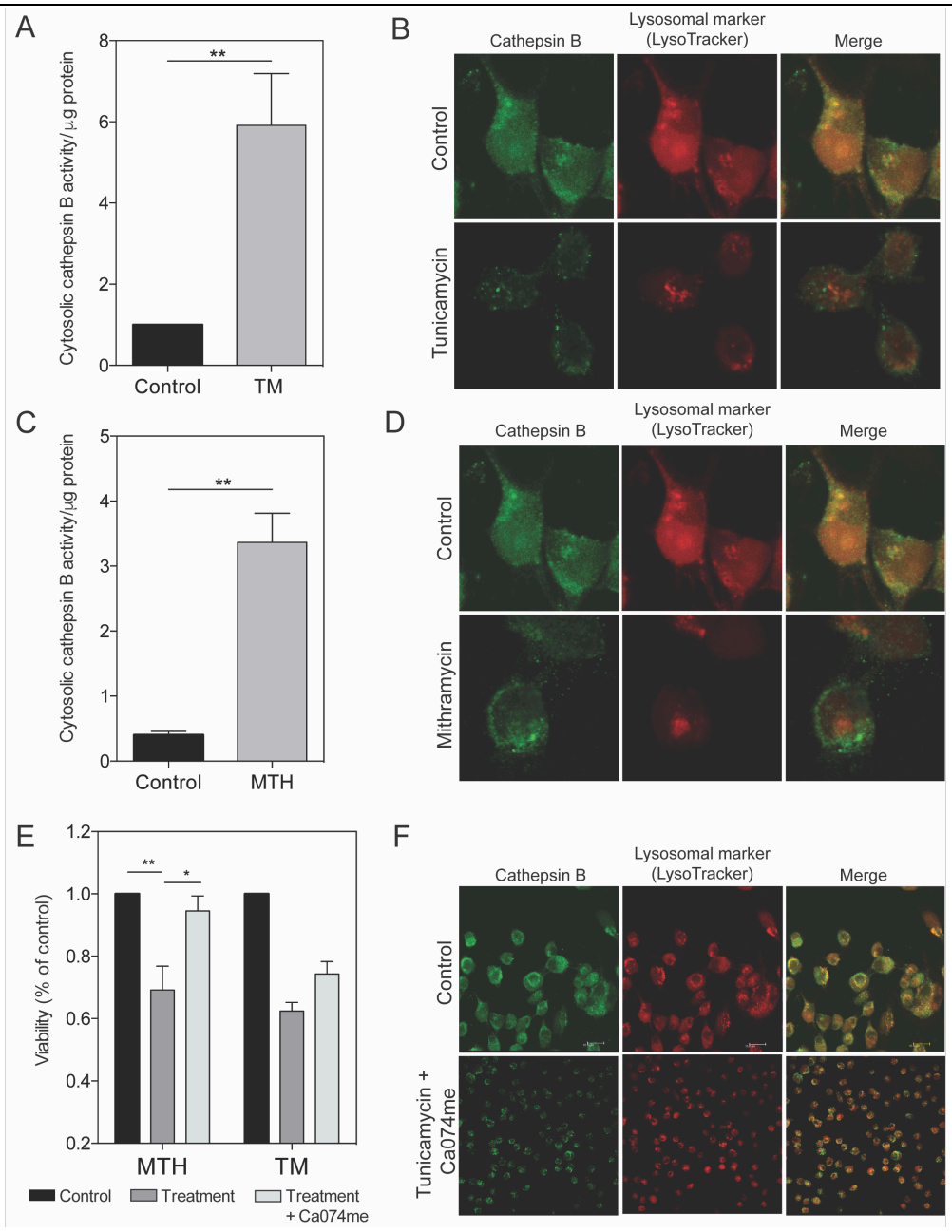

Figure 1.3: ER stress leads to a disruption in the lysosomal membrane
MIA PaCa-2 cells analyzed for lysosome membrane permeabilization. (A) Cells treated with 1 μM tunicamycin and analyzed for cytosolic cathepsin B activity. (B) Cells treated with 1 μM tunicamycin and stained with cathepsin B and lysotracker. Images taken at 60x. (C) Cells treated with 100 nM mithramycin and analyzed for cytosolic cathepsin B activity. (D) Cells treated with 100 nM mithramycin and stained with cathepsin B and lysotracker. Images taken at 60x. (E) Viability determined for cells treated with 100 nM mithramycin or 1 μM tunicamycin, with and without a cathepsin B inhibitor, Ca074me. (F) Cells treated with 1 μM tunicamycin, with and without Ca074me detected by immunofluorescence. Images taken at 40x and 60x.

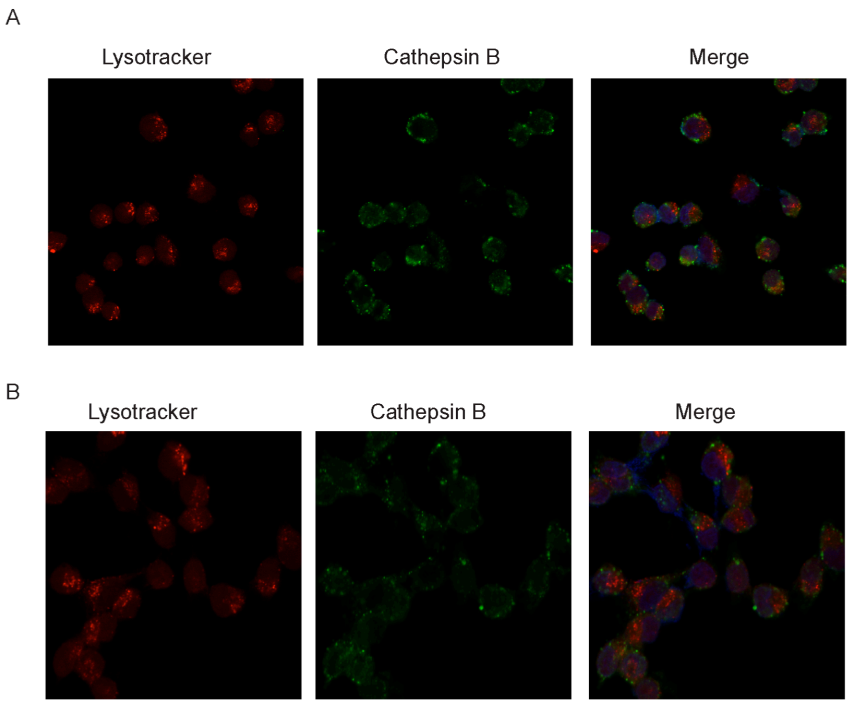

Supplementary Figure 1.4: Other known ER stress inducers also result in LMP
MIA PaCa-2 cells analyzed by immunofluorescence of cathepsin B and lysotracker after 6 hours of treatment with (A) 100 nM thapsigargin (TG) (B) 1 μM brefeldin A (BFA).

Since mitochondrial outer membrane permeabilization (MOMP) is also a commonly reported method of cell death, we sought to see if MOMP was another mechanism through which chronic ER stress led to cell death. MIA PaCa-2 cells were treated for 1 and 6 hours with TM, TG, BFA, and MTH, and assayed for disruption of mitochondrial membrane potential (MMP). Based on our results, we can conclude that while TM had a minor disruption in MMP compared to the positive control, FCCP, the other inhibitors did not affect MMP within 6 hours of treatment (data not shown).

Chronic ER stress results in a sustained accumulation of cytosolic calcium

Calcium imbalance in the cytosol is a known inducer of ER stress in a cell, as calcium is one of the co-factors needed for protein folding. Sustained calcium release from the calcium stores in the cellular organelles, in response to a drug or noxious stimuli, eventually leads to cell death. Therefore, we measured the amount of cytosolic calcium in cells treated with multiple pharmacological inhibitors simulating chronic ER stress. Treatment of MIA PaCa-2, S2-VP10, and S2-013 cells with 100 nM MTH, 100 nM TG, 1

μM TM, and 1 μM BFA resulted in a sustained accumulation of cytosolic calcium between 6-24 hours, measured using calcium orange dye-based assay method (Figure 1.4), as well as Fura-2 (data not shown). While 1 hour did not result in an appreciable amount of cytosolic calcium (data not shown), by 24 hours, we observed a sustained calcium accumulation in the cytosol.

MIA PaCa-2 cells treated with SP1 siRNA and pharmacological inhibitors showed the following calcium levels at 24 hours: untreated 100%, TG 143.5%, TM 131.0%, BFA 192.0% (Figure 1.4A), MTH 136.0% (Figure 1.4B), siSP1 113.2% (Figure 1.4C). S2-VP10 cells treated with pharmacological inhibitors showed the following calcium levels at 24 hours: untreated 100%, TG 131.9%, TM 177.6%, BFA 212.4% (Figure 1.4A), MTH 126.0% (Figure 1.4B). S2-013 cells treated with pharmacological inhibitors showed the following calcium levels at 24 hours: untreated 100%, TG 165.5%, TM 203.0%, BFA 245.3% (Figure 1.4A), MTH 147.7% (Figure 1.4B).

To determine if sustained accumulation of calcium was responsible for the cell death, we next used 10 μM of BAPTA (a calcium chelator) with each pharmacological inhibitor (data not shown). While there was a decrease in cytosolic calcium upon treatment with BAPTA, the viability of the cells was unaffected (data not shown). This finding suggests that even though induction of chronic ER stress led to an accumulation of cytosolic calcium at 24 hours, cytosolic calcium did not precipitate the UPR.

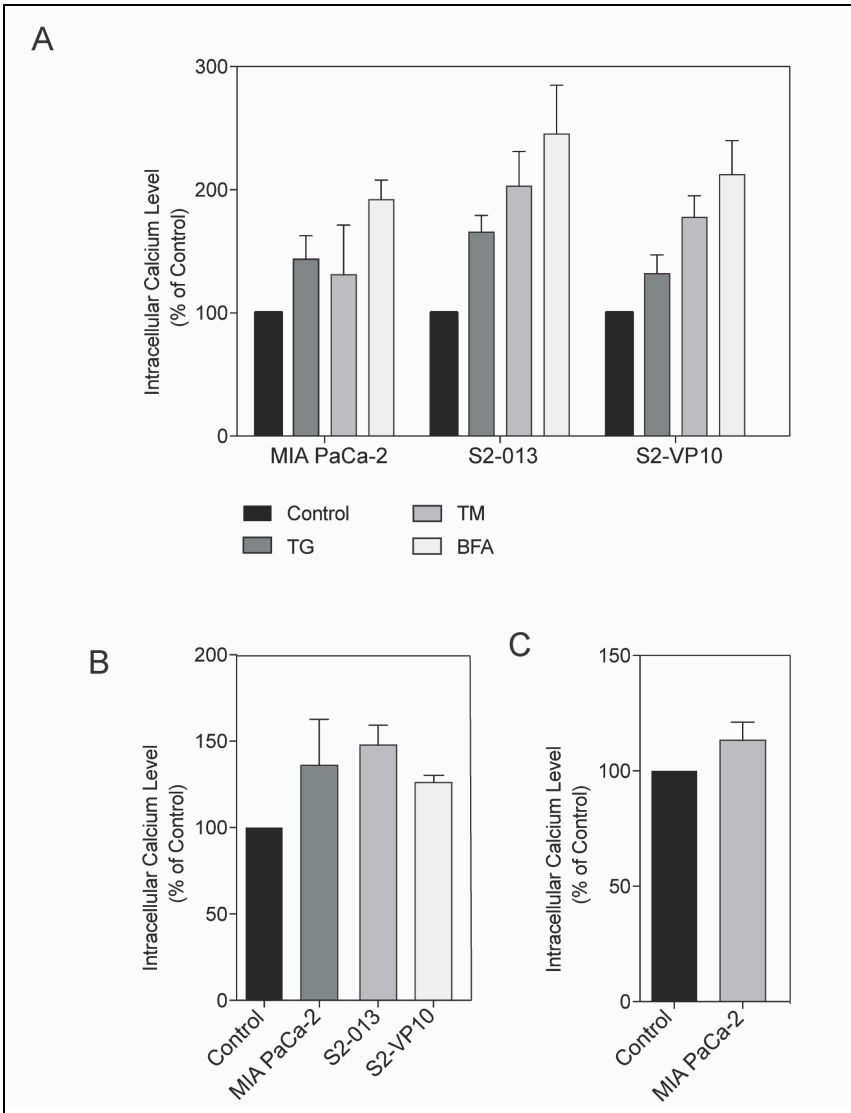

Figure 1.4: Chronic ER stress results in a sustained accumulation of cytosolic calcium
MIA PaCa-2, S2-VP10, and S2-013 cells treated with (A) known ER stress inducers and measured cytosolic calcium after 24 hours of treatment, and (B) mithramycin and measured cytosolic calcium after 24 hours of treatment, and (C) silenced with siSP1 measured cytosolic calcium after 24 hours of transfection.

DISCUSSION

ER stress is a “condition” due to an accumulation of unfolded proteins in the ER. A variety of cellular insults can result in the accumulation of unfolded or incorrectly folded proteins[52-54]. In response to ER stress, a cell can initiate the UPR to adapt and survive, thereby re-establishing ER homeostasis. However, severe or chronic UPR can breach the threshold for survival, and lead to cell death. ER stress is an important mechanism, which has been implicated in various pathologies, and has the potential to be targeted therapeutically[54, 55, 65, 66]. There have been prior studies that have described UPR as a druggable mechanism in cancer because of the distinct metabolic requirements of cancer cells, and the activity of UPR compared to normal cells[65, 66]. As a result, it is important to understand how this mechanism works in cancer to find druggable targets, which can preferentially induce cancer cell death in cancer cells, while avoiding cellular adaptation and survival.

Previous studies have determined that SP1 is necessary for an ER stress response[59], and cancer cell survival[15, 56]. In order to restore ER homeostasis, active GRP78 transcription is required. Interestingly, the RNA and protein expression of GRP78 remained relatively unchanged, as the cells failed to regain homeostasis following SP1 downregulation. Based on our data from the current investigation, in the absence of SP1, there is decreased binding of SP1 to the GRP78 promoter (Figure 1.2A). Without active transcription of GRP78, there is a breach in the threshold of stress that cells can handle, leading to cell death. By downregulating SP1 (Figures 1.1 and 1.2), we see a decrease in viability, in ERSE activity, and binding to the *GRP78* and *ATF6* promoters (ATF6 data not shown); whereas, tunicamycin did not affect SP1 binding (Supplementary Figure 1.3A). An increase in ERSE activity is one necessary step for a cell to re-establish homeostasis. Without SP1, *GRP78* is not transcribed, and is unable to help the cells recover from ER stress and turn off the activated UPR.

In previous studies, we have shown that triptolide works in two ways 1) it downregulates the substrate pool of O-GlcNAc, the modification of SP1, rendering it inactive; and 2) by causing chronic ER stress and cell death[15, 19, 23]. In our current study, we have shown that SP1 downregulation also causes chronic ER stress. To further characterize the cell

death mechanism induced by chronic ER stress, we studied lysosomal and mitochondrial cell death. Depending on the type of ER stress inducer, as well as the cell type, cancer cells can die by caspase-dependent or independent pathways upon LMP[60]. In AML and human monocytic leukemia/lymphoma, it has been shown that tunicamycin causes lysosome-mediated cell death, independent of the mitochondria[52]. In pancreatic cancer, bortezomib, a proteasome inhibitor, induces both LMP and MOMP[67]. Our group has published that triptolide results in LMP-mediated apoptosis, independent of MOMP[22]. However, triptolide in combination with TRAIL induces LMP and MOMP[16]. In the current study, we have shown that multiple ER stress inducers can result in LMP in PDAC (Figure 1.3), and initiate cell death, independent of MOMP.

To further explore ER stress-induced cell death, we studied the effect of ER stress inducers on cytosolic calcium. Calcium regulation is essential for survival of every cell. The ER is a major storage site for calcium, which can be taken up via the SERCA pump. Conversely, calcium can be released from the ER, for example, to aid in cytosolic protein folding. Further, in autophagy, calcium is necessary for the fusion of the autophagosome and lysosome[68]. Our results clearly show that acute UPR observed in the first 6 hours, initiated by either known ER stress inducers or SP1 downregulation, does not lead to an accumulation of cytosolic calcium. However, upon onset of chronic/prolonged ER stress, there is an accumulation of calcium in the cell that leads to cell death in 24 hours (Figure 1.4).

CONCLUSION

This study underscores the importance of ER stress and understanding the complex balance of adaptation vs. cell death in pancreatic cancer. The current study identified SP1 and GRP78 as potential targets for future therapeutics in PDAC; discovered a protective role of SP1 in cancer; as well as further detailed ER stress response in cell death mechanisms.

METHODS

Cell Culture and Treatment

Pancreatic cancer cell line, MIA PaCa-2 (obtained from ATCC) was cultured in DMEM; high glucose, supplemented with 10% FBS and 100 units/mL penicillin and 100 µg/mL streptomycin. S2-VP10 and S2-013 cell lines (a gift from Dr. Masato Yamamoto's lab, University of Minnesota) were grown and propagated in RPMI, supplemented with 10% FBS, 100 units/mL penicillin and 100 µg/mL streptomycin. All cells were maintained at 37°C in a humidified air atmosphere with 5% CO_2.

ON-TARGETplus SMARTpool human SP1 and GRP78 siRNA (Dharmacon) were used to silence expression of the respective genes in MIA PaCa-2 cells. Pool of 4 siRNA was used for all the above genes. Transfections were completed using DharmaFECT (Dharmacon) according to manufacturer's instructions. The following drugs were used for this study: mithramycin, tunicamycin, thapsigargin, brefeldin A (all from Sigma).

Cell Viability Assay

MIA PaCa-2 cells were seeded in a 96 well plate (7,000 cells/well) and allowed to adhere for 24 hours. Cells were transfected with 20 nM siRNA or treated with 100 nM mithramycin. Cell viability assays following siRNA or pharmacological inhibitors were performed using a WST-8 based cell cytotoxicity assay per the manufacturer's protocol (Dojindo) and expressed after normalizing to untreated cells.

Gene Expression Analyses

RT-PCR: RNA was isolated from the cells according to manufacturer's instructions using Trizol (Invitrogen). Total RNA (2 μg) was used to perform real-time PCR using the Quantitect SyBr green PCR kit (Qiagen) according to the manufacturer's instructions using Roche 480 real-time PCR system. All data were normalized to the housekeeping gene 18S (18s Quantitect Primer Assay; Qiagen). Quantitative RT-PCR primers for SP1, GRP78 (Qiagen).

Synthesized by Invitrogen/life technologies

ATF6 F: GGAGTATTTTGTCCGCCTGC/ R: ACTGGGCTATTCGCTGAAGG

XBP-u F: CAGACTACGTGCACCTCTGC/ R: GGCTGGTAAGGAACTGGGTC

XBP-s F:CTGAGTCCGCAGCAGGTG/ R: GGCTGGTAAGGAACTGGGTC

CHOP F: AGATGAGCGGGTGGCAGCGA/R: CCAGGCTTCCAGCTCCCAGC

Western blotting: Proteins from treated and untreated cell lysates were estimated using the BCA protein estimation assay (Thermo Scientific). Blots were probed for: anti-SP1; anti-BiP; anti-IRE1α; anti-PERK; anti-phospho-PERK (Thr980); anti-eIF2α; anti-phospho-eIF2α; anti-β-actin (all from Cell Signaling).

Luciferase Reporter Assay for ERSE

MIA PaCa-2 cells were seeded in a 24 well plate. Non-silencing and siSP1 were transfected in four wells each, and allowed to incubate for 15 hours. Cells were then transfected with the Cignal reporter plasmids for ERSE (Qiagen) and treated with 100 nM MTH and 1 μM TM for 8 and 24 hours. At each time point, wells were washed with PBS, and 100 μL of passive lysis buffer was added per well. After 15 minutes of rocking in passive lysis buffer, plates were stored at -80°C until ready to read. The dual luciferase kit (Promega) was used to measure activity using a luminometer. Each sample was treated in duplicate for each plasmid (duplicates for the negative reporter and duplicates for the ERSE reporter).

Immunofluorescence

MIA PaCa-2 cells were plated in chamber slides and incubated for 1-24 hours at 37°C. The slides were treated with 100 nM MTH, 1 μM TM, 100 nM TG, or BFA 1 μM; fixed with 2% paraformaldehyde, and permeabilized with CHAPS. The slides were incubated with 1:1000 dilution of rabbit polyclonal anti-cathepsin B antibody (Sigma) and a 1:1000 dilution of Alexa 488-conjugated donkey anti-mouse IgG (Molecular Probes) for cathepsin B staining. The slides were mounted using Prolong Gold anti-fade with 4',6-diamidino-2-phenylindole (Molecular Probes). Immunofluorescence images were obtained on a confocal microscope (Nikon Eclipse Ti) with a 40-100x oil-immersion objective. EZ-C software was used to obtain images.

Chromatin Immunoprecipitation

MIA PaCa-2 cells were treated with 100 nM MTH for 6 and 24 hours. Samples were collected and processed per the manufacturer's instructions (Pierce). GRP78 ChIP primer (GPH1026964(-) 01A; Qiagen) was used.

Calcium Measurement: Calcium orange-AM

Cells were seeded in a white 96-well plate, and allowed to attach for 24 hours at 37°C, and then treated with various ER stress inducers, including MTH and siSP1. After 24 hours of treatment, media was removed; cells were washed with phosphate-buffered saline (PBS), and loaded with 1.5 μL of 5 mmol/L Calcium Orange-AM (in 20% pluronic acid in DMSO) in serum free media for 1 hour. After incubation, the cells were washed with PBS three times, and fresh PBS was added for measurement of calcium. Luminescence measurements were obtained at 550 nM. A clear 96-well plate was used to determine viability, and the results were normalized to viability.

Cathepsin B Assay

Cells were seeded in a 6-well plate, and allowed to adhere for 24 hours. Cells were treated with 1 μM TM and 100 nM MTH for 1 hour each. To measure cytosolic cathepsin B activity, the cytosolic fraction was isolated using a cytosolic buffer (25 mM HEPES, 120 mM KCl, 0.15 mM $CaCl_2$, 10 mM K_2HPO_4, 5 mM $MgCl_2$, 2 mM EDTA, 2 mM ATP, 10 mM DTT, pH 7.6) containing 20 μg/mL Streptolysin O for 20 minutes on ice. Cells were then washed without Streptolysin O, and incubated at 37°C for 20 minutes to selectively permeabilize the plasma membrane. The cells were then centrifuged at high speed to separate the cells and cytosol. Cathepsin B activity was determined using a cathepsin B selective substrate, N-carbobenzoxy-arginyl-arginine-naphthylamide (Bachem), as described by McDonald and Ellis[69]. Activity was expressed as units/mg protein in each sample.

***In vivo* Study**

Athymic nude mice were injected with 10^6 MIA PaCa-2 cells suspended in Matrigel (Corning), subcutaneously in the right flank. Tumor size was measured weekly and mice

were randomized when tumors reached an average of 250 mm^3. Mice were randomized into saline, MTH 0.3 mg/kg, and MTH 0.6 mg/kg groups. MTH was administered intraperitoneally, three times per week. Mice were sacrificed when tumors reached 900 mm^3. The University of Minnesota Institutional Animal Care and Use Committee (IACUC) approved all procedures.

Statistical Analysis

Values are expressed as the mean +/- SEM. All *in vitro* experiments were performed at least three times. The significance between any two samples was analyzed by t-test, values of $p<0.05$ were considered statistically significant.

CHAPTER 2: ENDOPLASMIC RETICULUM STRESS IN PDAC CAN LEAD TO CHEMORESISTANCE

Inhibition of GRP78 sensitizes pancreatic cancer cells to chemotherapy and potentiates cell death

Patricia Dauer[1], Nikita S Sharma[2,3], Vineet K Gupta[2,3], Alice Nomura[2,3], Vikas Dudeja[2,3], Ashok Saluja[2,3], Sulagna Banerjee[2,3]

1 Department of Pharmacology, University of Minnesota, Minneapolis Minnesota
2 Department of Surgery, University of Miami, Miami, FL
3 Sylvester Comprehensive Cancer Center, Miami, FL

Under final review at Molecular Oncology

SUMMARY

Background: Chemoresistance is a major therapeutic challenge that plays a role in the poor statistical outcomes in pancreatic cancer. Unfolded Protein Response (UPR) is one of the homeostatic mechanisms in cancer cells that have been correlated with chemoresistance in a number of cancers including pancreatic cancer.

Methods: MIA PaCa-2, S2-VP10, and SU.86.86 pancreatic cancer cell lines were used for the following study. The significance of glucose regulatory protein 78 (GRP78), nuclear factor, erythroid 2-like 2 (NRF2) and ATP-binding cassette (ABC) transporter expression was established using the *LSL-Kras*^{G12D}; *LSL-Trp53*^{R172H}; *Pdx-1-Cre* (KPC) mouse model for mRNA and protein expression, as well as serum expression for GRP78. Genetic silencing of *GRP78* and *specificity protein 1* (*SP1)* was combined with chemotherapeutics *in vitro* to determine viability, ABC transporter activity, total cellular ATP and ATPase, antioxidant response activity, and reactive oxygen species (ROS) production. MIA PaCa-2 cells were injected into athymic nude mice subcutaneously, and treated with two doses of mithramycin (SP1 inhibitor), gemcitabine, or the combination of gemcitabine and mithramycin for four weeks. The effect of SP1 downregulation on GRP78 was determined, as well as the relative cell death in each group.

Results: In the current study, we showed that modulating GRP78, the master regulator of the UPR, could have a profound effect on multiple pathways that mediate chemoresistance. Our study showed for the first time that knockdown of *GRP78* could diminish efflux activity of ABC transporters, and it could decrease the antioxidant response resulting in an accumulation of ROS. We also show that these effects could be mediated by the activity of SP1, a transcription factor overexpressed in pancreatic cancer. Thus, inhibition of SP1 negatively affects the UPR, deregulates the antioxidant response of NRF2, as well as ABC transporter activity by inhibiting GRP78-mediated ER homeostasis.

Conclusion: SP1 and NRF2 have been classified as non-oncogene addiction genes and thus are imperative to understanding the molecular mechanism of resistance. Our results show that the combination of gemcitabine and mithramycin attenuates

chemoresistance, resulting in more cell death and smaller tumor size *in vivo*. These findings have clinical relevance as both SP1 and GRP78 are overexpressed in pancreatic cancer patients and increased expression of these proteins are indicative of poor prognosis. Understanding how these proteins may regulate the chemosensitivity of this aggressive cancer may pave the way for development of efficacious therapy for this devastating disease.

INTRODUCTION

Pancreatic cancer is a devastating disease with relatively unchanged survival statistics for 70 years[70]. In 2017, it is estimated that 53,670 people will be diagnosed with pancreatic cancer, and 43,090 people will die from the disease[70]. FOLFIRINOX (oxaliplatin, irinotecan, leucovorin, and 5-fluorouracil (5-FU) combination therapy) offers a slight survival benefit compared to gemcitabine alone, but only a small subset of patients can withstand the toxicity[50, 71]. One of the main reasons for the poor survival statistics in this disease is due to drug resistance to these standards of care, like gemcitabine, paclitaxel, and 5-FU.

There are multiple mechanisms of chemoresistance employed by cancer cells. The unfolded protein response (UPR) contributes to chemoresistance, a homeostatic mechanism, which ameliorates stressful conditions to ensure cell survival. In order to survive the pressure created by the tumor microenvironment, including hypoxia and nutrient deprivation, tumor cells utilize the UPR pathways[4, 33, 72, 73]. Multiple components of the UPR have been linked to advanced tumor stage and chemoresistance in cancer[32, 74-76]. For example, overexpression of protein disulfide isomerase family A member 5 (PDIA5) in chronic myeloid leukemia shows increased resistance to Imatinib[33]. Overexpression of X box protein 1s (XBP1s) has been found in triple negative breast cancer, a resistant subset of breast cancer[33, 77]. XBP1s also correlates with higher tumor grade, chemoresistance, and shorter survival in lymphoma[32].

Glucose regulatory protein 78 (GRP78), the regulator of the UPR, has previously been correlated with poor patient prognosis in multiple cancers, including pancreatic cancer[4, 32, 73, 78, 79]. Based on correlation studies and direct overexpression leading to chemoresistance, numerous proteins in the UPR pathway have been targeted with small molecules in hopes to attenuate chemoresistance[33, 74, 75, 79]. In spite of a generous body of literature correlating chemoresistance to expression of genes involved in UPR (Table 2.1), there have been almost no studies to elucidate the mechanism(s) by which UPR contributes to chemoresistance.

Table 2.1: UPR Activation in Multiple Cancers

Cancer	UPR Component	Conclusion	Described by	Year
Lung	CHOP	Correlates with high tumor stage and shorter survival	Kim, KM. *et al.*[80]	2012
Breast	GRP78, XBP1	Correlates with ER-negative	Fernandez, PM. *et al.*[77] Scriven, P. *et al.*[81]	2000 2009
Colon	GRP78, CHOP	Correlates with malignancy and tumor stage	Rask, K. *et al.*[82] Xing, X. *et al.*[83]	2000 2006
Gastric	GRP78, GRP94	Correlates with tumor size, invasion, metastasis, and stage	Zheng, HC. *et al.*[84] Langer, R. *et al.*[85]	2008 2008
Liver	GRP78, ATF6, XPB1, HSP27, HSP70	Correlates with histological grade, venous infiltration, CD147 expression	Shuda, M. *et al.*[86] Luk, JM. *et al.*[87] Tang, J. *et al.*[88]	2003 2006 2012
Prostate	GRP78	Correlates with survival, castration resistance, recurrence	Pootrakul, L. *et al.*[89] Tan, SS. *et al.*[90]	2006 2011
Kidney	GRP78	Correlates with tumor grade, stage, invasion, metastasis, survival	Fu, W. *et al.*[91] Kuroda, K. *et al.*[92]	2010 2011
Skin	GRP78	Correlates with metastasis, survival	Zhuang, L. *et al.*[93]	2009
Ovary	GRP78	Correlates with malignancy	Huang, LW. *et al.*[94]	2012
Lymphoma	XBP1, GRP94, IRE1, GADD34	Correlates with tumor grade, resistance, survival	Balague, O. *et al.*[95] Mozos, A. *et al.*[96] Boelens, J. *et al.*[97]	2009 2011 2013
Pancreas	GRP78	Correlates with tumor stage, poor survival.	Niu Z. *et al*[78]	2015

Upregulation of the oxidative stress response pathway is another mechanism of decreasing chemotherapy-driven apoptosis. Management of oxidative stress decreases reactive oxygen species (ROS) accumulation in a cell, which in turn enhances detoxification and inhibits apoptotic cell death of tumor cells[98, 99]. The major transcription factor responsible for regulating oxidative stress response is Nuclear factor, erythroid 2-like 2 (NRF2). NRF2 is downstream of the PKR-like endoplasmic reticulum kinase sensor in the UPR, and is one transcription factor that has been shown to regulate ABCC-subfamily expression[100]. NRF2 normally acts like a tumor suppressor, but over-activation its antioxidant response elements (ARE) activity leads to cell survival of normal and malignant cells[99-101]. It has previously been reported that gemcitabine upregulates the NRF2 pathway, helping to mediate resistance[4, 102].

Another well-known mechanism of chemoresistance is through the ATP-binding cassette (ABC) transporter family. ABC-transporters drive the efflux of xenobiotics, including

chemotherapeutics. High transporter activity keeps intracellular chemotherapeutic concentrations low, thereby decreasing their overall effectiveness. The most common transporters involved in chemoresistance are BRCP (ABCG2), MDR1 (ABCB1), and MRPs (ABCCs)[103-107].

A previously published study from our laboratory showed higher GRP78 expression in tumor ducts compared to non-tumor tissue[23]. It was recently reported that GRP78 correlates with poor prognosis and chemoresistance in pancreatic cancer[78, 79]. Further, it was shown that gemcitabine-resistant cell lines have higher GRP78 expression compared to gemcitabine-sensitive cell lines[79]. It has also been reported that patients with pancreatic cancer have an upregulation of ABC transporters, particularly ABCC3 and ABCC5[105, 108]. However, it is unclear whether the ABC expression regulation correlates with PDAC tumor stages[105, 108].

Specificity protein 1 (SP1) regulates many biological functions, including cell growth, differentiation, survival, as well as tumor progression and metastasis[15, 24, 26, 28, 56]. Multiple studies have underscored the importance of SP1 in malignant tissues[15, 24, 28]. Interestingly, it has been reported in colon, gastric, pancreatic, and breast cancers that SP1 is overexpressed, whereas minimal to no SP1 expression is detected in normal differentiated cells[15, 24, 28]. We have recently published that upon downregulation of SP1, transcriptional regulation of GRP78 is adversely affected and cannot recover from chronic ER stress, which leads to cell death[109].

In this manuscript, we show for the first time that modulation of GRP78 expression by either overexpressing or silencing has a profound effect on a number of independent pathways that are responsible for chemoresistance. We further show that the effect of GRP78 modulation is mediated by the activity of SP1, a transcription factor that plays a significant role in maintaining ER homeostasis. Thus, inhibition of SP1 deregulates the antioxidant response of NRF2 as well as ABC transporter activity by inhibiting GRP78-mediated ER homeostasis via the unfolded protein response.

RESULTS

Based on studies listed in Table 2.1, GRP78 appears to correlate with tumor size, stage, malignancy, and chemoresistance. The correlation of GRP78 and chemoresistance was established just recently in pancreatic cancer. For our current study, we used multiple established cell lines. Supplementary Figure 2.1 below shows the mRNA expression of GRP78 (y-axis, also known as HSPA5), and NRF2 (x-axis), according to the publicly available RNAseq data on the Cancer Cell Line Encyclopedia.

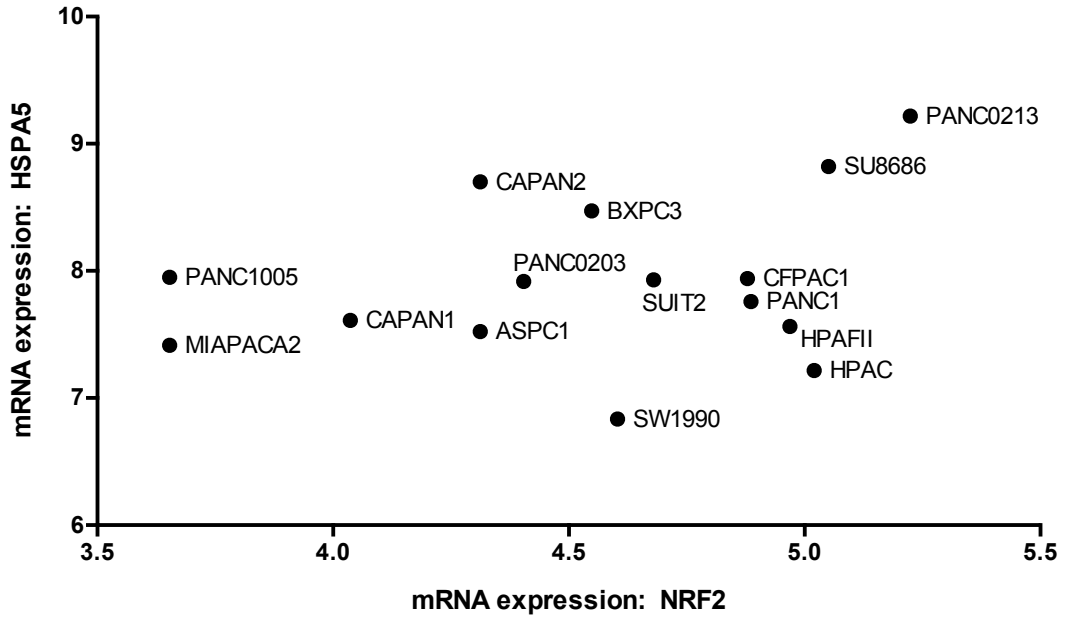

Supplementary Figure 2.1: Comparison of GRP78 and NRF2 mRNA expression between multiple cell lines
mRNA expression of GRP78 (y-axis) and NRF2 (x-axis) of multiple pancreatic cancer cell lines from CCLE RNAseq data.

GRP78 expression correlates with tumor progression

We found significantly increased GRP78 mRNA expression in tumor bearing mice ($8.82e^{-6}$) compared to 1 month ($7.76e^{-7}$) and 3 month mice ($1.62e^{-6}$) (Figure 2.1A). Serum protein level of GRP78 was also significantly increased (0.53 ng/mL) compared to the non-tumor bearing controls (0.02 ng/mL) (Figure 2.1B). Further, we analyzed human patient serum for levels of GRP78, and found a similar increase in GRP78

expression (15 ng/mL) compared to healthy controls (below detection limit) (Figure 2.1C). Consistent with our mRNA data, we looked at GRP78 protein expression in the KPC pancreata by immunofluorescence staining, and found an increase in the ductal expression of GRP78 in the tumor-bearing group compared to the non-tumor group (Figure 2.1D).

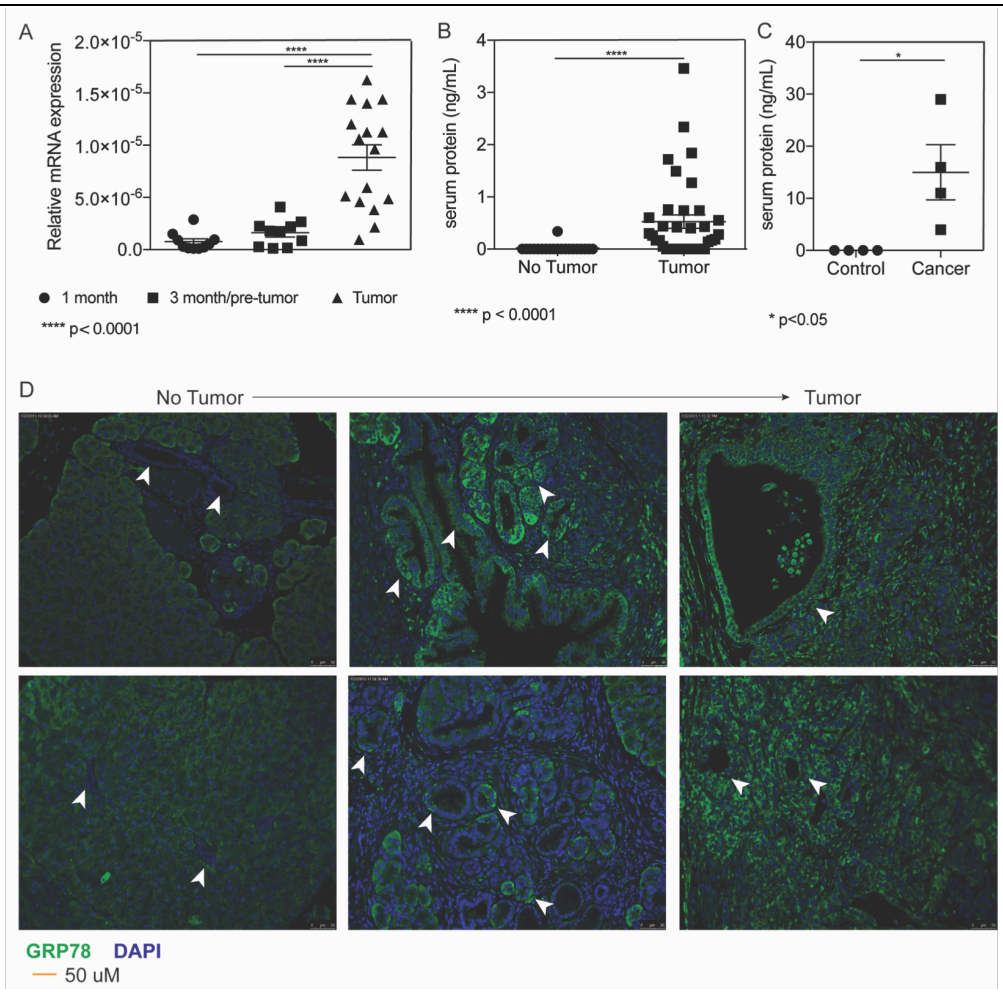

Figure 2.1: GRP78 expression correlates with tumor progression
Analysis using KPC pancreata ranging from 1-9 months found that (A) GRP78 mRNA expression is overexpressed in pancreata with tumor compared to 1 or 3 month old KPC mice, and (B) GRP78 in serum from mice with tumors compared to mice without tumors was significantly greater. Serum from human patients also had elevated GRP78 compared to healthy controls (C). GRP78 protein expression (FITC) was found to be overexpressed in the ductal/pseudo-ductal regions in the tumor-bearing mice compared to mice without tumors (highlighted by arrows). Images were acquired at 20x magnification. (D).

Silencing GRP78 combined with chemotherapeutics increases cell death

Three pancreatic cancer cell lines: MIA PaCa-2, SU.86.86, and S2-VP10 were used to demonstrate the chemoresistance to relevant PDAC drugs (gemcitabine, paclitaxel, and 5-FU). Figure 2.2A is a dose response curve for each cell line with the three drugs after 48 hours of treatment. To determine if silencing GRP78 would diminish chemoresistance in the same cell lines, cells were transfected with siGRP78 and treated with gemcitabine, paclitaxel, or 5-FU for 24-48 hours. We found that combining chemotherapeutics (using greater than IC_{50} concentrations) with siGRP78 resulted in more cell death than silencing or drug treatment alone in 24 and 48 hours (Figure 2.2B, Supplementary Figure 2.1A-B). In addition to cell viability, apoptosis was detected using immunofluorescence by probing with a cleaved caspase 3 antibody. MIA PaCa-2 (Figure 2.2C, Supplementary Figure 2.2A) and S2-VP10 (Supplementary Figure 2.2B) were transfected with non-silencing (NS) siRNA, NS + gemcitabine, siGRP78, or siGRP78 + gemcitabine for 24 hours. Our results show increased cleaved caspase 3 in siGRP78 + gemcitabine compared to gemcitabine or NS alone.

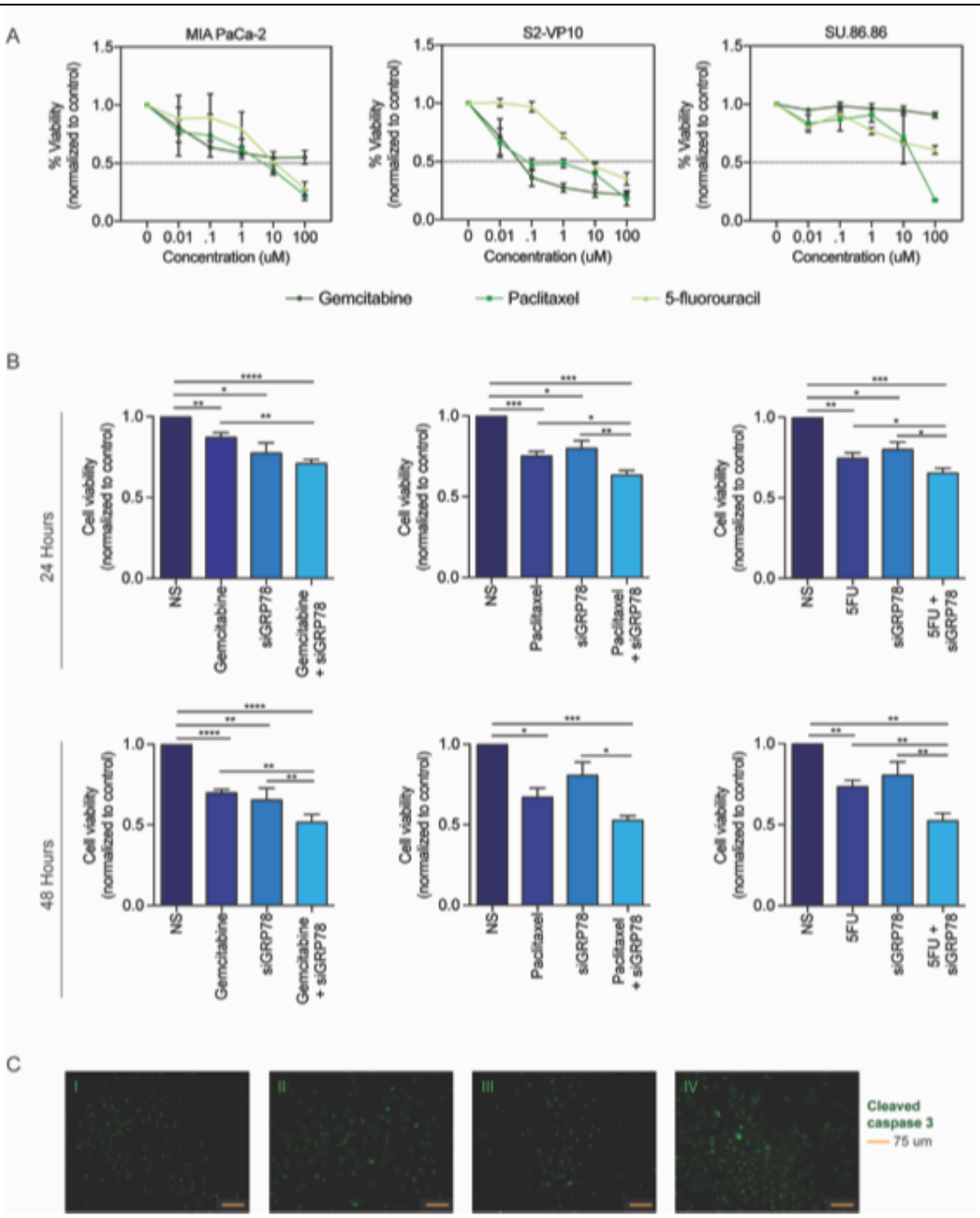

Figure 2.2 Silencing GRP78 combined with chemotherapeutics increases cell death.
MIA PaCa-2, SU.86.86, and S2-VP10 cells were all treated with a dose response (0-100 μM) of gemcitabine, paclitaxel, and 5-fluorouracil for 48 hours (A). MIA PaCa-2 cells transfected with siGRP78 and treated with 400 nM gemcitabine, 50 nM paclitaxel, or 5 μM 5-FU for 24 and 48 hours resulted in decreased viability compared to treatment or silencing alone (B). MIA PaCa-2 cells transfected with NS siRNA (C-I), 400 nM gemcitabine (C-II), siGRP78 (C-III), or siGRP78 + gemcitabine (C-IV) for 24 hours. Cells were fixed and probed with a cleaved caspase 3 antibody for apoptosis, and images were acquired at 20x magnification.

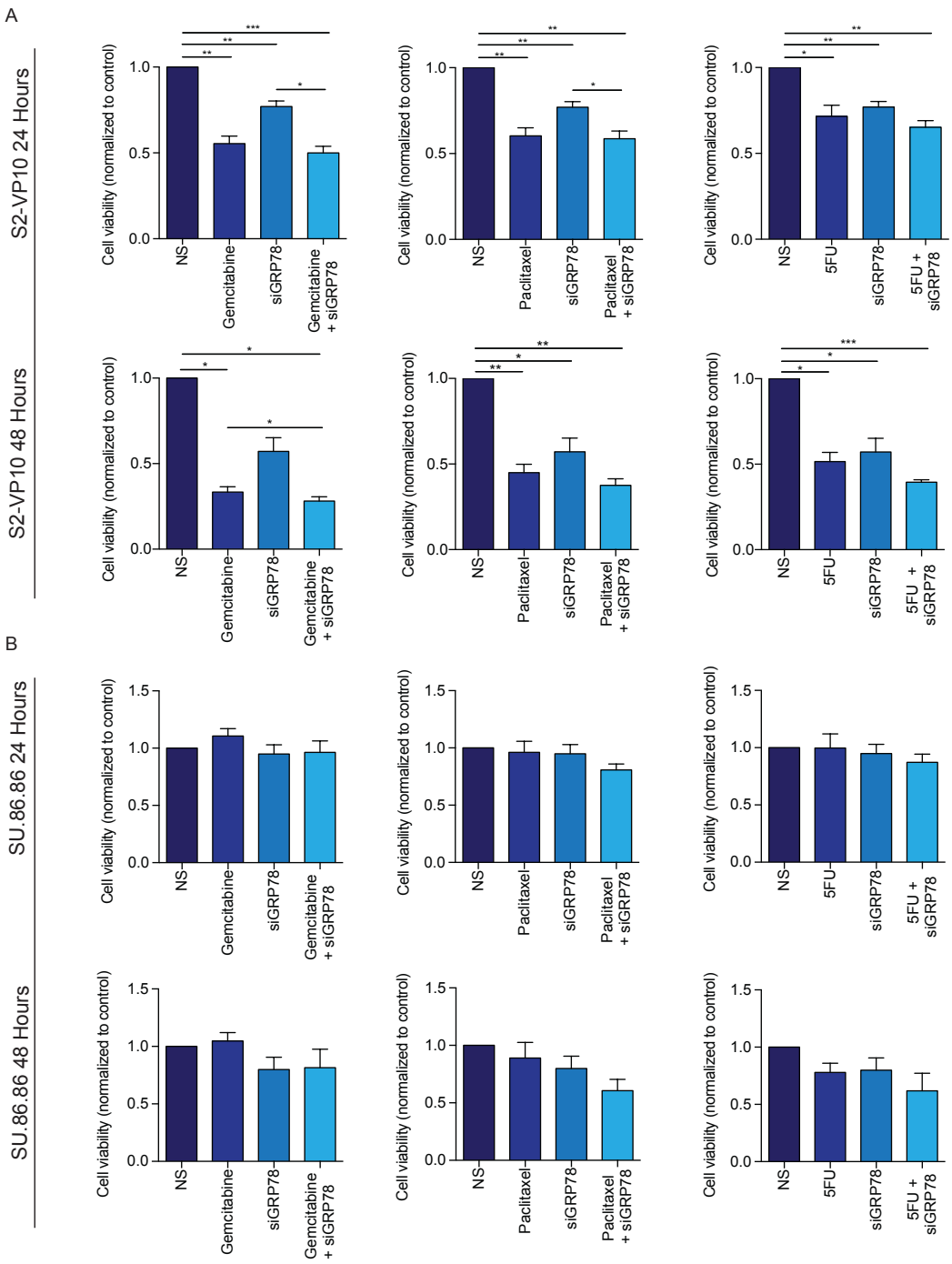

Supplementary Figure 2.1: Silencing GRP78 combined with chemotherapeutics decreases viability in pancreatic cancer cell lines
(A) S2-VP10 cells transfected with siGRP78 and treated with 100 nM gemcitabine, 50 nM paclitaxel, or 5 μM 5-FU for 24 and 48 hours resulted in decreased viability compared to treatment or silencing alone. (B) Su.86.86 cells transfected with siGRP78 and treated with 400 nM gemcitabine, 50 nM paclitaxel, or 5 μM 5-FU for 24 and 48 hours resulted in decreased viability compared to treatment or silencing alone.

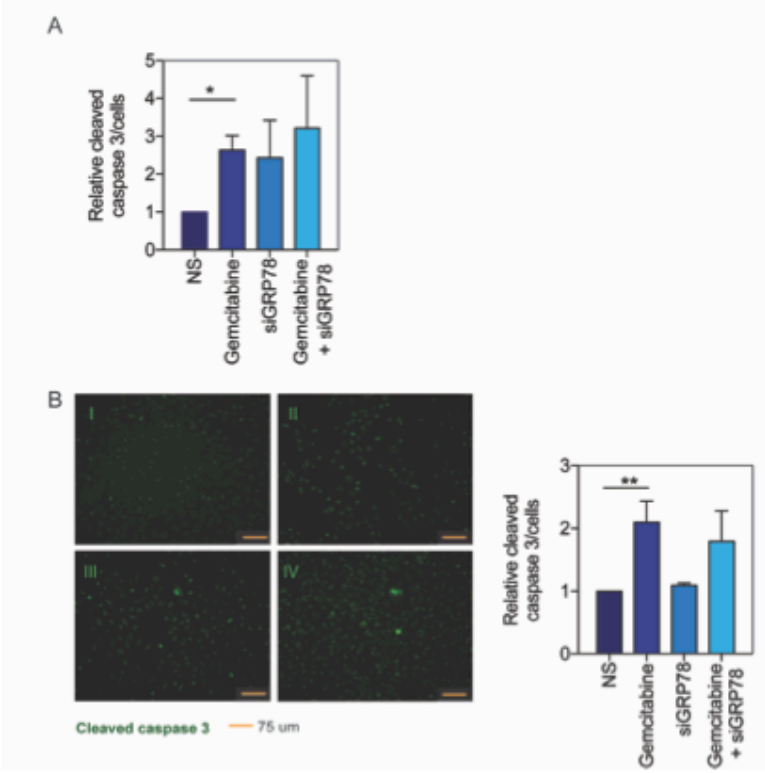

Supplementary Figure 2.2: Silencing GRP78 combined with gemcitabine results in more cell death.
(A) Quantitation of cleaved caspase 3 staining after MIA PaCa-2 cells were transfected with siGRP78 and treated with 400 nM gemcitabine 24 hours. (B). S2-VP10 cells transfected with NS siRNA (B-I), 100 nM gemcitabine (B-II), siGRP78 (B-III), or siGRP78 + gemcitabine (B-IV) for 24 hours, and stained with cleaved caspase 3 for apoptosis, and the respective quantitation. Images were acquired at 20x magnification.

Silencing GRP78 combined with chemotherapeutic compounds decreases ABC transporter activity in pancreatic cancer cells

ABC-transporters are a known mechanism of chemoresistance. Our results showed numerous ABC transporters to be overexpressed in KPC tumors compared to 1 month KPC without tumors (Table 2.2). Further, using a dye-efflux assay, we found that gemcitabine and paclitaxel alone both increased the % efflux of cells (27.1% and 2.9%, respectively). Conversely, non-silencing (0.35-0.77%) and siGRP78 (0.43-0.88%) had minimal efflux activity. When MIA PaCa-2 cells were silenced with siGRP78 and treated

with gemcitabine, the % efflux decreased back to baseline (0.68%). siGRP78 and paclitaxel had a similar trend as gemcitabine, and the combination decreased the % efflux to 0.56% (Figure 2.3A).

Table 2.2: mRNA expression of ABC transporters in KPC mice

	1 month	SEM	3 month/pre-tumor	SEM	Tumor	SEM
ABCA1	6.011E-07	2.69E-07	1.117E-06**	7.82E-07	1.125E-05**	1.41E-06
ABCB1	4.539E-08	2.05E-08	3.096E-08**	1.63E-08	2.172E-06**	7.95E-07
ABCC1	6.210E-07	3.60E-07	6.897E-07**	3.58E-07	5.478E-06**	1.25E-06
ABCC2	4.731E-06	3.32E-06	3.076E-05	2.46E-05	5.852E-05	4.22E-05
ABCC4	1.050E-07	5.19E-08	1.302E-07**	7.25E-08	2.941E-06**	7.21E-07
ABCC5	8.264E-07	3.34E-07	1.167E-06*	4.71E-07	4.990E-06*	7.94E-07
ABCG2	2.247E-07	6.90E-08	1.008E-05	7.53E-06	2.493E-06	1.29E-06

*<0.001 ** <0.0001

The dye efflux assay utilizes verapamil to effectively block transport, but also as a calcium channel blocker, blocks calcium channels. We next wanted to determine the effect on viability and calcium changes when blocking transporters using verapamil with and without siGRP78 or drugs. The combination of verapamil and drugs in MIA PaCa-2 cells (Figure 2.3B, Supplementary Figure 2.3A) and S2-VP10 cells (Supplementary Figure 2.3B) decreased cell viability in 24 hours more than verapamil or drug alone. Next, we transfected MIA PaCa-2 cells with NS, siGRP78, NS + verapamil, or siGRP78 + verapamil for 1 and 6 hours, and stained cells with ER tracker and Fluo4 (calcium dye). Pearson coefficients were calculated for each group. After 1 hour, r ranged from 0.3166 - 0.7254 (data not shown). However, in 6 hours NS had an r value of 0.8848; siGRP78 r = -0.1272; verapamil r = -0.5227; and siGRP78 + verapamil r = -0.4092 (Figure 2.3C), indicating a negative correlation between calcium and ER tracker.

ABC transporters are fueled by ATP. In order to determine how GRP78 (an ER resident protein) effectively decreases the ABC transporter activity, we silenced GRP78 and measured the total ATP and ATPase per condition described in MIA PaCa-2 cells. Results are expressed as relative luciferase units (RLU) per µg/mL protein. Gemcitabine alone increased ATP (4.62) as compared with non-silenced (1.74) and siGRP78 (3.26).

Gemcitabine with siGRP78 decreased the total ATP (4.02) compared to gemcitabine alone (Figure 2.3D). The amount of ATPase corresponds with the total cellular ATP. ATPase is expressed as μM phosphate per μg/mL protein. Gemcitabine had an increase in the ATPase ($7.59e^{-4}$) compared to NS (0) or siGRP78 ($2.80e^{-4}$) (Figure 2.3E), indicating that more ATP is being utilized. Gemcitabine with siGRP78 decreased the amount of ATPase compared to gemcitabine alone (3.94), indicating that less ATP is being utilized with the combination.

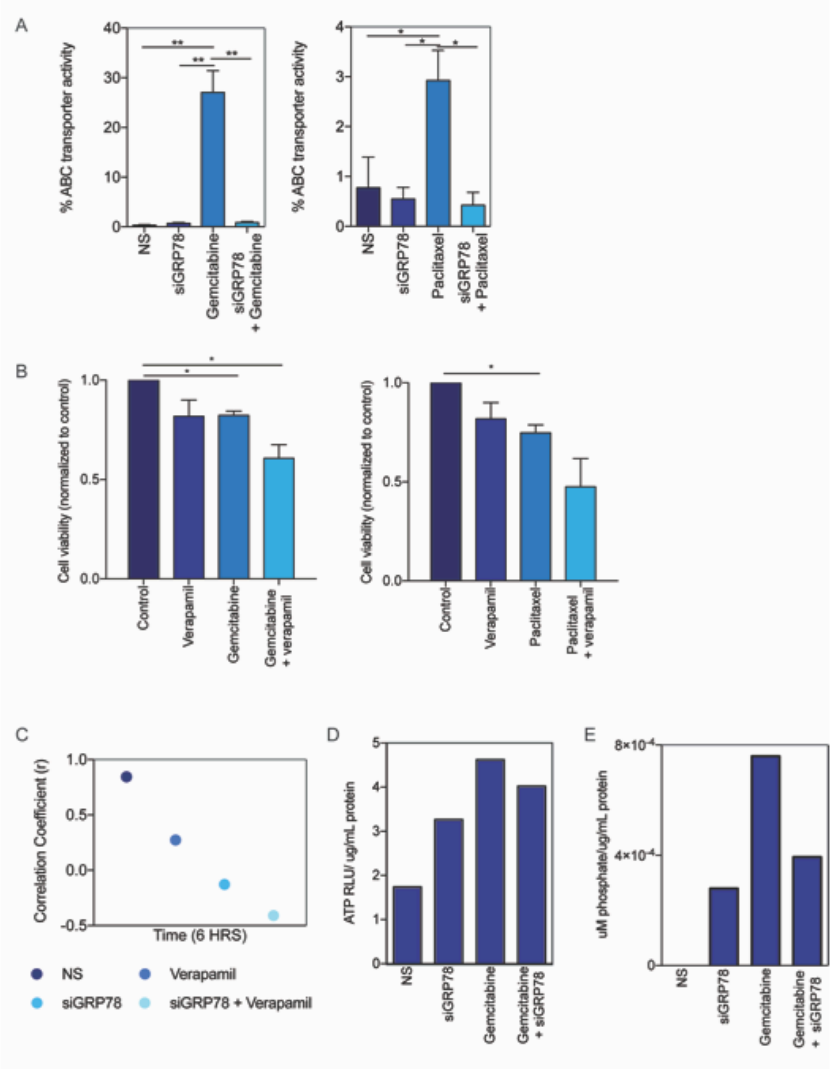

Figure 2.3: GRP78 combined with chemotherapeutic compounds decreases ABC transporter activity in pancreatic cancer cells

MIA PaCa-2 cells transfected with siGRP78 and treated with 400 nM gemcitabine or 50 nM paclitaxel for 8 hours +/- verapamil, and analyzed by flow cytometry (A). MIA PaCa-2 cells were treated with verapamil + chemotherapeutics for 24 hours to determine cell viability (B). Pearson coefficient was calculated for ER tracker and calcium co-localization in MIA PaCa-2 cells transfected with siGRP78 and treated with 100 μM verapamil for 6 hours (C). MIA PaCa-2 cells transfected with siGRP78 and treated with 400 nM gemcitabine for 24 hours to measure total ATP (D) and ATPase (E). Figures are representative of three experiments.

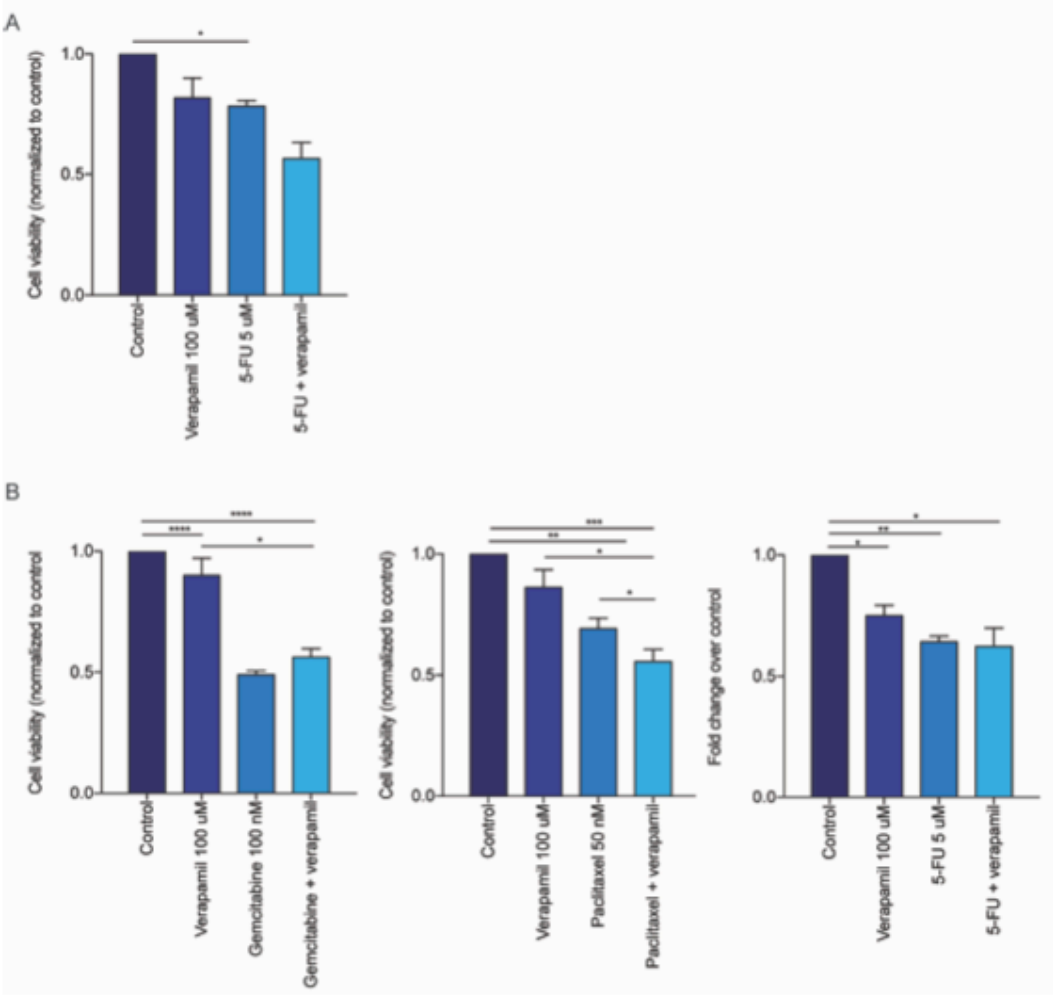

Supplementary Figure 2.3: Verapamil combined with chemotherapeutic compounds decreases cell viability in pancreatic cancer cells
(A) MIA PaCa-2 cells were treated with 5 μM 5-FU and 100 μM verapamil for 24 hours to determine cell viability. (B) S2-VP10 cells were treated with 100 μM verapamil and either 100 nM gemcitabine, 50 nm paclitaxel, or 5 μM 5-FU for 24 hours to determine cell viability.

Silencing GRP78 combined with chemotherapeutic compounds decreases antioxidant response in activity in pancreatic cancer cells

NRF2 is also an important mechanism of chemoresistance, by binding to the antioxidant response elements and transcribing detoxification genes, as well as some ABC-transporters. We found that NRF2 mRNA expression is overexpressed in full tumor KPC pancreata ($4.35e^{-5}$) compared to 1 month ($3.33e^{-6}$) and 3 month pancreata without tumors ($1.69e^{-5}$) (Figure 2.4A). In terms of activity, gemcitabine modestly increased the

NRF2 activity in MIA PaCa-2 cells (1.71 RLU), as measured by a luciferase reporter of the antioxidant response elements (representative results shown). siGRP78 modestly decreased NRF2 activity (0.62 RLU), and when combined with gemcitabine (1.23 RLU), it decreases the activity closer to non-silenced cells (NS) (1.06 RLU) (Figure 2.4B). S2-VP10 cells had a similar trend, but resulted in much more NRF2 activity. Gemcitabine increased the NRF2 activity (3632 RLU), siGRP78 was slightly higher than NS (1055 RLU), and when combined with gemcitabine (1915 RLU), it decreases the activity closer to NS (320 RLU) (Figure 2.4C). Further, we observed that the total ROS detected with DCFDA dye was increased in the siGRP78 + gemcitabine compared to NS, siGRP78, or treatment alone in MIA PaCa-2 (Figure 2.4D) as well as in S2-VP10 (Figure 2.4E), indicating that the UPR-NRF2/ARE signaling is not able to decrease the amount of ROS being produced in the combination treatment.

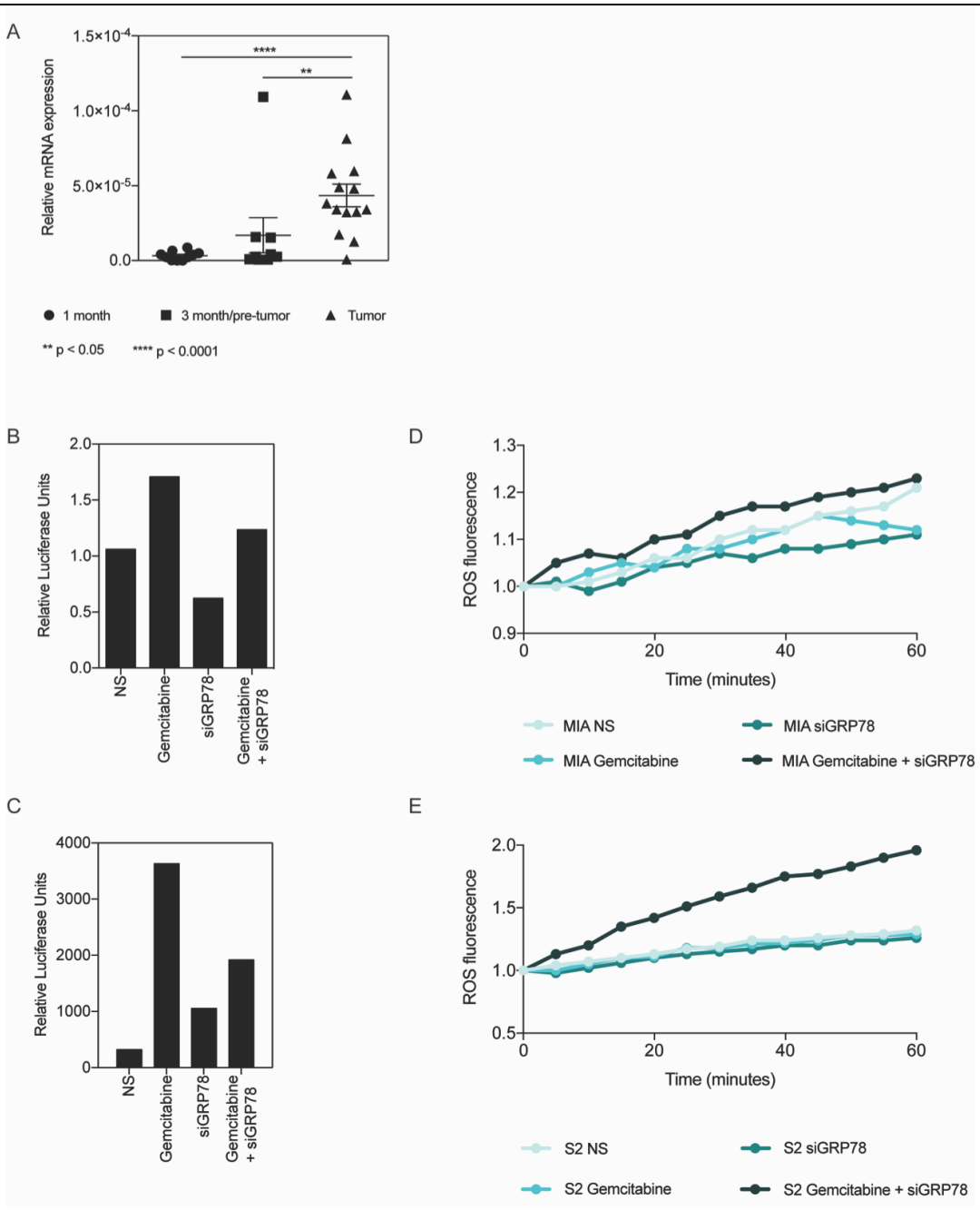

Figure 2.4: Silencing GRP78 combined with chemotherapeutic compounds decreases antioxidant response in activity in pancreatic cancer cells

Analysis using KPC pancreata ranging from 1-9 months found that (A) NRF2 mRNA expression is overexpressed in pancreata with tumor compared to 1 or 3 month old KPC mice. MIA PaCa-2 cells transfected with siGRP78 and treated with 400 nM gemcitabine for 24 hours to measure ARE activity (B). S2-VP10 cells transfected with siGRP78 and treated with 100 nM gemcitabine for 24 hours to measure ARE activity (C). ROS measurement of MIA PaCa-2 (D) and S2-VP10 (E) cells after 24 hours of treating with gemcitabine and siGRP78.

SP1 is required for ER homeostasis and affects chemoresistance in pancreatic cancer cells, similarly to GRP78

We have previously shown that SP1 is required for ER homeostasis in pancreatic cancer[109]. MIA PaCa-2 (Figure 2.5A) and S2-VP10 cells (Supplementary Figure 2.4A) were treated with NS siRNA, NS + gemcitabine, siSP1, or siSP1 + gemcitabine for 24-48 hours. We observed similar chemo-sensitivity as with siGRP78 when comparing cell viability with silencing SP1. In addition to cell viability, apoptosis of cells untreated vs. treated was detected using immunofluorescence by probing with a cleaved caspase 3 antibody. Again, we observed similar results as with silencing GRP78, and found that combining siSP1 with drugs resulted in more cell death. (Figure 2.5B, Supplementary Figure 2.4B-C).

Using a dye-efflux assay, we found that gemcitabine and paclitaxel alone both increased the % efflux of MIA PaCa-2 cells (26.9% and 3.0%, respectively). Conversely, non-silencing (0.90-1.85%) and siSP1 (0.13-1.18%) had minimal efflux activity. The combination of siSP1 and gemcitabine decreased the % efflux towards baseline (5.83%), whereas siSP1 and paclitaxel modestly decreased efflux (0.7%) (Figure 2.5C). We also determined the total ATP and ATPase per condition in MIA PaCa-2 cells. Gemcitabine alone increased the ATP (4.62) compared to NS (1.72) and siSP1 (2.92) (Figure 2.5D). Gemcitabine with siSP1 decreased the total ATP compared to gemcitabine alone (3.23). The amount of ATPase corresponds with the total cellular ATP, in that gemcitabine had an increase in the ATPase ($7.59e^{-4}$), indicating that more ATP is being utilized compared to NS (0) or siSP1 ($1.41e^{-4}$) (Figure 2.5E). Gemcitabine with siSP1 decreased the amount of ATPase compared to gemcitabine alone ($2.15e^{-4}$), indicating that less ATP is being utilized.

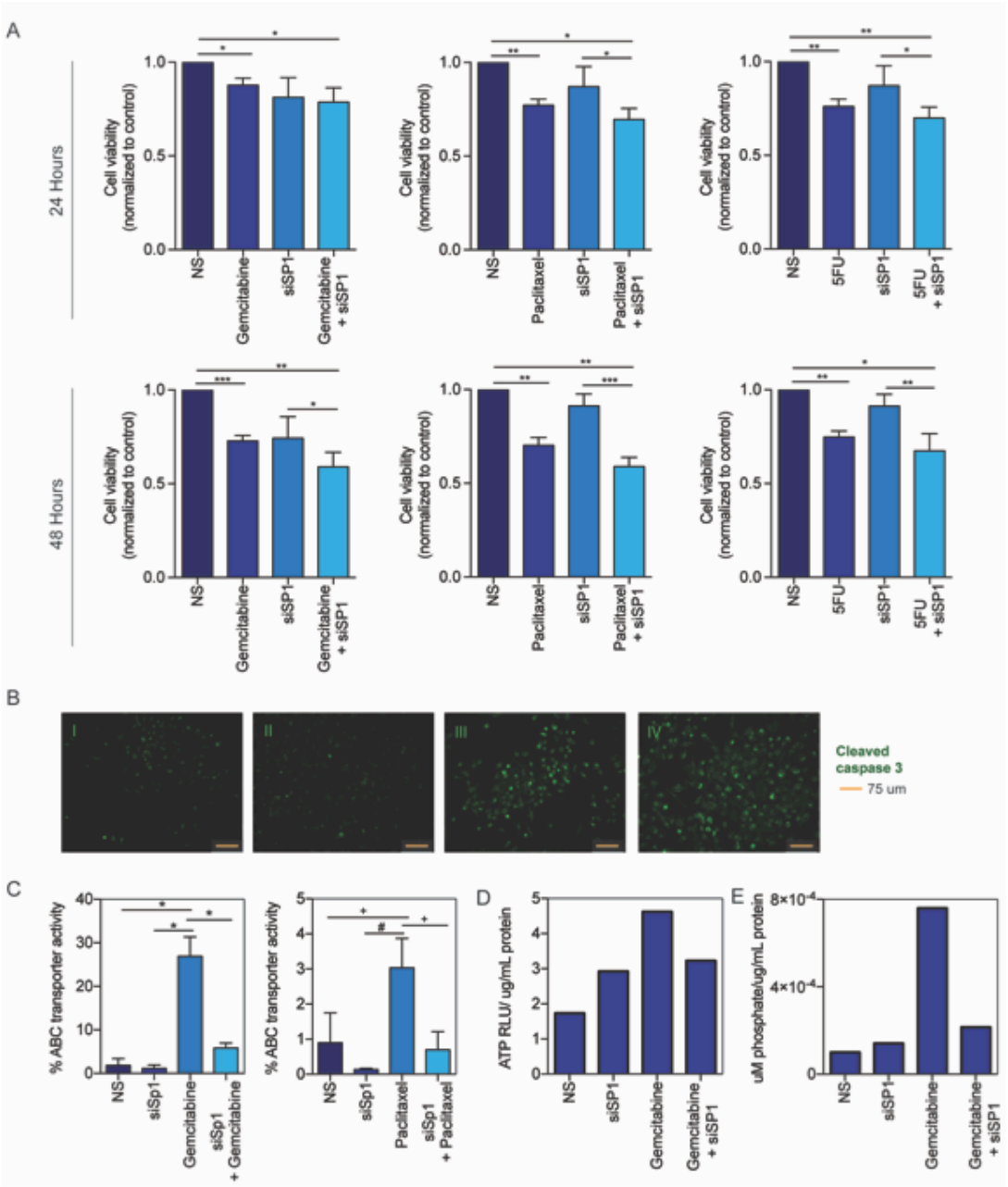

Figure 2.5: SP1 is required for ER homeostasis and affects chemoresistance in pancreatic cancer cells, similarly to GRP78

MIA PaCa-2 cells transfected with siSP1 and treated with 400 nM gemcitabine, 50 nM paclitaxel, or 5 μM 5-fluorouracil for 24 and 48 hours resulted in decreased viability compared to treatment or silencing alone (A). MIA PaCa-2 cells transfected with NS siRNA (B-I), 400 nM gemcitabine (B-II), siSP1 (B-III), or siSP1 + gemcitabine (B-IV) for 24 hours, and probed with a cleaved caspase 3 antibody for apoptosis. Images were acquired at 20x magnification. MIA PaCa-2 cells transfected with siSP1 and treated with 400 nM gemcitabine or 50 nM paclitaxel for 8 hours +/- verapamil, and analyzed by flow cytometry (C). ♦=0.07 •=0.08. MIA PaCa-2 cells transfected with siSP1 and treated with 400nM gemcitabine for 24 hours to measure total ATP(D) and ATPase(E).

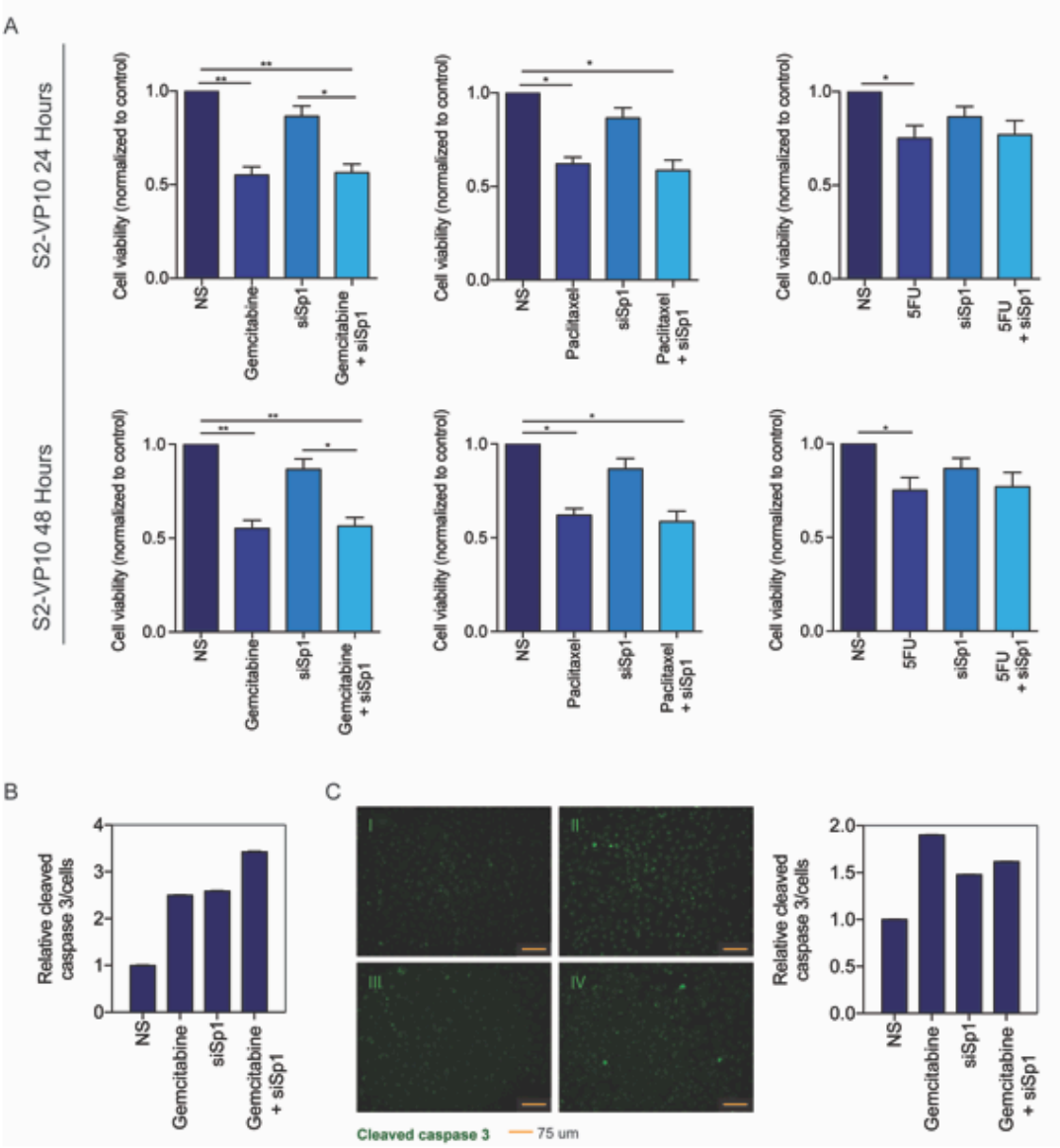

Supplementary Figure 2.4: SP1 is required for ER homeostasis and affects chemoresistance in pancreatic cancer cells, similarly to GRP78.
S2-VP10 cells transfected with siSP1 and treated with 100 nM gemcitabine, 50 nM paclitaxel, or 5 μM 5-fluorouracil for 24 and 48 hours resulted in decreased viability compared to treatment or silencing alone (A). (B) Quantitation of cleaved caspase 3 staining after MIA PaCa-2 cells were transfected with siSp1 and treated with 400 nM gemcitabine 24 hours. (C). S2-VP10 cells transfected with non-silencing siRNA (NS) (C-I), 100 nM gemcitabine (C-II), siSP1 (C-III), or siSP1 + gemcitabine (C-IV) for 24 hours, and stained with cleaved caspase 3 for apoptosis, and the respective quantitation.

Inhibition of SP1 *in vivo* sensitizes tumors to gemcitabine therapy

In vivo subcutaneous injection of MIA PaCa-2 cells into athymic nude mice were injected with either saline, 0.3 mg/kg mithramycin (MTH; SP1 inhibitor), 0.6 mg/kg MTH, 50 mg/kg gemcitabine (GEM), 0.3 mg/kg MTH and GEM, or 0.6 mg/kg MTH and GEM. Both combinations of MTH and GEM resulted in less tumor volume (0.3 MTH/GEM 304.0 mm^3; 0.6 MTH/GEM 307.9 mm^3) than 0.3 mg/kg MTH (365.1 mm^3), 0.6 mg/kg MTH (316.3 mm^3), or GEM (407.2 mm^3) (Figure 2.6A). Further, cleaved caspase 3 was increased in both 0.3 MTH/GEM (7.10) and 0.6 MTH/GEM (8.54) groups compared to single treatments (0.3 MTH 6.56; 0.6 MTH 5.91; GEM 5.24) and control (4.31) (Figure 2.6B).

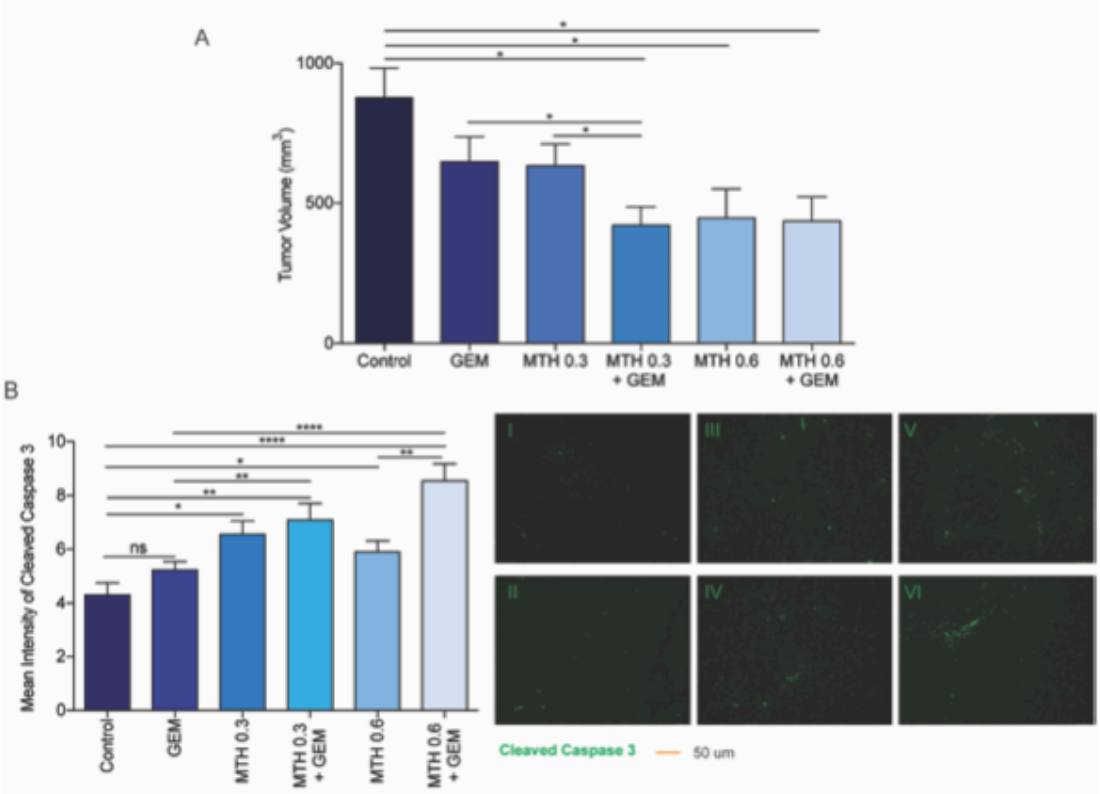

Figure 2.6 Inhibition of SP1 *in vivo* overcomes gemcitabine-induced chemoresistance.
MIA PaCa-2 cells injected subcutaneously into athymic nude mice, and treated with gemcitabine (50 mg/kg twice weekly), mithramycin (0.3 mg/kg or 0.6 mg/kg thrice weekly), or a combination of 0.3 mithramycin and gemcitabine, or 0.6 mithramycin and gemcitabine. Tumor volume measured at the endpoint (A). Tumors were probed with a cleaved caspase 3 antibody and quantified with Image J. Images were acquired at 20x magnification (B).

Supplementary Figure 2.5 provides histological evidence that mithramycin sufficiently downregulates (A) SP1 and (B) GRP78.

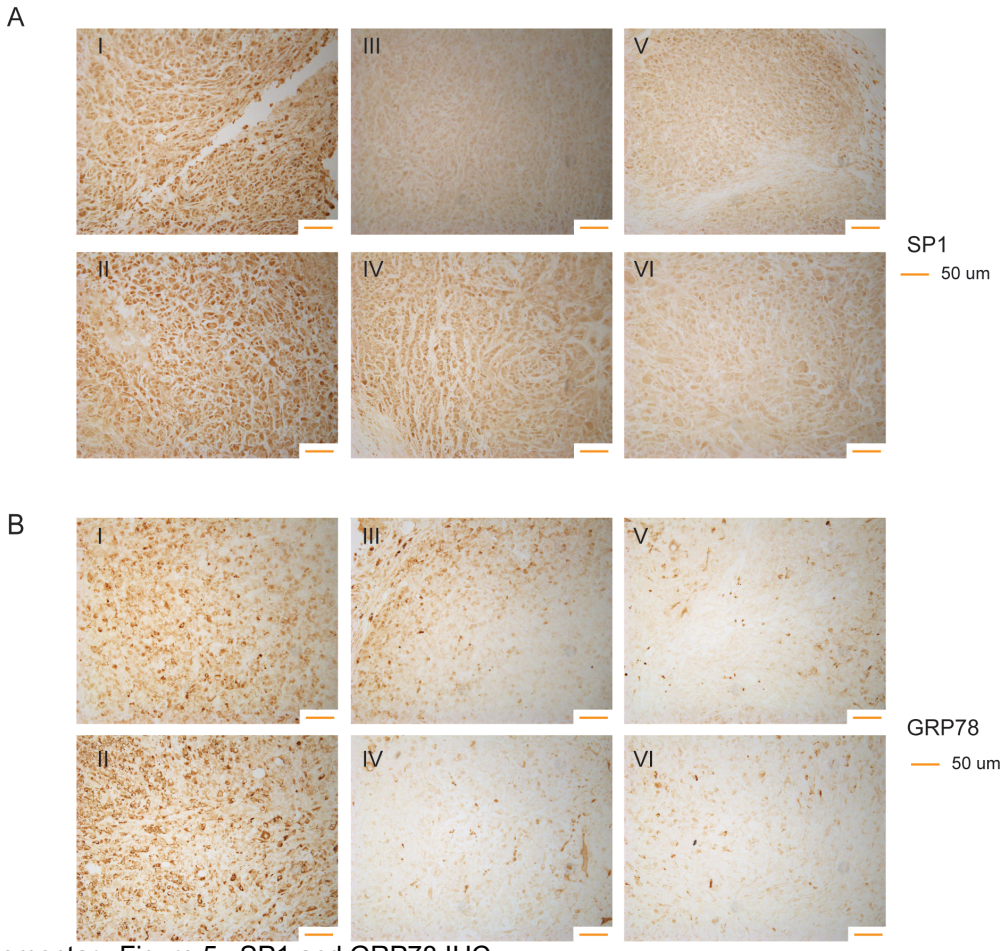

Supplementary Figure 5: SP1 and GRP78 IHC
MIA PaCa-2 subcutaneous tumors were stained for (A) SP1 and (B) GRP78. Each group compares Control (I); Gemcitabine 50 mg/kg (II); Mithramycin 0.3 mg/kg (III); Mithramycin 0.3 mg/kg + Gemcitabine (IV); Mithramycin 0.6 mg/kg (V); and Mithramycin 0.6 mg/kg + Gemcitabine (VI). Images were acquired at 20x magnification.

DISCUSSION

Various stressful conditions such as hypoxia, nutrient deprivation, pH changes or poor vascularization can be growth limiting for tumor cells, and thus activate the UPR[4, 72, 73]. As the cancer cells undergo rapid proliferation, the need for increased protein and other bimolecular synthesis contributes to an increased ER stress response in cancer cells[4, 72]. The ER is the main site for the translation of excess nutrition into metabolic and inflammatory responses. In tumor cells, ER stress may restore homeostasis and make the adjacent environment hospitable for tumor survival and tumor expansion, thus, is considered cytoprotective[73, 110, 111]. This makes the ER stress response one of the key survival responses in cancer.

Chemoresistance in cancer has been shown to occur via a number of mechanisms. Some studies suggest that GRP78 membrane localization contributes to pro-proliferative pathways[74, 75]. While GRP78 membrane localization is a novel and interesting concept in cancer biology, our study finds that chemoresistance in pancreatic cancer cells can be mediated by an overexpression and increased activity of ABC transporter genes. Our data show that the expression of a number of genes in this superfamily correlates with the expression of GRP78 (Table 2.2). The ABC transporters typically efflux the chemotherapeutic drugs from the cells thereby minimizing their accumulation in the cells. These pumps are regulated by the ATP in the cells and are transcriptionally regulated by the transcription factor, NRF2, which binds to antioxidant response element in the promoter gene of these genes leading to their upregulation. Normal substrates for the ABC transporters include glutathione and glucuronide conjugates, which can be mediated through NRF2-ARE activity[106, 107], which suggests that NRF2 and ABC transporters can alternatively work in tandem to promote chemoresistance. Further, Kras mutations have been shown to increase transcription and basal levels of NRF2 in cancer, which minimize intracellular ROS accumulation and maintain cancer cell survival[99].

ABC transporters have been an attractive target for many years, because of their role in chemoresistance[112]. A suggested strategy for battling chemoresistance is to decrease the efflux of the ABC transporters[107]. Verapamil is a first generation multidrug resistant

(MDR) modulator, whereas tariquidar and zosuquidar are third generation modulators, which have demonstrated fewer pharmacokinetic interactions with anti-neoplastics[107, 113]. Downregulation of GRP78 results in sensitizing the pancreatic cancer cells to multiple chemotherapeutic agents currently used in pancreatic cancer (Figure 2.2). Our results indicated that this was due to a decrease in the activity of the ABC transporters in these cells. Since ABC transporters depend on ATP hydrolysis, we estimated the ATPase activity in pancreatic cancer cells following GRP78 inhibition and drug treatment. GRP78 has ATP binding sites to help in protein folding. We demonstrate that siGRP78 modestly increases the total cellular levels of ATP and ATPase, which could indicate this reduction is partly due to less GRP78 utilization of ATP. Additionally, we have shown that siGRP78 decreases cellular viability, which is also an ATP-driven mechanism. Interestingly, our data also showed that gemcitabine with siGRP78 decreased the amount of ATPase compared to gemcitabine alone, which could indicate that less ATP is being utilized by the cell to drive ABC transporters. (Figure 2.3D). Similarly, inhibition of SP1 also showed increased sensitivity to gemcitabine by deregulation of ABC transporters (Figure 2.5C) and these effects could be observed both *in vitro* (Figure 2.5) and *in vivo* (Figure 2.6).

CONCLUSION

There have been many efforts to target the UPR in recent years, including proteasome inhibitors, and inhibitors targeting GRP78, HSP90, PERK, and IRE1alpha[32]. GRP78, one of the regulators of the UPR, is an attractive target because it is responsible for maintaining homeostasis in the ER. Recently, a small molecule GRP78 inhibitor called IT-139, was shown to sensitize chemoresistant PDAC cells to gemcitabine[79]. Our previously published data shows that GRP78-mediated ER homeostasis is dependent on SP1 activity and inhibition of SP1 prevents the homeostasis and pushes the UPR to a chronic ER stress phase, leading to cancer cell death[109]. Our study is clinically relevant, because mithramycin (SP1 inhibitor) is undergoing clinical trials for lung, esophagus, breast, and GI cancers. Interestingly, SP1 and NRF2 have been recently described as non-oncogene addiction genes[114, 115]. Thus, understanding the interaction between multiple stress pathways (Unfolded Protein Response, Oxidative Stress) can contribute to development of better therapeutic targets to ameliorate the therapeutic resistance.

METHODS

Cell Culture and Treatment

MIA PaCa-2 (obtained from ATCC) was cultured in DMEM; high glucose, supplemented with 10% FBS and 100 units/mL penicillin and 100 µg/mL streptomycin. S2-VP10 (a gift from Dr. Masato Yamamoto's lab, University of Minnesota) and SU.86.86 (ATCC) were grown and propagated in RPMI, supplemented with 10% FBS, 100 units/mL penicillin and 100 µg/mL streptomycin. All cells were maintained at 37°C in a humidified air atmosphere with 5% CO_2.

ON-TARGETplus SMARTpool (pool of 4 siRNA) human SP1 (Dharmacon, Cat # L-026959-00-0020) and GRP78 siRNA (Dharmacon, Cat # L-008198-00-0020) were used for silencing experiments. Transfections were completed using DharmaFECT (Dharmacon) according to manufacturer's instructions. Evidence of silencing GRP78 and SP1 are provided in Supplementary Figure 6.

Human HSPA5 siRNA (SMARTpool) Target Sequences
GCGCAUUGAUACUAGAAA; GAACCAUCCCGUGGCAUAA;
GAAAGAAGGUUACCCAUGC; AGAUGAAGCUGUAGCGUAU

Human ON-TARGETplus Non-targeting siRNA #2 Target Sequence
UGGUUUACAUGUUGUGUGA

Human SP1 siRNA (SMARTpool) Target Sequences
GCCAAUAGCUACUCAACUA; GAAGGGAGGCCCAGGUGUA;
GGGCAGACCUUUACAACUC; CUACAGAGGCACAAACGUA

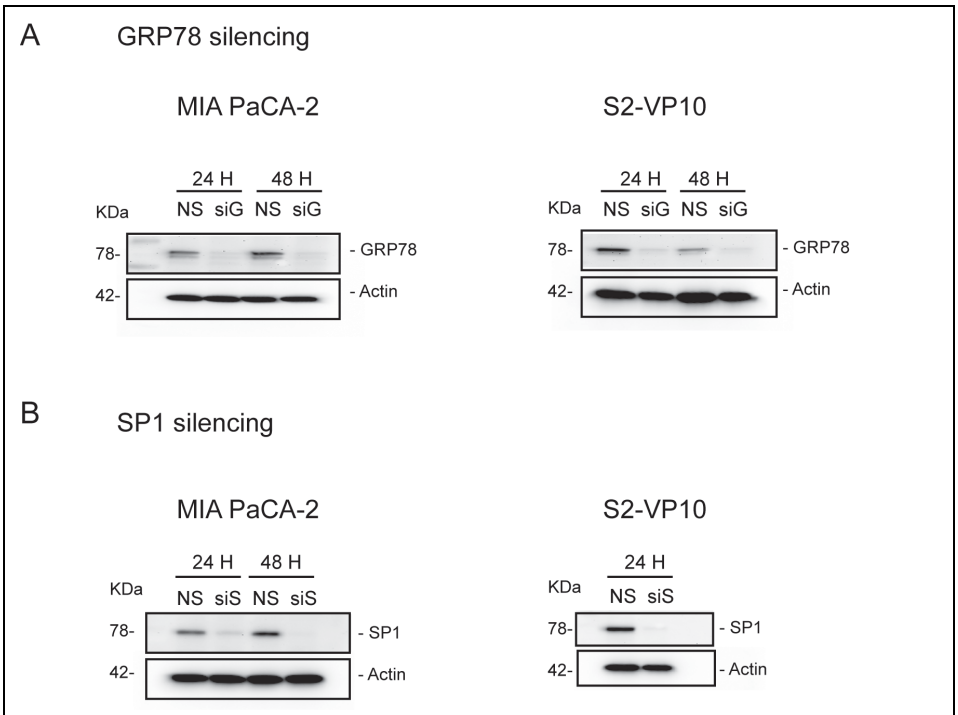

Supplementary Figure 2.6: Evidence of silencing
Protein from MIA PaCa-2 and S2-VP10 cells was used to verify silencing *in vitro* for (A) GRP78 and (B) SP1.

KPC Tumor Analyses

LSL-Kras^{G12D}; *LSL-Trp53*^{R172H}; *Pdx-1-Cre* (KPC) mice of various ages (1-9 months) were euthanized and pancreata were analyzed for mRNA and protein expression of GRP78, NRF2, and ABC transporters. Mice were sorted according to age and tumor status into non-tumor and full tumor groups; i.e. the 3 month KPC mice with tumors were placed in the tumor group (ranging from 3-9 months).

Gene Expression Analyses

RT-PCR: RNA was isolated from the cells according to manufacturer's instructions using Trizol (Invitrogen). Total RNA (2 μg) was used to make cDNA and perform real-time PCR using the Quantitect SyBr green PCR kit (Qiagen) according to the manufacturer's instructions using Roche 480 real-time PCR system. All data were normalized to the housekeeping gene 18S (Qiagen, Cat # QT00199367). Quantitative RT-PCR primers for SP1 (Qiagen, Cat # QT01870449), HSPA5 (GRP78) (Qiagen, Cat #

QT 00096404).

ELISA

KPC or human serum was used to analyze the GRP78 serum levels, using the Enzo ELISA kit, per manufacturer's instructions. GRP78 antibody is immobilized in a pre-coated plate. 100 μL of serum was pipetted in each well of a 96 well plate in duplicates, and allowed to bind overnight at 4°C. The following morning, the serum was removed and fresh GRP78 standards were prepared and pipetted in duplicates. 100 μL of biotin-conjugated GRP78 antibody was added to each well, followed by 100 μL HRP-avidin secondary. Color formation was achieved using a TMB substrate for 30 minutes, and was detected at 450 nm using a microplate reader.

Immunofluorescence

Paraffin-embedded KPC mouse tissues were deparaffinized in xylene and then rehydrated in graded ethanol. After citrate antigen retrieval, tissues were blocked with Dako protein block, and incubated with primary (GRP78, Abcam ab21685) at 1:1000 dilution. Slides were washed with PBS and incubated with Alexa Fluor 488 anti-rabbit secondary antibody for 1 hour. Slides were washed with PBS, and mounted with prolong gold with DAPI (Invitrogen).

MIA PaCa-2 and S2-VP10 cells were plated in chamber slides and incubated for 1-24 hours at 37°C. The slides were treated with 400 nM (MIA PaCa-2) or 100 nM (S2-VP10) gemcitabine; fixed with 2% paraformaldehyde. The slides were incubated with 1:1000 dilution of rabbit polyclonal anti-cleaved caspase 3 antibody (Cell Signaling) and a 1:1000 dilution of Alexa 488-conjugated donkey anti-rabbit IgG (Molecular Probes). The slides were mounted using Prolong Gold anti-fade with 4',6-diamidino-2-phenylindole (Molecular Probes). Immunofluorescence images were obtained on a Leica DM6B with a 20x objective. Cleaved caspase was quantified using Image J software.

Immunohistochemistry

Paraffin-embedded KPC mouse tissues were deparaffinized in xylene and then rehydrated in graded ethanol. Slides were steamed with pH 9 antigen retrieval (Dako).

Endogenous peroxidases were blocked with a 3% hydrogen peroxide solution. Tissues were then blocked with Dako protein block, and incubated with primary antibody overnight. Slides were stained with anti-SP1 (Cell Signaling, Cat # 9389) and anti-GRP78 (Cell Signaling, Cat # 3177) at 1:200 dilutions. Slides were washed with PBS, incubated with secondary anti-rabbit antibody, conjugated to horseradish peroxidase, for 30 minutes. Slides were washed again with PBS. Diaminobenzidine Peroxidase Substrate Kit (Vector Laboratories) was then added to slides. Primary antibody was omitted for negative controls. Slides were mounted with permount. Images were obtained on a Leica DM6B with a 20x objective.

Cell Viability Assay

MIA PaCa-2, S2-VP10 and SU.86.86 cells were seeded in a 96 well plate (7,000 cells/well) and allowed to adhere for 24 hours. Cells were transfected with 20 nM non-silencing siRNA (NS), siGRP78, or siSP1. Drug treatments used 400 nM (MIA PaCa-2) or 100 nM (S2-VP10) gemcitabine, 50 nM paclitaxel, or 5 μM 5-FU, unless otherwise specified. Cell viability assays following siRNA or pharmacological inhibitors were performed using a WST-8 based cell cytotoxicity assay per the manufacturer's protocol (Dojindo) and expressed after normalizing to untreated cells.

Dye Efflux Assay

MIA PaCa-2 cells were plated in a 6 well plate. NS, siGRP78, and siSP1 were transfected in two wells each, and allowed to incubate for 15 hours. Cells were then treated with 400 nM gemcitabine or 50 nM paclitaxel for 8 hours. Cells were then gently scraped and were transferred equally into two flow cytometry tubes. In one set, NucBlue live dye was added, and incubated on ice. In the second set of tubes, NucBlue live dye was added, along with 100 μM verapamil, and incubated at 37°C for 30 minutes, and subsequently moved to ice. Flow cytometry was performed using the Pacific Blue and AmCyan. The percent of inhibition was calculated by: (+Verapamil) – (-Verapamil).

ATP Measurement

MIA PaCa-2 and S2-VP10 cells were seeded in a 6 well plate. NS, siGRP78, and siSP1

were transfected in two wells each, and allowed to incubate for 15 hours. Cells were then treated with 400 nM (MIA PaCa-2) or 100 nM (S2-VP10) gemcitabine for 24 hours. Total cellular ATP was measured using the ENLITEN ATP assay system (Promega). Briefly, 1 μL trichloroacetic acid was added to 100 μL cell lysate to extract the ATP. Each sample was then neutralized with 900uL TAE (pH 8.0). A standard curve ranging from 10^{-7} M to 10^{-11} M was prepared using the provided 10^{-7} M ATP standard. Luminescence was recorded for each sample and standard.

ATPase Activity Assay

MIA PaCa-2 and S2-VP10 cells were seeded in a 6 well plate. NS, siGRP78, and siSP1 were transfected in two wells each, and allowed to incubate for 15 hours. Cells were then treated with 400 nM (MIA PaCa-2) or 100 nM (S2-VP10) gemcitabine for 24 hours. Cells were lysed in lysis buffer and analyzed for ATPase per manufacturer's instructions (Sigma). After assay incubation, plate was read at 620 nm for standards, blanks, and unknowns on a spectrophotometer.

ARE Reporter Assay

MIA PaCa-2 and S2-VP10 cells were seeded in a 24 well plate. NS, siGRP78, and siSP1 were transfected in two wells each, and allowed to incubate for 15 hours. Cells were then transfected with the Cignal reporter plasmids for ARE (Qiagen) and treated with 400 nM (MIA PaCa-2) or 100 nM (S2-VP10) gemcitabine for 24 hours. Wells were washed with PBS, and 100 μL of passive lysis buffer was added per well. After 15 minutes of rocking in passive lysis buffer, plates were stored at -80°C until ready to read. The dual luciferase kit (Promega) was used to measure activity using a luminometer. Each sample was treated in duplicate for each plasmid (duplicates for the negative reporter and duplicates for the ARE reporter).

Reactive Oxygen Species Assay

MIA PaCa-2 and S2-VP10 cells were seeded in black, clear bottom 96 well plates. NS, siGRP78, and siSP1 were transfected in two wells each, and allowed to incubate for 15 hours. Cells were then treated with 400 nM (MIA PaCa-2) or 100 nM (S2-VP10) gemcitabine, 50 nM paclitaxel, and 5 uM 5-FU for 24 hours. Media was removed and

replaced with 5 uM H2DCFDA/phenol-free media for 1 hour at 37°C. Cells were washed with PBS, and phenol-free media was replaced. ROS was measured at 5 minute intervals for 1 hour, with 492/517 ex/em filters. Results were expressed as ROS fluorescence per viability using a WST-8 cell cytotoxicity assay (Dojindo).

In vivo Study

8-week-old athymic nude mice were injected subcutaneously (right flank) with 10^6 MIA PaCa-2 cells suspended in Matrigel (Corning). Mice were randomized when the average tumor size reached 135 mm^3. Mice were randomized into the following groups: 1. saline; 2. mithramycin 0.3 mg/kg; 3. mithramycin 0.6 mg/kg; 4. gemcitabine 50 mg/kg; 5. mithramycin 0.3 mg/kg + gemcitabine 50 mg/kg; and 6. mithramycin 0.6 mg/kg + gemcitabine 50 mg/kg. Saline and all mithramycin groups had 7 mice each; gemcitabine had 5 mice. Mithramycin was administered intraperitoneally three times per week. Gemcitabine was administered intraperitoneally 2 times per week. Tumors were measured weekly with a digital caliper. Mice were euthanized when tumors reached 900 mm^3. The University of Minnesota Institutional Animal Care and Use Committee (IACUC) approved all procedures.

Statistical Analysis

Values are expressed as the mean +/- SEM. All *in vitro* experiments were performed at least three times. The significance between any two samples was analyzed by t-test, values of $p<0.05$ were considered statistically significant.

CHAPTER 3: ER stress sensor, glucose regulatory protein 78 (GRP78) is responsible for maintenance of "stemness" by regulating redox balance and DNA damage in pancreatic cancer

Unpublished data

Data and analysis performed by Patricia Dauer

SUMMARY

Background: Endoplasmic reticulum (ER) stress and the unfolded protein response (UPR) signaling have been shown to be dysregulated in multiple cancer types. Glucose regulatory protein 78 (GRP78), the master regulator of the UPR is thought to play a role in proliferation, invasion, and metastasis in cancer. Cancer stem cells (CSCs) make up a crucial component of the tumor heterogeneity in pancreatic cancer, as well as other cancers. Even though UPR and CSCs have a role in multiple overlapping functions in tumors, there have been few studies connecting the concepts of CSCs and UPR. In the current study, we aimed to define what role GRP78 plays in the aggressive biology of pancreatic cancer.

Methods: Transcriptomic and proteomic analyses were conducted to compare S2-VP10 control cells versus S2-VP10 shGRP78 cells. Cancer stem cell mRNA expression and key assays [colony formation, reactive oxygen species (ROS), invasion] were performed.

Results: We found that shGRP78 dysregulates multiple transcriptomic and proteomic pathways important in cancer. GRP78 downregulation decreases stemness and self-renewal properties *in vitro. In vivo* studies resulted in delayed tumor initiation, as well as less tumor growth in the shGRP78 groups. Further, Downregulation of GRP78 results in fatty acid metabolism dysregulation.

Conclusion: Our studies show that downregulation of GRP78 disrupts multiple pathways that are key in proliferation, survival, fatty acid metabolism, and cell organization and biogenesis. Further, this study shows for the first time a connection to cancer stem cells, which are attributed to aggressive properties like chemoresistance and metastasis.

INTRODUCTION

Pancreatic cancer was a devastating disease 50 years ago, and it remains a devastating disease today. In 2018, it is estimated that 55,440 people will be diagnosed with pancreatic cancer, and 44,330 people will die from the disease in the United States[1]. Compared with the 20 most prevalent cancers in the United States, pancreatic cancer is the only type that has a five-year survival rate of less than 10% for all stages[1]. The only treatment option, which has shown to have curative potential, is surgical resection. However, less than 20% of patients are eligible for surgery upon diagnosis[1]. For those patients that surgery is an option, a number will have tumor recurrence within 5 years. The five-year survival rate after surgical resection can range up to 29%[116-123]. Suffice it to say, there is a need to understand the basic biology of pancreatic cancer further, in order to understand how to treat advanced stage patients better.

One mechanism, which has been shown to be useful in oncogenic reprogramming, is the unfolded protein response (UPR). Endoplasmic reticulum (ER) stress and UPR signaling have been shown to be dysregulated in cancer[33, 73, 124]. ER stress is caused by a variety of physiological or xenobiotic pressures on the cell, like glucose deprivation, hypoxia, or chemotherapeutics. This in turn can disrupt the protein folding homeostasis in the ER, which activates an adaptive response, namely the UPR, which consists of three branches of unique downstream signaling to help recover from cellular stress. When inactivated, the three UPR branches are kept silent by close association with glucose regulatory protein 78 (GRP78), a mostly ER associated chaperone protein.

The ER is also a major site for the synthesis of sterols and phospholipids, which are important membrane components. Maintenance of lipid homeostasis is important for normal cells, as well as cancer cells[30, 125-127]. It has been demonstrated that inhibition of GRP78 in breast cancer dysregulates lipid metabolism: reducing fatty acid oxidation and resulting in an increase in cellular fatty acids[128].

This seemingly innocuous homeostatic mechanism can be hijacked by cancer cells to aid in tumor growth, migration, transformation, and angiogenesis[33, 73]. GRP78, the master regulator of the UPR, has been reported to be upregulated in multiple cancers[74,

[78, 124, 129]. In pancreatic cancer, it was recently reported that GRP78 is also overexpressed [78]. GRP78 is thought to play a role in proliferation, invasion, and metastasis in cancer[74, 78]. Additionally, there are a few studies showing that GRP78, and ER-resident protein, can translocate and be secreted[74]. In head and neck cancer, GRP78 is overexpressed, and it was reported that knocking down GRP78 decreased tumor initiation[129].

In vitro studies show that knocking down GRP78 in immortalized endothelial cells decreases proliferation, survival, and migration[74]. GRP78-/- mouse models are embryonic lethal[40, 127]. Heterozygous GRP78 mouse models are viable, but display an increase in ER stress proteins[40, 41, 130]. Studies have also shown that knocking down GRP78 decreases invasion and metastatic growth *in vivo*[74]. Another study using an inducible knockdown of GRP78 (*Grp78*$^{f/f}$; *Mx1-Cre)* results in decreased hematopoietic stem cells, decreased lymphoid progenitors decrease viability, increased UPR and cell death[130]. These studies suggest that GRP78 may play an important role in the survival of normal stem cells, but its role in cancer stem cells (CSCs) is unclear.

CSCs have been identified to play a major role in tumor recurrence because of their ability to promote tumor initiation, growth, metastasis, and chemoresistance[124, 131-135]. CSCs make up a crucial component of the tumor heterogeneity in pancreatic cancer, as well as other cancers. Even though UPR and CSCs have a role in multiple overlapping functions in tumors, there have been few studies connecting the concepts of CSCs and UPR. As the master regulator of the UPR, GRP78, few recent studies have suggested a role of GRP78 in maintaining the survival of CSCs[136, 137]. Additionally, Li *et al.* recently published that downregulation of inositol-requiring enzyme 1 alpha (IRE1α), one of three transmembrane sensors, resulted in a decrease of colon cancer stem cells[138].

In the current study, we aimed to define what role GRP78 plays in the biology of pancreatic cancer. We aimed to study this role, and determine if GRP78 is essential in maintaining the aggressive phenotype of pancreatic cancer by using a shGRP78 stable cell line.

RESULTS

GRP78 is an essential protein for maintaining the UPR, and has been shown to be important for cell survival[30]. This led us to inquire how GRP78 is important for cell survival, and why cancer stem cells seem to have more of it. For the following experiments, we created a stable shGRP78 clonal cell line with S2-VP10 cells.

GRP78 knockdown decreases "stemness" and self-renewal properties in pancreatic cancer

We first observed that the shGRP78 cells had a slower doubling cycle than the control cells. When we performed a proliferation assay by ECIS, we indeed found that the shGRP78 cells had a significant decrease in cell proliferation when compared to control cells (Figure 3.1A).

Previous data published by Nomura, *et al* suggests that ER stress is important for cancer stem cells, because when sorted, CD133+ cells had more GRP78 and other heat shock protein (HSP)-family mRNA expression compared to CD133- cells[13]. In the current study, we found that shGRP78 cells had decreased CD133 mRNA expression in addition to significantly downregulated self-renewal genes (Figure 3.1B).

Using an *in vitro* surrogate assay for stemness, we next performed a limiting-dilution colony formation assay. Control and shGRP78 cells were both plated in multiple dilutions ranging from 100,000 cells - 1 cell in a methylcellulose-based medium. After 6 days, the number of colonies in the 100,000 control cells was too many to count accurately, and was subsequently excluded. The number of colonies formed in each of the remaining groups was counted. shGRP78 cells had significantly fewer colonies formed than the control cells using both 10,000 and 1,000 cells (Figure 3.1C). No colonies were detected with 100, 10, or 1 cell.

Nomura *et al.* has shown that CD133+ cells significantly induce invasion *in vitro*[132]. We showed that shGRP78 cells resulted in less CD133 expression (Figure 3.1B). To further demonstrate that GRP78 may play a role in maintaining the CSC and self-renewal phenotype in pancreatic cancer, we next looked at invasion. We used a Boyden

chamber assay with control or shGRP78 cells, to determine the number of invaded cells in 24 hours. We found that shGRP78 cells had a significant reduction in the number of invaded cells compared to the control cells (Figure 3.1D).

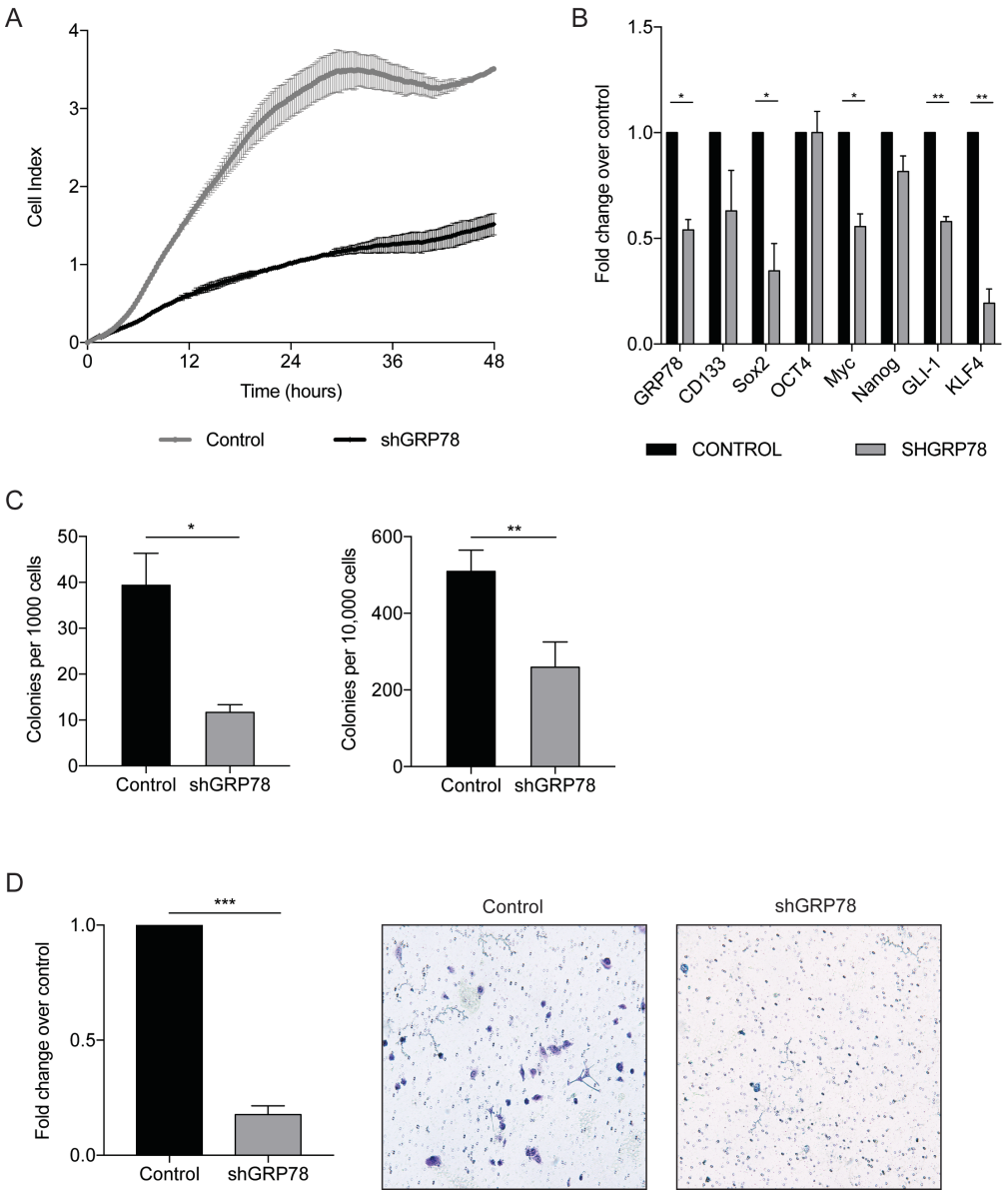

Figure 3.1: shGRP78 have decreased "stemness" and self-renewal phenotype
Control and shGRP78 cells were analyzed for cell proliferation (A) and stemness and self-renewal properties. (B) mRNA expression of CD133 and self-renewal genes (B) colony formation assay (C) cell invasion. Invasion images were taken with a 4x objective and counted with Image J software.

Tumor initiation and size are significantly reduced in GRP78 knockdown mice

GRP78 knockdown has been reported to decrease tumor initiation in head and neck cancer[129]. Additionally, it has been shown to decrease proliferation and growth in other cancers[40, 73, 128]. To determine if GRP78 knockdown delays tumor initiation and growth, we injected 10,000 or 100,000 cells into athymic nude mice. We noted when each mouse formed a tumor, and tumor volume was measured weekly.

When we injected 10,000 cells, 5/5 control mice formed tumors within 16 days, whereas only 2/5 shGRP78 mice formed tumors (Figure 3.2A). Based on this data, the tumor initiation frequencies were calculated, and 1/6214 control cells has probability to initiate a tumor, whereas only 1/45217 shGRP78 cells had the probability of initiating a tumor In the group that we injected 100,000 cells, we found that 5/5 control mice formed tumors within 11 days, and 4/5 shGRP78 mice formed tumors (Supplementary Figure 3.1A). In addition to delayed tumor initiation, shGRP78 mice (both groups) had significantly smaller tumor volumes (Figure 3.2B, Supplementary Figure 3.1B) and significantly less tumor weight in the shGRP78-10,000 cell group (Figure 3.2C) compared to control mice after 4 weeks post-implantation. Even though the Control-100,000 cells group had significantly greater tumor volumes than the corresponding shGRP78 group, many of the S2-VP10 tumors result in ascites and/or ulceration, thereby reducing the overall tumor weight upon necropsy (Supplementary Figure 3.1C).

Examination of the H&E from the control and shGRP78 mice resulted in an unanticipated result of a pronounced accumulation of lipids in and around the tissues of the shGRP78 mice (Figure 3.2D). The tissues were stained with GRP78, in order to verify that there is indeed a reduction of GRP78 *in vivo* (Figure 3.2E). We also observed more apoptotic cells in the shGRP78 mice, when stained with TUNEL (Figure 3.2F).

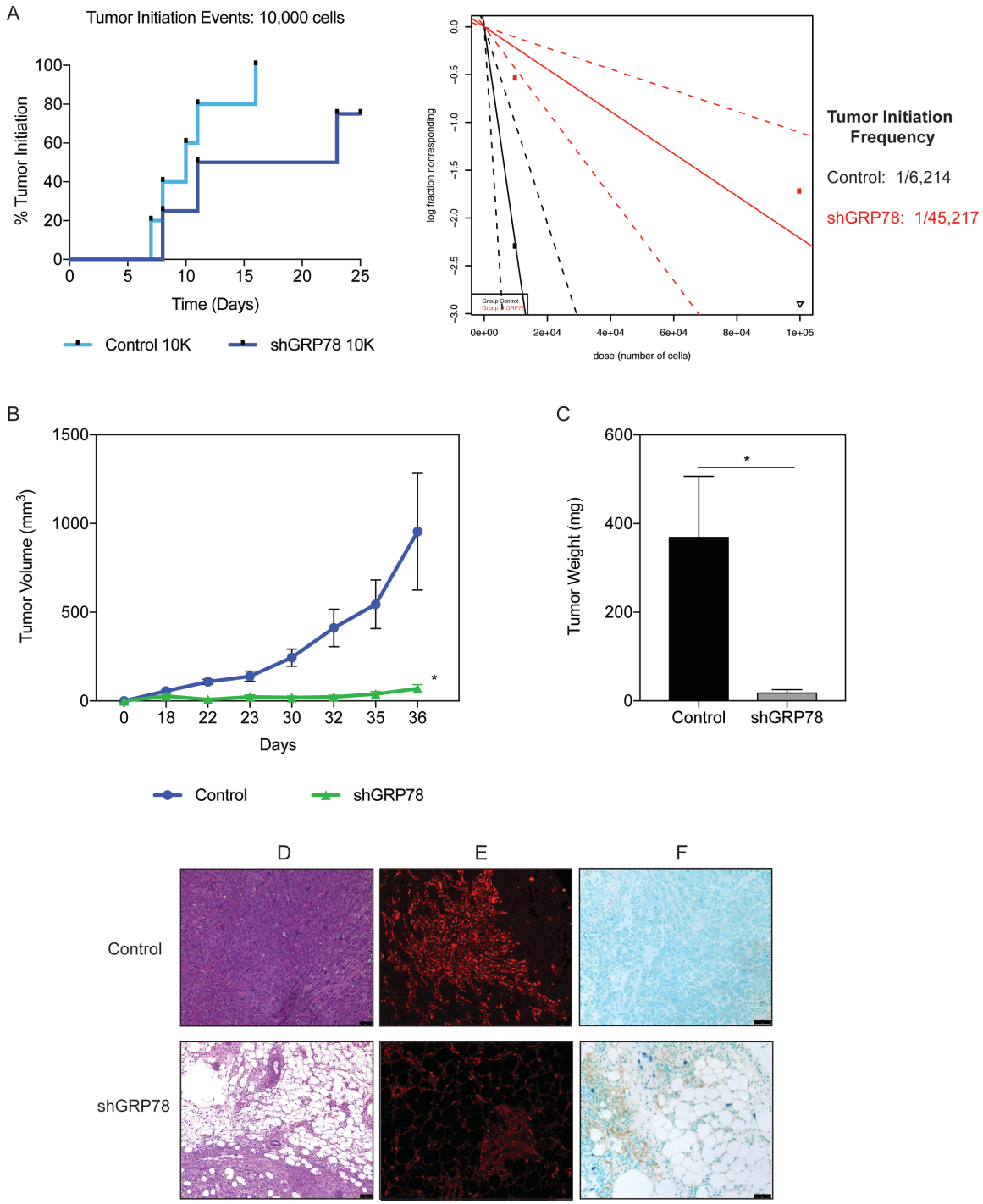

Figure 3.2: GRP78 knockdown results in delayed tumor initiation and smaller tumors
Athymic nude mice were injected with 10,000 cells. (A) Tumor initiation was monitored daily for 25 days. Tumor initiation frequency was determined based on total at 25 days. (B) Tumor volume was measured weekly for 36 days. (C) Tumor weights were noted at endpoint. (D) H&E of control and shGRP78 tumors. Control and shGRP78 tissues stained with (E) GRP78 and (F) TUNEL. Images were acquired with a 20x objective.

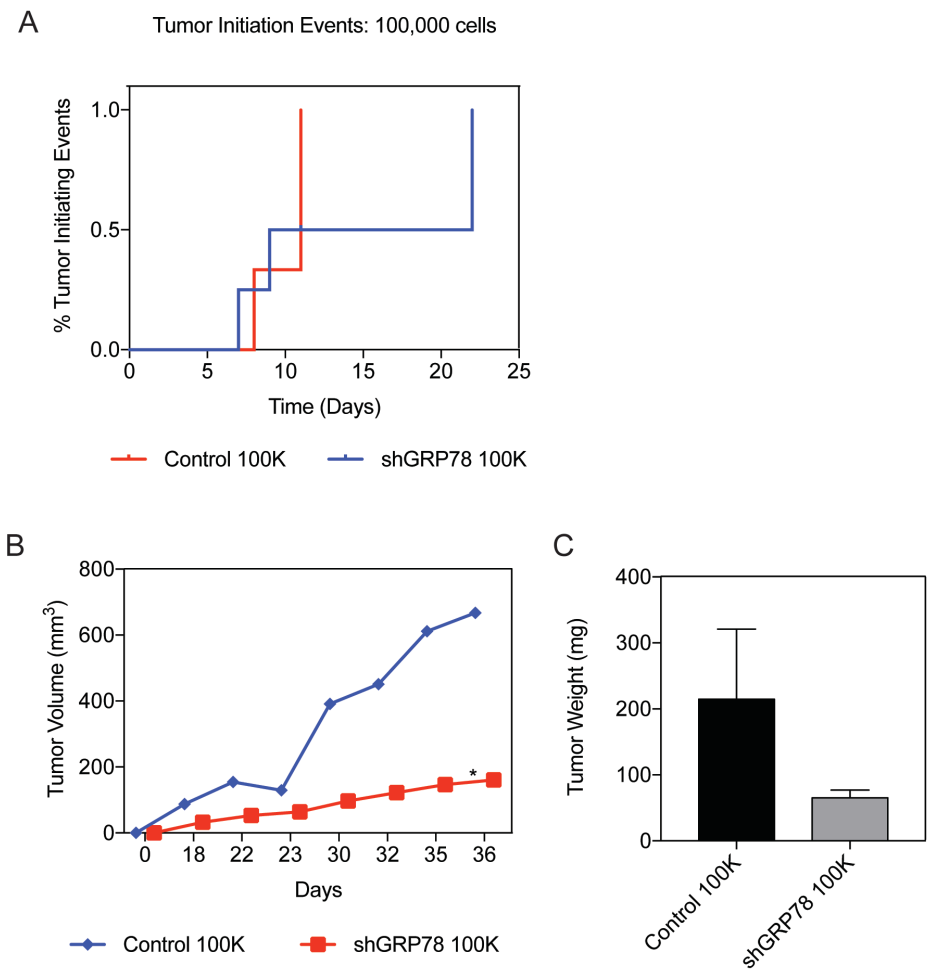

Supplementary Figure 3.2: GRP78 knockdown results in delayed tumor initiation and smaller tumors

Athymic nude mice were injected with 100,000 cells. (A) Tumor initiation was monitored daily for 25 days. (B) Tumor volume was measured weekly for 36 days. (C) Tumor weights were noted at endpoint.

Downregulation of GRP78 leads to deregulated lipid metabolism

Due to the unexpected finding of lipids in the H&E stained tissues, we decided to check the fatty acid metabolism in shGRP78 cells compared to controls. When GRP78 was inhibited in breast cancer, Cook *et al.* also found a change in lipid metabolism[128]. In that study, GRP78 inhibition reduced fatty acid oxidation and increased cellular fatty acids[128]. These effects could be caused by alterations in fatty acid uptake, lipid biosynthesis, or beta-oxidation. In the current investigation, we found multiple downregulated genes using a human fatty acid metabolism qPCR array (Figure 3.3A). Genes downregulated

included acetyl-CoA transferase, acyl-CoA dehydrogenase, acyl-CoA thioesterase, and acyl-CoA synthetase; glycerol kinase and glycerol dehydrogenase; lipase; protein kinases; and the solute carriers (fatty acid transporters). These *in vitro* results were consistent with mRNA from our subcutaneous tumors using the same fatty acid metabolism qPCR array (Supplementary Figure 3.2).

Due to the fatty acid metabolism dysregulation, and based on the observations that shGRP78 results in slower proliferation, stemness, and invasion (Figure 3.1), we next supplemented cells with saturated (SFA) and unsaturated fatty acids (UFA), to see if shGRP78 cells would behave more like the control cells. It has been reported that SFAs induce ER stress, but UFAs can inhibit ER stress. We treated control and shGRP78 cells with palmitic acid (SFA), linoleic acid (UFA), or oleic acid (UFA) for 24 hours and determined cell viability, proliferation, and invasion ability. Supplementation of fatty acids did not significantly affect cell viability (data not shown), but increased proliferation and migration of shGRP78 cells (Figure 3.3B), and modestly increased the invasiveness of cells *in vitro,* determined using a Boyden chamber invasion assay (Figure 3.3C).

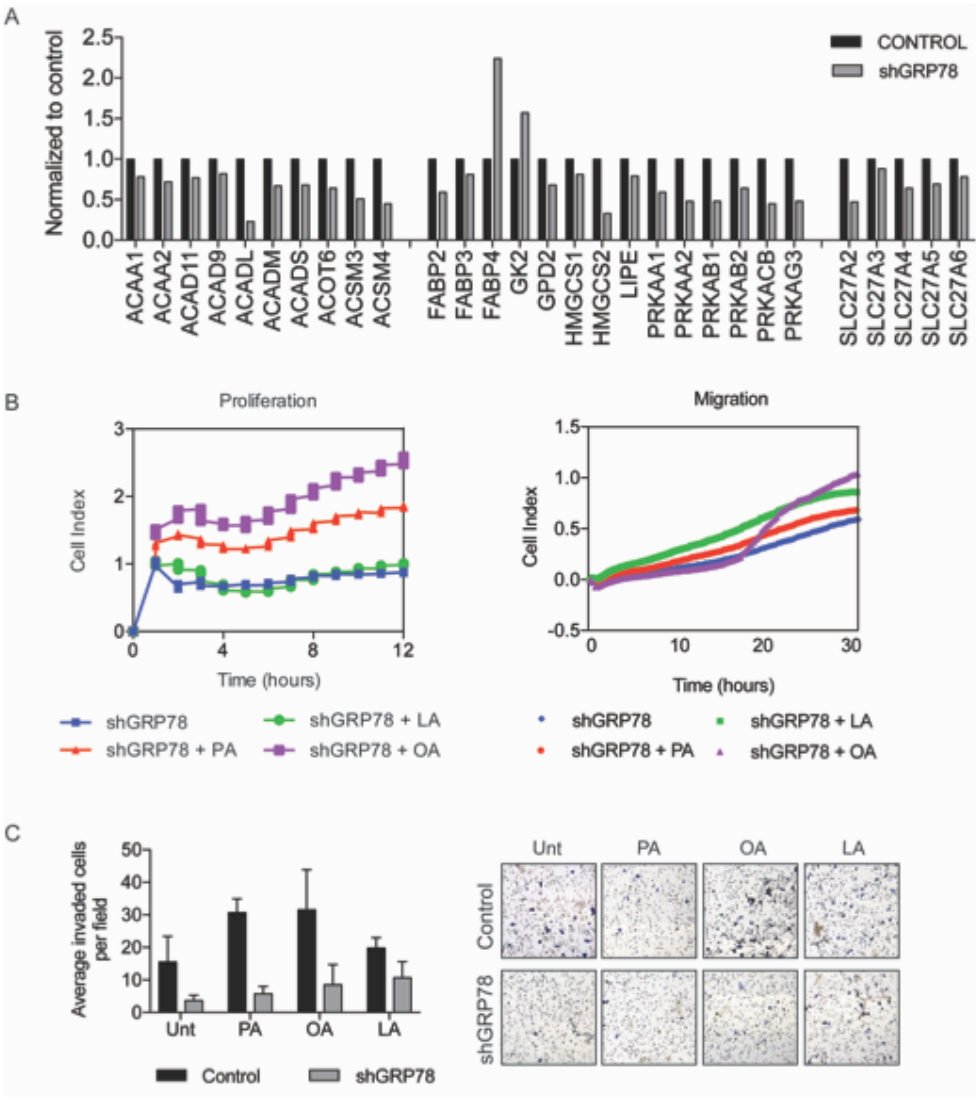

Figure 3.3: Downregulation of GRP78 results in deregulated fatty acid metabolism shGRP78 has dysregulated fatty acid metabolism genes *in vitro* (A). (B) The addition of fatty acids to shGRP78 cells slightly increased cell proliferation in 12 hours, and cell migration in 30 hours, (C) Fatty acid supplementation modestly increases cell invasion using a Boyden chamber assay. Invasion images were taken with 5x objective and counted using Image J software.

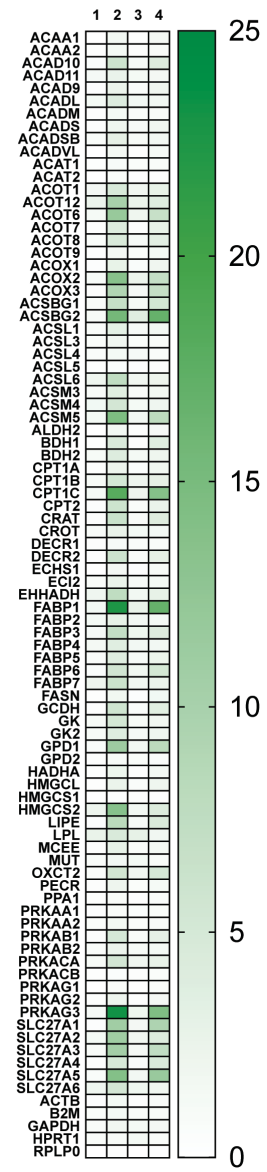

Supplementary Figure 3.2: Downregulation of GRP78 results in deregulated fatty acid metabolism shGRP78 has dysregulated fatty acid metabolism genes *in vivo*.

Transcriptomic and proteomic analyses show GRP78 plays an important role in DNA damage and repair

In order to elucidate the role that GRP78 and the UPR may play in CSCs and the aggressive phenotype of pancreatic cancer, we conducted a transcriptomic analysis of

our shGRP78 cells versus our controls. We found that many genes were significantly deregulated (Figure 3.4A). Supplementary Figure 3.3A lists the top 55 significantly deregulated canonical pathways. Among them are IL-1 signaling, which Nomura *et al* has reported in *Molecular Cancer Research* leads to epithelial to mesenchymal transition (EMT) and invasion in pancreatic cancer[139]. Drug resistance by drug efflux and xenobiotic metabolic signaling pathways were also deregulated, which supports the previous study in Chapter 2. Additionally, metabolic pathways including the pentose phosphate pathway were deregulated in the shGRP78 cells compared to controls. The top 25 dysregulated canonical pathways sorted by z-score are in Supplementary Figure 3.3B. Among them are NRF2-oxidative stress signaling and growth factor signaling pathways. Further, the top deregulated genes are organized according to function in Figure 3.4B. There were 2971 genes dysregulated in shGRP78 cells compared to control, which are represented as 100 circles (100%). The number of colored circles is directly proportionate to the number of genes for that cellular function, in respect to the total number of genes. For example, 63/2971 genes are related to DNA damage response, which is 2.1% of total deregulated genes.

Next, we conducted a qualitative mass spectrometry analysis of shGRP78 versus control cells. Though, we did not observe significant differences in the pathways dysregulated (data not shown). We next conducted a quantitative iTRAQ proteomic analysis between shGRP78 and control cells. Figure 3.4C are two heatmaps showing the upregulated (red) and downregulated (green) proteins of shGRP78 when compared to control cells.

We found multiple canonical pathways dysregulated by GRP78 knockdown, including actin cytoskeleton signaling and protein ubiquitination. We also found significantly deregulated NRF2-mediated oxidative stress response, glutathione depletion, and G2/M DNA damage checkpoint regulation (Table 3.1). 268 proteins were involved in cell death and survival ($p=3.91E^{-4}$-$2.38E^{-13}$); 164 proteins involved in cellular assembly and organization ($p=3.53E^{-4}$-$3.99E^{-10}$); 198 proteins involved in cellular function and maintenance ($p=5.35E^{-4}$-$3.99E^{-10}$); 172 proteins involved in cell morphology ($p=5.35E^{-4}$-$1.08E^{-8}$); and 161 proteins involved in cellular movement ($p=2.86E^{-4}$-$2.79E^{-7}$) (Table 3.2).

Table 3.1: Significantly deregulated pathways in shGRP78 cells

Pathway	p-value
Actin Cytoskeleton Signaling	4.82E-08
Protein Ubiquitination	3.32E-06
NRF2-mediated Oxidative Stress Response	6.14E-04
Glutathione Depletion-Phase II Reactions	2.77E-02
Cell Death	2.89E-02
Cell Cycle: G2/M Damage Checkpoint Regulation	2.93E-02

Table 3.2: Significantly deregulated molecular functions in shGRP78 cells

Molecular Function	p-value	No. of Molecules
Cell Death and Survival	3.91E-04 - 2.38E-13	268
Cellular Assembly and Organization	3.53E-04 - 3.99E-10	164
Cellular Function and Maintenance	5.35E-04 - 3.99E-10	198
Cell Morphology	5.35E-04 - 1.08E-08	172
Cellular Movement	2.86E-04 - 2.79E-07	161

We identified multiple dysregulated proteins and categorized according to their cellular component (Figure 3.4D), molecular function (Figure 3.4E), and biological function (Figure 3.4F). We separated dysregulated proteins into cytoplasm (231), nucleus (250), ER (29), or membrane (282). The biological functions identified were: cell differentiation (62), metabolic process (364), transport (148), cell death (32), cell organization and biogenesis (206). We further categorized according to molecular function: protein binding (469), catalytic activity (237), DNA binding (109), and transporter activity (49). The top significantly deregulated genes/gene clusters are identified in Supplementary Figure 3.3C, where the q-value ranged from 0.001-0.05.

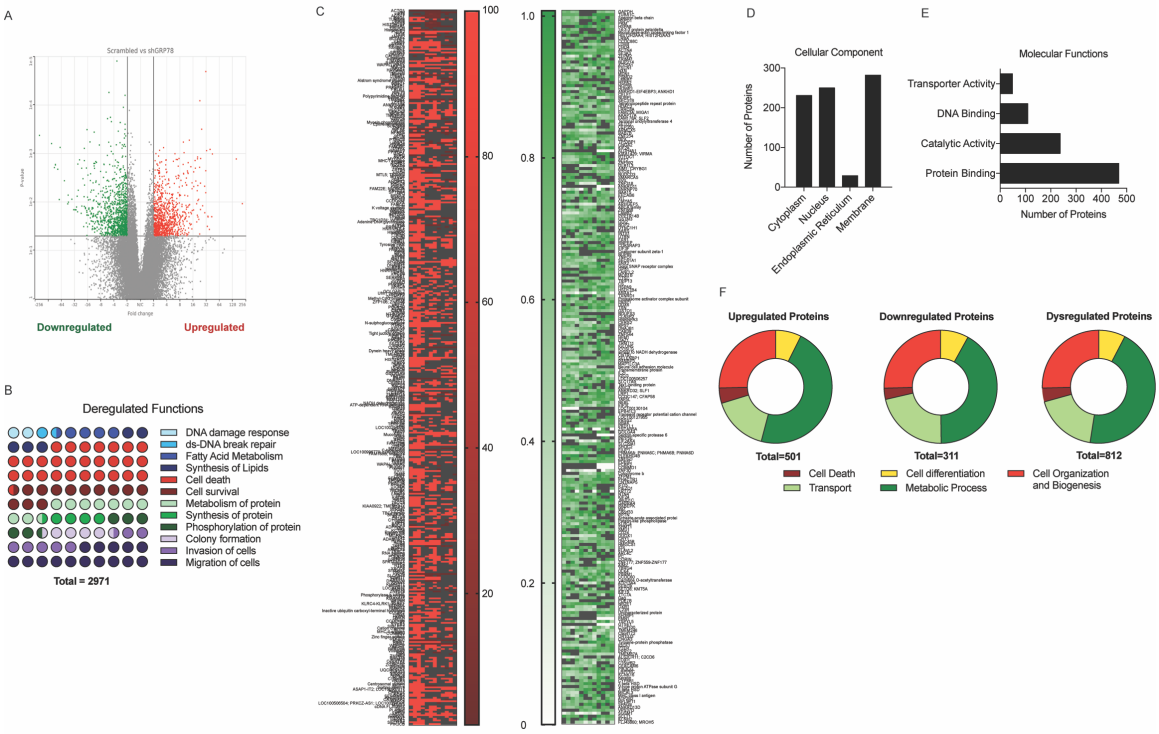

Figure 3.4: Transcriptomic and proteomic analyses show GRP78 plays an important role in DNA damage and repair

Transcriptomic analysis was performed on shGRP78 versus control cells (A-B). (A) Volcano plot depicting the significantly deregulated genes (red=upregulated; green=downregulated). (B) Dot plot depicting the percentage of significantly deregulated genes by function. iTRAQ proteomic analysis was performed on shGRP78 versus control cells (C-F). (C) Heatmaps showing upregulated (red) and downregulated (green) genes. Deregulated genes were sorted according to (D) cellular component (E) molecular function, and (F) biological function.

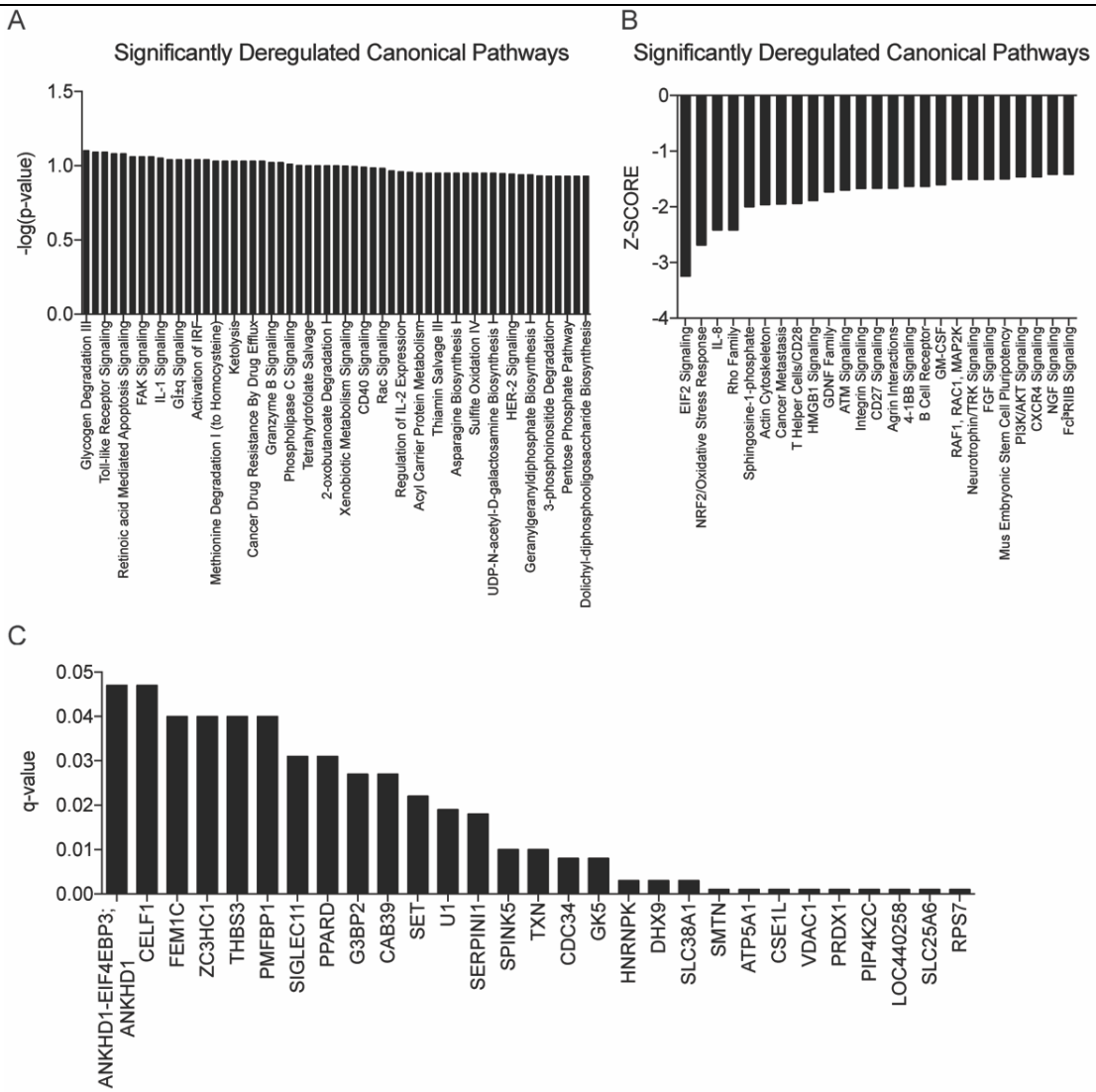

Supplementary Figure 3.3: Significantly deregulated canonical pathways
Transcriptomic analysis was performed on shGRP78 versus control cells (A-B). (A) The top 55 canonical pathways significantly deregulated. (B) The top 25 deregulated pathways sorted by z-score. iTRAQ proteomic analysis was performed on shGRP78 versus control cells, and (C) depicts the top canonical pathways deregulated.

GRP78 inhibition leads to deregulated redox balance in the cells leading to dysregulation of DNA damage and repair pathways

Another attribute of pancreatic CSCs, which Nomura *et al.* described, is maintaining a low level of reactive oxygen species (ROS) production in CD133+ cells compared to CD133- cells[133]. This suggests that CSCs maintain a low level of ROS through the UPR-

Nuclear factor, erythroid-2-like-2 (NRF2) signaling activation. Interestingly, we found that shGRP78 cells have a higher ROS baseline compared to control cells (Figure 3.5A), indicating a loss of a functional prosurvival-NRF2 mechanism, that may result in more DNA damage, ROS production, and cell death, which we observed in our transcriptomic and proteomic analyses (Figure 3.4).

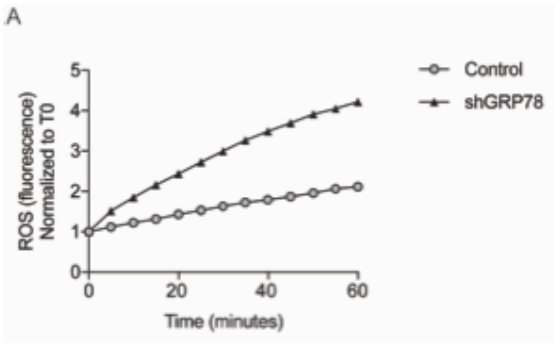

Figure 3.5: GRP78 knockdown leads to deregulated redox balance (A) ROS fluorescence of control and shGRP78 measured at 5-minute intervals over 60 minutes.

Treatment with N-acetyl-cysteine rescues GRP78 knockdown cells from DNA damage and cell death.

In order to determine if the cellular damage and DNA repair processes were the aspects of UPR that are important for maintaining “stemness” in pancreatic cancer, we next performed assays using an anti-oxidant, N-acetyl-cysteine (NAC). We found that treatment of 10 mM NAC for 24 hours lowered ROS levels, measured over 60 minutes, in comparison to control cells (Figure 3.6A). We also found that treating control and shGRP78 cells with 10 mM NAC for 24 hours rescued cell viability (3.9-fold and 5.3-fold over untreated control cells, respectively) (Figure 3.6B). Further, we observed that untreated shGRP78 had a 2.8-fold increase in caspase 3/7-mediated cell death when compared to untreated control cells. Whereas, treatment with 10 mM NAC for 24 hours rescued shGRP78 cells from caspase 3/7 mediated apoptosis (0.65-fold change normalized to control) (Figure 3.6C).

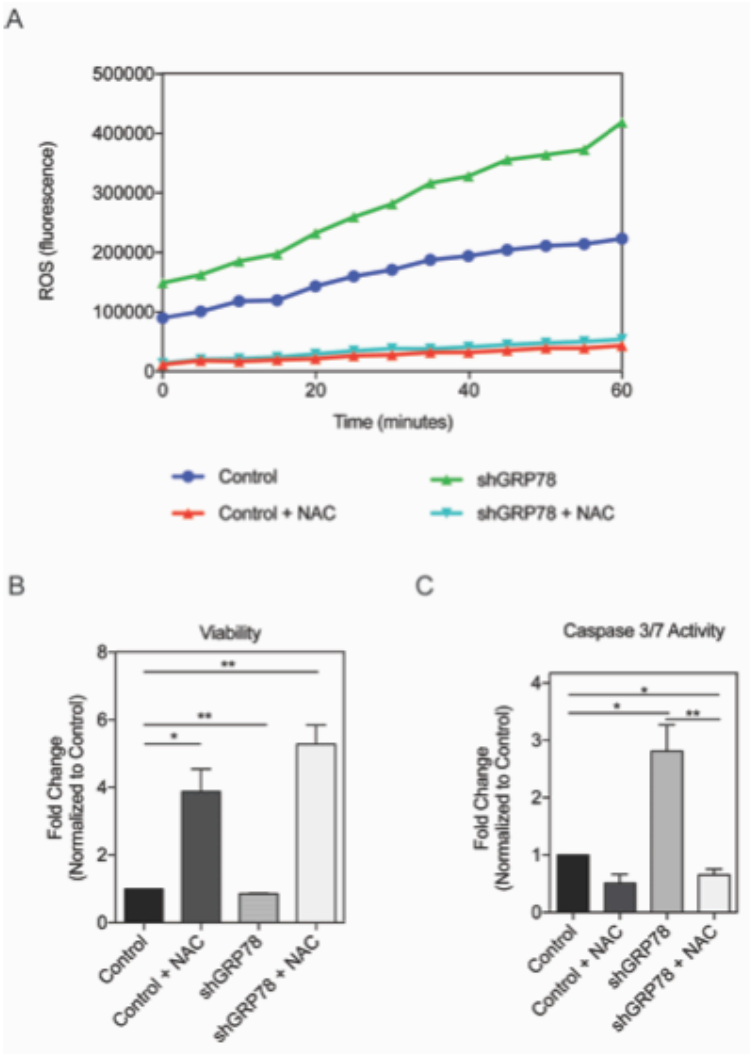

Figure 3.6: Antioxidant, NAC, rescues shGRP78 from DNA damage-induced cell death Control and shGRP78 cells were treated +/- 10 mM N-acetyl-cysteine (NAC) for 24 hours. (A) ROS fluorescence was measured at 5-minute intervals over 60 minutes, (B) Cell viability after 24 hours NAC treatment, and (C) Caspase 3/7-mediated activity after 24 hours of NAC treatment.

DISCUSSION

A number of events can occur once the UPR is activated, which can have various outcomes on a tumor cell. For example, nuclear factor kappa-light-chain-enhancer of activated B cells (NF-κB) activation leading to anti-apoptotic signaling; caspase 12 activation and apoptosis; G_1 arrest and apoptosis; G_0 arrest and tumor cell dormancy; p38 activation and dormancy; or an increase in vascular endothelial growth factor (VEGF) secretion and angiogenesis, which leads to aggressive growth and metastasis[73].

ER stress has been implicated in and could be potentially having opposing roles during several different stages of tumor development. During early tumorigenesis and before angiogenesis, UPR activation can induce G_1 arrest and activate p38, both of which can promote cell dormancy. If the pro-apoptotic branches of the UPR are also activated, cancer cells with mutations in the apoptotic machinery will be selected in order to evade cell death. ER stress also induces pro-survival NF-κB and inhibits p53-dependent apoptotic signals. In the event of a pro-survival UPR activation, ER stress can promote aggressive growth of these cancer cells by enhancing their angiogenesis[73].

In this study, we showed that knocking down GRP78 dramatically altered genes involved in DNA damage, oxidative stress signaling, and cell death (Figure 3.4). We demonstrated the significant transcriptional and proteomic alterations ultimately affected cell proliferation. Further, we characterize for the first time, a connection with the UPR and stemness and self-renewal in pancreatic cancer (Figure 3.1). CSCs are capable of self-renewal, pluripotency, and metastasis, and remain elusive targets for current pancreatic ductal adenocarcinoma (PDAC) therapies. Thus, pharmacological targets of GRP78 or the UPR may be useful in combination with drugs that target rapidly proliferating cells, as well as the surrounding stromal cells.

Knocking down GRP78 in pancreatic cancer seems to have a profound effect on the oxidative stress signaling, as well as fatty acid metabolism. ER stress can lead to lipogenesis and altered metabolism, whereas lipids and aberrant metabolism can lead to ER stress[125]. What is known is that cancer cells require more lipid production for survival[126]. Fatty acid synthase (FASN) is a multi-enzyme protein that catalyzes fatty

acid synthesis. FASN expression correlates with cancer progression, poor therapeutic response to gemcitabine, and survival (TCGA)[126, 140]. In addition, inhibiting FASN with orlistat has shown to decrease stemness in pancreatic cancer[140].

It has been reported that multiple cancer cell lines require unsaturated lipids[126]. In hypoxia (solid tumors), enzymatic reactions for *de novo* lipid synthesis are inactive, because they require oxygen[126]. As a result, cancer cells require exogenous unsaturated lipids, which can be acquired by desaturation of *de novo* fatty acids or by fatty acid uptake. Cells normally satisfy their fatty acid requirements from blood when triglycerides and low-density lipoproteins are hydrolyzed by lipoprotein lipase[126]. However, cancer cells are rapidly proliferating, and as a result, *de novo* lipid biogenesis provides most necessary lipids[127]. Inhibition of GRP78 has been shown to downregulate sterol regulatory element-binding protein (SREBP) transcription factors in breast cancer[128]. SREBP1 and 2 play an important role in regulating lipid metabolism, and regulating multiple metabolic genes [stearoyl-CoA desaturase (SCD1), FASN, acetyl-CoA carboxylase (ACC)]. Inhibiting SREBP can also result in decreased unsaturated lipids, resulting in cell death[126].

CONCLUSION

Pancreatic cancer is characteristically an aggressive cancer type. One reason for the aggressive phenotype is because of the tumor heterogeneity; for example, PDAC has rapidly proliferating epithelial cells, cancer stem cells, and a dense surrounding stroma that creates a hypoxic environment. Interestingly, the UPR plays a role in each component, making PDAC exponentially more complicated. In our current study we have demonstrated that targeting the UPR, by downregulating GRP78, could be a method of targeting cancer stem cells, which could have promising clinical applications in treating PDAC.

METHODS

Cell Culture and Treatments

S2-VP10 (a gift from Dr. Masato Yamamoto's lab, University of Minnesota) cells were cultured in RPMI 1640 containing 10% fetal bovine serum and 1% penicillin/streptomycin. Cells were treated with 1 uM palmitic acid (Sigma), 10 uM linoleic acid (Sigma), or 400 uM oleic acid (Sigma) in 1% BSA. Cells were treated with 10 mM N-acetyl-cysteine (Sigma).

Plasmid

Four pGFP-C-shLenti-HSPA5 plasmids and one pGFP-C-shLenti-scrambled target were acquired from Origene (Cat # TL312303).

Generation of Stable Cell Line

S2-VP10 cells were transfected with one of four sh-GRP78 plasmids or scrambled sh plasmid (Origene). 1 μg/mL puromycin selection was applied after 48 hours post transfection. After verifying GFP expression, cells were collected and brought to a Flow Cytometry Core Facility. Cells were gated by GFP-positive expression, and sorted single cells into each well of a 96 well plate. Clones were propagated and maintained in RPMI with 1 μm puromycin.

Transcriptomic Analysis

Aliquots of RNA were derived from the qRT-PCR samples. Three control replicates and three shGRP78 replicates were analyzed. The RNA was quality tested using a Bioanalyzer 2100 (Agilent Technologies). cDNA was created by reverse transcription of oligo-dT purified polyadenylated RNA and fragmented, blunt-ended, and then ligated to barcoded adaptors. Then, the library was size selected, and the selection process was validated and quantified by capillary electrophoresis and qPCR, respectively. Samples were load on the HiSeq 2500 (Illumina Inc.) to generate around 25 million paired-end 50bp reads for each sample. Quality control was conducted by FastQC 0.11.2 according to http://www.bioinformatics.babraham.ac.uk/projects/fastqc. The mean inner distance

was established using the insertion size metrics feature of Picard-tools. The resulting TopHat data served as input to other Cufflinks tools 2.2.0. Transcripts were also assembled using Cufflinks, with stipulating the reference transcriptome *Homo sapiens*. All cufflinks assemblies were merged with Cuffmerge. Differentially expressed genes (DEGs) were calculated with Cuffdiff and presented the data in terms of fragments per kilobase of transcript per million mapped reads (FPKMs). Visualization of data from Cuffdiff outputs was used CummeRbund v2.0.0[141]. Ingenuity Pathway Analysis (Qiagen) was used for pathway enrichment analysis.

iTRAQ Proteomic Quantification

Four control cell pellets and four shGRP78 pellets were prepared for iTRAQ MS/MS. To each cell pellet (each containing ~50 μg protein) 30 μL of dissolution buffer (0.5 M triethylammoniumbicarbonate (TEAB), pH 8.5) was added. Samples were denatured with 2% SDS, and reduced with 100 mM tris-(2-carboxyethyl) phosphine (TCEP). Samples were incubated for 1 hour at 60°C, and then 1 μL of 84 mM iodoacetamide solution was added, and incubated at 30°C in the dark. Promega Sequencing Grade trypsin was added to each sample, and then incubated at 37°C overnight. 8Plex iTRAQ reagents were prepared the following day by adding 50 μL isopropanol to each reagent. Each reagent was then transferred to one sample each. Sample-reagent mixtures were incubated at 2 hours at room temperature, and then the reactions were quenched with water, and combined into one tube. Sample was then vacuum dried, and washed three times with water.

Gene Expression Analyses

RT-PCR: RNA was isolated from the cells according to manufacturer's instructions using Trizol (Invitrogen). Total RNA (2 μg) was used to make cDNA and perform real-time PCR using the Quantitect SyBr green PCR kit (Qiagen) according to the manufacturer's instructions using Roche 480 real-time PCR system. All data were normalized to the housekeeping gene 18S (18s Quantitect Primer Assay; Qiagen). Primers for HSPA5 (GRP78), CD133, SOX2, OCT4, NANOG, GLI-1, Myc were acquired from Qiagen.

Fatty Acid Metabolism Array (Qiagen) was used to study expression level of genes involved in fatty acid metabolism as described by manufacturer's instructions.

ECIS

Proliferation was measured by Electric Cell-substrate Impedance Sensing (ECIS). Control and shGRP78 cells were seeded in 8W10E+ PET array with or without fatty acid supplementation (See Cell Culture and Treatments). Impedance (Z), capacitance (C) and resistance (R) were monitored for 48 hours by an ECIS Model ZΘ instrument (Applied BioPhysics Inc.) and normalized to Z0.

Colony Formation Assay

One million control and shGRP78 cells were prepared in 1 mL PBS. Cells were then serially diluted, and 100 μL of the diluted cells was added to the cell resuspension solution (R&D Systems). This mixture was added to 1.8 mL of methyl cellulose media, and plated in a 6-well plate with a blunt cannula.

Reactive Oxygen Species Assay

shGRP78 and control cells were seeded in black, clear bottom 96 well plates. Media was removed and replaced with 5 uM H2DCFDA/phenol-free media for 1 hour at 37°C. Cells were washed with PBS, and phenol-free media was replaced. ROS was measured at 5-minute intervals for 1 hour, with 492/517 ex/em filters. Results were expressed as ROS fluorescence per viability using a WST-8 cell cytotoxicity assay (Dojindo).

Cell Viability Assay

shGRP78 and control cells were seeded in a 96 well plate (7,000 cells/well) and allowed to adhere for 24 hours. Cell viability assay was performed using a WST-8 based cell cytotoxicity assay per the manufacturer's protocol (Dojindo) and expressed after normalizing to untreated cells.

Caspase 3/7 Activity

shGRP78 and control cells were seeded in a white 96 well plate (10,000 cells/well) and allowed to adhere for 2 hours. Cells were then treated with 10 mM N-acetyl-cysteine for 24 hours. Caspase 3/7 analysis was performed per manufacturer's protocol (Promega). Caspase results were normalized to cell viability, which was plated in tandem.

Boyden Chamber Invasion Assay

Boyden chamber invasion inserts (Corning biocoat) were rehydrated for at least one hour in serum free medium at 37°C. Cells were plated into the inserts in serum free medium. The wells contained the attractant: 10% fetal bovine serum containing medium. After 24 hours, the top of the insert was washed with PBS, and inserts were fixed in methanol and stained with crystal violet. Membranes were analyzed using a light microscope. Cells were counted using Image J software.

***In vivo* Study**

10,000 cells (control or shGRP78), and 100,000 cells (control or shGRP78) were resuspended in 50:50 PBS:matrigel mixture, and injected into the right flanks of athymic nude mice (5 mice per group). Tumor formation was monitored daily, and tumor volume was measure using a digital calipers. When the endpoint of the experiment was reached, mice were sacrificed, and tissues were resected and sent to pathology for embedding and preparation of H&E and unstained slides. All procedures were approved by the University of Miami Institutional Animal Care and Use Committee (IACUC).

Immunohistochemistry

Paraffin-embedded tissues were deparaffinized in xylene and then rehydrated in graded ethanol. TUNEL staining was completed per manufacturer's instructions (Abcam, Cat # ab206386). Briefly, slides were permeabilized with a proteinase K solution, and covered with TdT equilibration buffer. Tissues were then labeled with a TdT labeling reaction mixture for 1.5 hours, and then a conjugate solution for 30 minutes. DAB solution was added for 15 minutes, and then slides were washed with water. Slides were counterstained with methyl green and mounted with permount. Images were obtained on

a Leica DM6B with a 20x objective.

Immunofluorescence

Slides were deparaffinized in xylene and rehydrated through graded ethanol solutions. Antigen retrieval was completed in a steamer using Reveal Decloaker (Biocare Medical) and blocked with Dako serum block. Primary antibody for GRP78 (Cell Signaling) was diluted 1:200 in Sniper (Biocare Medical). Alexa 555-conjugated donkey anti-rabbit IgG (Molecular Probes) secondary antibody was diluted 1:1000. The slides were mounted using Prolong Gold anti-fade with 4',6-diamidino-2-phenylindole (Molecular Probes). Immunofluorescence images were obtained on a Leica DM6B with a 20x objective.

Statistical Analysis

Values are expressed as the mean +/- SEM. All *in vitro* experiments were performed at least three times. The significance between any two samples was analyzed by t-test, values of $p<0.05$ were considered statistically significant.

CHAPTER 4: SPECIFICITY PROTEIN 1-MEDIATED ONCOGENIC SIGNALING AND TUMOR MICROENVIRONMENT CROSSTALK

Inactivation of cancer-associated-fibroblasts (CAF) disrupts oncogenic signaling in pancreatic cancer cells and promotes its regression

Patricia Dauer[1,2], Xianda Zhao[3], Vineet K Gupta[1], Nikita Sharma[1], Kousik Kesh[1], Prisca Gnamlin[1], Vikas Dudeja[1], Selwyn M Vickers[3,4], Sulagna Banerjee[1]*, Ashok Saluja[1]*

1 Department of Surgery, University of Miami, FL, USA
2 Department of Pharmacology, University of Minnesota, MN, USA
3 Department of Surgery, University of Minnesota, MN, USA
4 Department of Surgery, University of Alabama, AL, USA

Previously published in *Cancer Research*. 2017 DEC 19.
DOI: 10.1158/0008-5472.CAN-17-2320[142]

SUMMARY

Background: Resident fibroblasts that contact tumor epithelial cells (TEC) are thought to become irreversibly activated as cancer-associated-fibroblasts (CAFs), which stimulate oncogenic signaling in TEC.

Methods: Transcriptome analysis of CAFs after 6 and 24 hours of triptolide treatment. Transforming growth factor-beta (TGF-β) and downstream effectors were analyzed with and without triptolide. Multiple markers of stromal activation were analyzed [vitamin A and lipid droplet expression, alpha smooth muscle actin (α-SMA) expression, extracellular matrix (ECM) secretion]. Finally, the effects of preventing TGF-β secretion were analyzed in TEC through specificity protein 1 (SP1) and SMAD activity.

Results: In this study, we evaluated the transcriptomic profiling conducted after treatment with triptolide revealed deregulation of the TGF-β signaling pathway in CAFs, resulting in an apparent reversal of their activated state to a quiescent, non-proliferative state. TEC exposed to media conditioned by drug-treated CAFs exhibited a decrease in oncogenic signaling as manifested by downregulation of the transcription factor SP1. This inhibition was rescued by treating TEC with recombinant TGF-β.

Conclusion: Given promising early clinical studies with Minnelide™, our findings suggest that approaches to inactivate CAFs and prevent tumor-stroma crosstalk may offer a viable strategy to treat pancreatic cancer.

INTRODUCTION

Pancreatic cancer is one of the most devastating cancers with a dismal 5-year survival rate of less than 6% (www.cancer.gov)[143]. Recent studies suggest that the dense desmoplastic stroma, consisting of intense fibrosis, increased production of extracellular matrix (ECM), and proliferation of myofibroblast-like cells[129, 144], contributes to the aggressiveness and chemotherapeutic resistance, thereby leading to poor survival. This fibro-inflammatory stroma, besides demonstrating multiple pro-cancerous features, contributes to an increase in tumor interstitial fluid pressure thus inhibiting delivery of anticancer therapies to the tumor cells[12, 44, 45]. However, stroma-targeted therapies have not been beneficial in terms of survival or prognosis[48]. An ideal therapeutic regimen for pancreatic ductal adenocarcinoma (PDAC) would thus be a combination of antitumorigenic drugs that are minimally toxic, and anti-stromal to deplete the dense stroma and/or disrupt its crosstalk with the tumor cells[145, 146].

The PDAC stroma consists of activated fibroblasts, also known as cancer associated fibroblasts (CAFs), immune cells, vasculature, and an abundance of ECM proteins[5]. This reactive milieu of cells modulates both tumor epithelial cells (TECs) and its microenvironment to promote tumor progression. CAFs secrete chemokines and cytokines that are pro-tumorigenic and help the tumor proliferate and metastasize. Whilst stromal cells do not exhibit the genetic transformations seen in malignant pancreatic cancer cells, they are altered by cytokines, and growth factors secreted by inflammatory cells and tumor cells[147, 148]. In the initial phases of tumor development, stroma production is stimulated by cancer-cell derived growth factors including transforming growth factor-β (TGF-β), hepatocyte growth factor (HGF), fibroblast growth factor (FGF), and epidermal growth factor (EGF)[149]. These tumor-derived factors and immune cell derived factors activate the quiescent stellate cells in the pancreas and make them myofibroblast-like. During these transformations under the influence of the tumor, the activated stellate cells further transform to cancer-associated fibroblasts. In their activated state, CAFs secrete ECM components, primarily type I and III collagen, fibronectin, and proteoglycans. Till date it has not been elucidated if CAFs can revert to normal quiescent fibroblasts[150, 151].

Studies in our laboratory have shown that triptolide, a diterpene triepoxide from the

Chinese plant *Tripterygium wilfordii*, induces cell death in pancreatic cancer cells, and is effective in reducing tumor growth and locoregional spread in several complementary models of pancreatic cancer[20]. For ease of clinical application, we have developed a water-soluble prodrug, Minnelide™ for this compound[9, 11, 14, 152-154]. Mechanistically, we have demonstrated that Minnelide™ downregulates heat shock protein 70 (HSP70) via inhibition of the activity of the transcription factor specificity protein 1 (SP1), thereby leading to pancreatic cancer cell death[15, 22]. Our recent publications showed that in addition to being effective against the epithelial pancreatic cancer cells, Minnelide™ also depletes the stroma by preventing the synthesis of hyaluronan and collagen stabilization. Furthermore, treatment with Minnelide™ reduces the viability of CAFs isolated from the pancreatic tumors[12]. Our pre-clinical studies show that at a dose of 0.4 mg/kg, Minnelide™ is an effective cytotoxic compound that targets multiple pathways in a tumor cell. At this dose, Minnelide™ eliminates stromal cells and decreases ECM components like collagen and hyaluronan (HA), thereby relieving the pressure on blood vessels allowing them to be functional, which results in better drug delivery[12]. Minnelide™ has just completed the Phase I clinical trial against advanced gastrointestinal malignancies and is currently awaiting Phase II trials. The Phase I has yielded very encouraging results with significant tumor responses observed in terms of reduced tumor activity on PET-CT and many patients with partial response or stable disease[155] (Manuscript under preparation). This Phase I trial revealed that the maximum tolerated dose for Minnelide™ is 0.67 mg/m2. This roughly translates to 0.2 mg/kg in mice. At this dose, Minnelide™ depletes the stromal ECM, resulting in relieving the interstitial pressure on the blood vessels and leading to better drug delivery[12].

In the current study, we performed an exhaustive transcriptome analysis on CAFs and determined that the profound effect of Minnelide™ on the pancreatic tumor stroma is due to inactivation of CAFs in the tumor. This further results in a low ECM production via suppression of the TGF-β signaling pathway in CAFs. Inactivation of CAFs lead to a decreased “cross-talk” between the tumor and the stroma, leading to decreased oncogenic signaling, suppressed tumor growth, and invasion.

RESULTS

Transcriptomic analysis of Cancer Associated Fibroblast after triptolide treatment

To study which pathways in CAFs were being downregulated by triptolide, we next conducted a transcriptome analysis based on RNA-Seq. Cell lines CAF-1, CAF-5, and CAF-7 were either untreated or treated with triptolide (100 nM) for 6 hours or 24 hours. All samples had around 25 million paired reads with over 90% mapped uniquely mapped[142]. A total of 3859 differentially expressed genes (DEGs) were identified between control group and triptolide 24 hour group with a false discovery rate (FDR) of 0.05 (Figure 4.1A-B). To further analyze the pathways that are deregulated by triptolide, we conducted pathway enrichment analysis and found that most significantly downregulated pathways were the RAR/RXR signaling pathway and TGF-β signaling (Figure 4.1C). Interestingly, RAR/RXR pathway is a retinoic acid (RA) stimulated pathway. In the presence of RA, which is a morphogen derived from vitamin A, RA translocates to the nucleus and stimulates the RAR/RXR to bind to their response elements (RARE), resulting in transcription of genes that regulate differentiation, survival, and TGF-β secretion. Our analysis showed that several genes in the TGF pathway (Supplementary Figure 4.1B) and RAR/RXR pathway[142] were being differentially regulated.

IPA analysis showed that TGF-β signaling pathway was significantly downregulated in CAFs (Figure 4.1D). Furthermore, the downstream genes of TGF-β signaling pathway were also downregulated in triptolide treated group (Figure 4.1E-F). Interestingly, in the TECs, these pathways were not among the top significant pathways that were deregulated (data not shown).

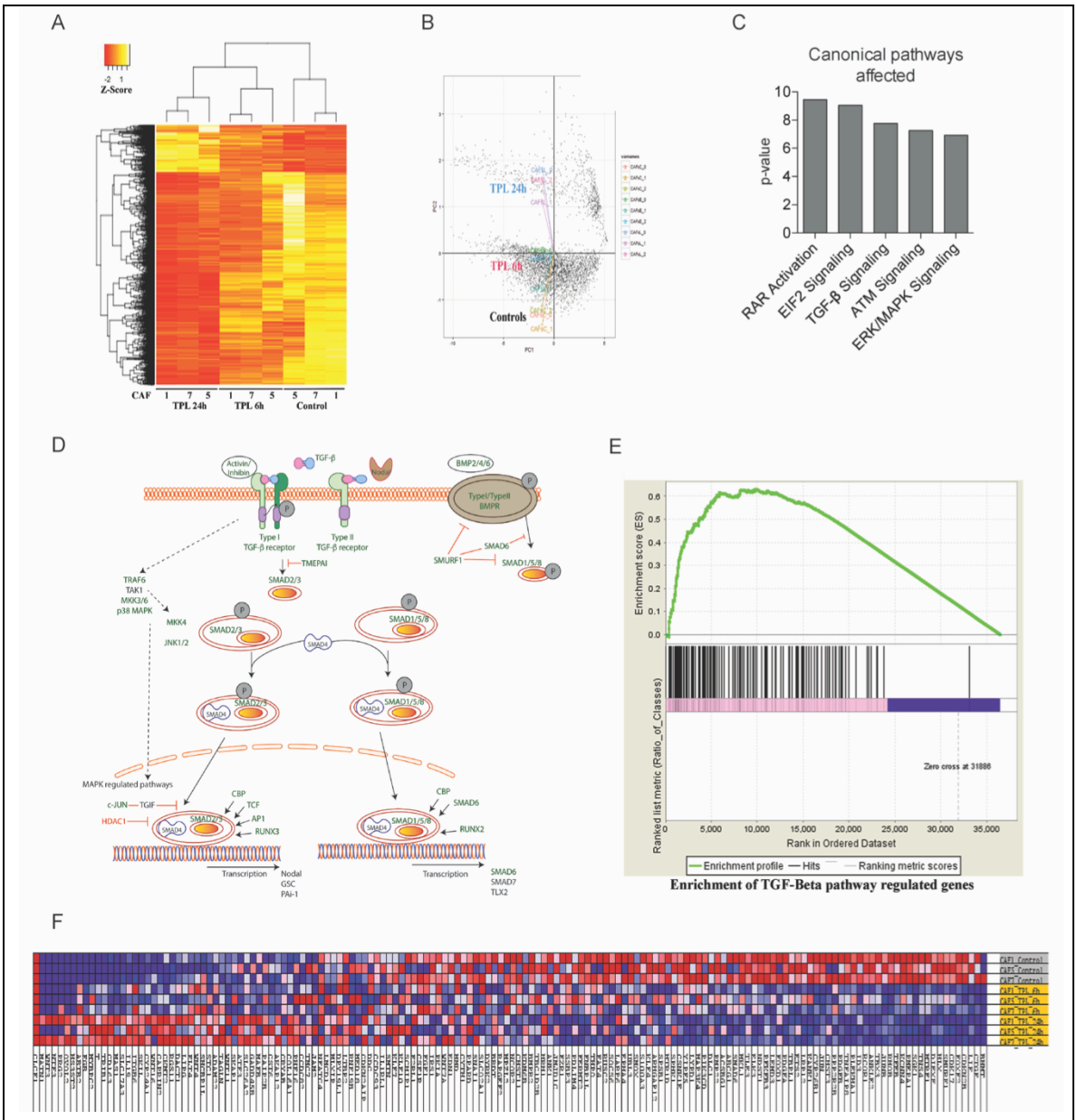

Figure 4.1: Transcriptome analysis of triptolide treated CAFs
Differentially expressed genes in CAFs before and after triptolide treatment were shown in heatmap (A). Principal component analysis showed three distinct groups of all samples that correlate to different treatments (B). Pathways that are significantly deregulated in 24 hours triptolide treatment samples were shown as bar plot (C). Visualization of TGF-β pathway in response to triptolide treatment in CAFs. Green label means downregulated genes and red label means upregulated genes (D). GSEA indicated obvious suppressive role of triptolide on TGF-β pathway downstream genes' expression (E). Heatmap of TGF-β pathway downstream genes' expression before and after triptolide treatment. Red means high expression and blue means low expression (F).

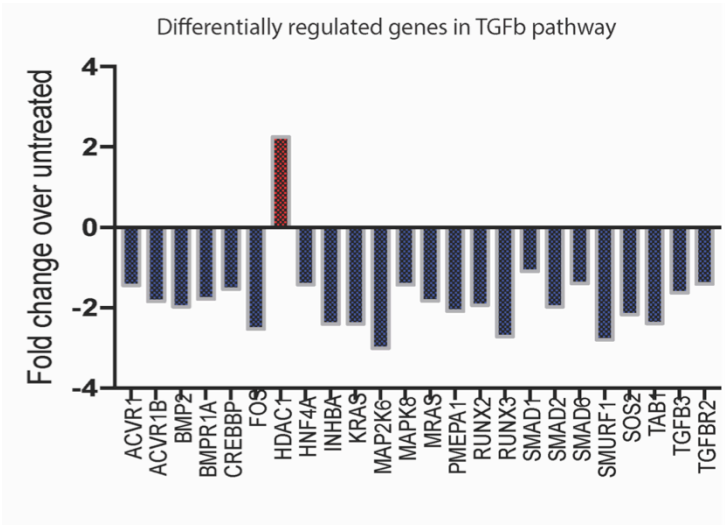

Supplementary Figure 4.1: Analysis of the RNAseq data showed the TGF-β pathway and RAR/RXR (not shown) to be the top two deregulated pathways in CAFs after treatment with Minnelide.

Triptolide downregulated the TGF-β pathway in CAFs at a sub-lethal dose

It is well known that upon activation, the stromal cells, specifically fibroblasts, secrete TGF-β. Our results confirmed this (Figure 4.2A-B). Since our transcriptomics analysis was done at a dose of 100 nM triptolide, we next studied the effect of low dose of triptolide on the TGF-β signaling. We treated the CAFs with a very low dose of 25 nM triptolide and analyzed all the components of the TGF-β pathway. Our study showed that the autocrine TGF-β signaling pathway in the CAFs was downregulated even at 25 nM triptolide. The expression of TGF-β was significantly decreased both at the RNA level (Figure 4.2C) as well as secretion level in both cells and supernatant (Figure 4.2D-E). Additionally, effectors of TGF-β pathway (SMAD2, 3, 4) were downregulated both at the RNA (Figure 4.2F) and protein level (Figure 4.2G). In addition, several other genes that were directly being regulated by the TGF-β signaling were also downregulated (Figure 4.2F). The expression and secretion of the TGF-β, as well as all its components that were decreased by triptolide treatment were rescued when treated with recombinant TGF-β (Figure 4.2G-F).

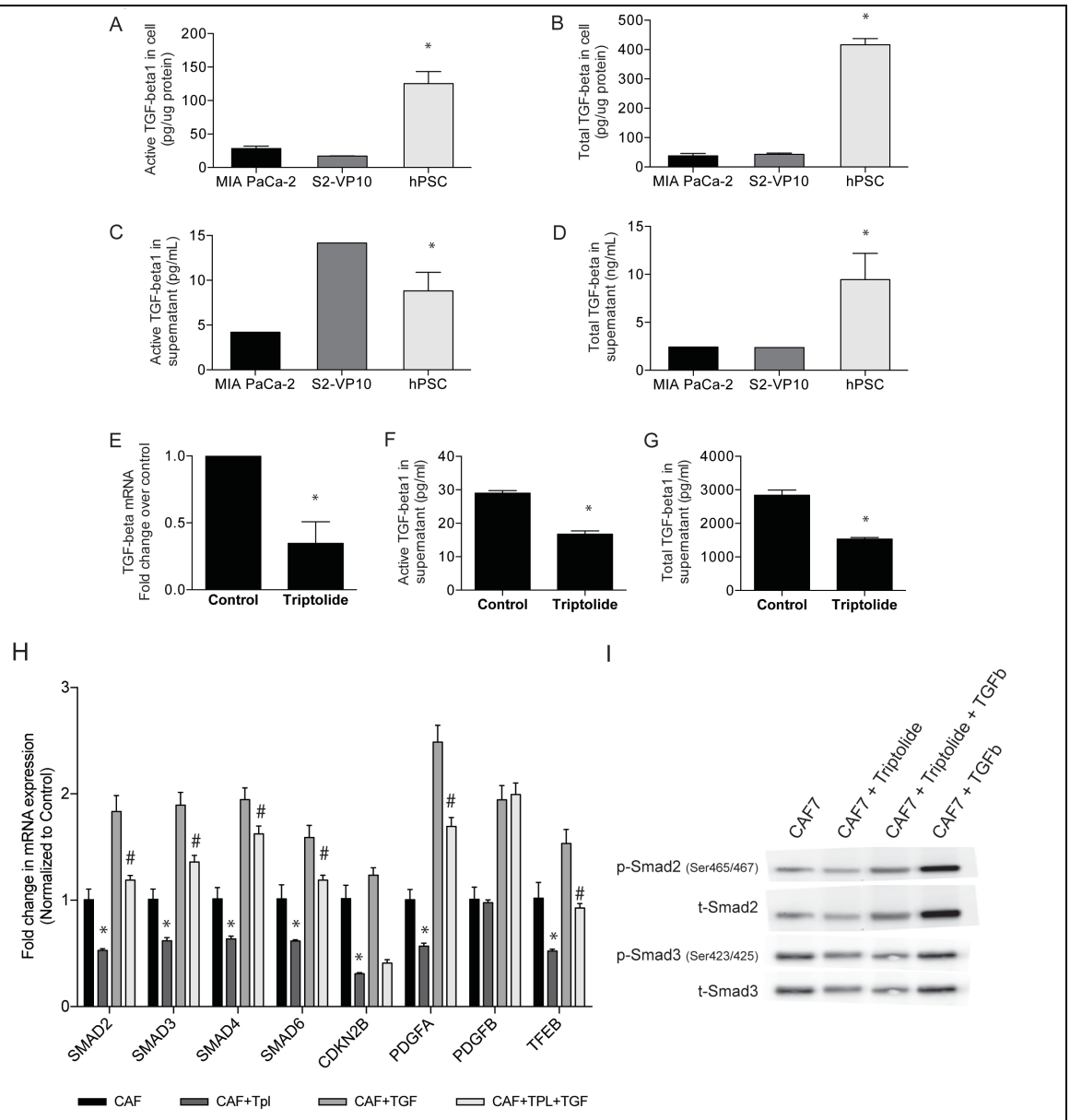

Figure 4.2: Triptolide downregulated TGF-β pathway in the CAFs
Activated pancreatic stellate cells (PSCs) produced more active as well as total TGF-β compared to the TECs in culture supernatant (A) as well as in the cell lysate (B) as seen by the ratio of the active:total TGF-β. Treatment with 25 nM triptolide (sub-lethal) decreased mRNA expression (C) as well as active:total TGF-β in hPSC supernatant (D) as well as in cell lysates (E). mRNA expression of several genes in the TGF-β pathway were downregulated by triptolide treatment of activated PSC. This was rescued by addition of recombinant TGF-β (F). Triptolide treatment also downregulated the activity of SMAD2 and SMAD3 proteins as seen by decreased phosphorylation in western blot. This was rescued by addition of recombinant TGF-β (G).
* signifies $p<0.05$ in control vs. triptolide treatment; # signifies $p<0.05$ in triptolide treated vs. TGF-β + triptolide treated samples.

Downregulation of TGF-β pathway in CAFs reverted them from activated to inactivated state

Activation of pancreatic stellate cells (PSCs) is characterized by loss of Vitamin A droplets in these cells and a subsequent increase in α-SMA expression. Thus, an increase in Vitamin A and lipid droplet accumulation in the fibroblast as well as a loss of α-SMA would indicate an inactivation of CAFs. We observed that treatment with lose dose triptolide decreased proliferation of CAFs, without affecting their viability (Figure 4.3A).

To study if this was due to "inactivation" of CAFs, we next analyzed the vitamin A droplets in these cells after treatment with triptolide. Our results showed that treatment with triptolide increased vitamin A accumulation (seen by monitoring fluorescence at 338 nm) in CAFs. Interestingly, upon treatment with TGF-β in the presence of triptolide, the vitamin A fluorescence decreased to that observed in untreated cells (Figure 4.3B). This indicated that TGF-β was capable of reverting the triptolide-induced inactivation. This was further supplemented by our IPA analysis of the RAR/RXR pathway. We observed an increased expression of retinol binding protein (RBP) in our triptolide treated CAFs[142]. RBP is required for stabilization of retinol in the cells, thus, this further conformed to our hypothesis that triptolide was indeed inactivating the CAFs, resulting in accumulation of vitamin A. To confirm this observation further, we next performed an Oil Red staining on the CAF cells. We observed an increased Oil Red stain in the triptolide treated CAFs, which decreased upon treatment with TGF-β (Figure 4.3C).

α-SMA is a classic marker for activation of PSCs. When in their quiescent state, PSCs do not express α-SMA. However, upon activation, this protein is upregulated. Treatment of CAF cells with triptolide decreased the α-SMA+ cells as seen by flow cytometry (Figure 4.3D).

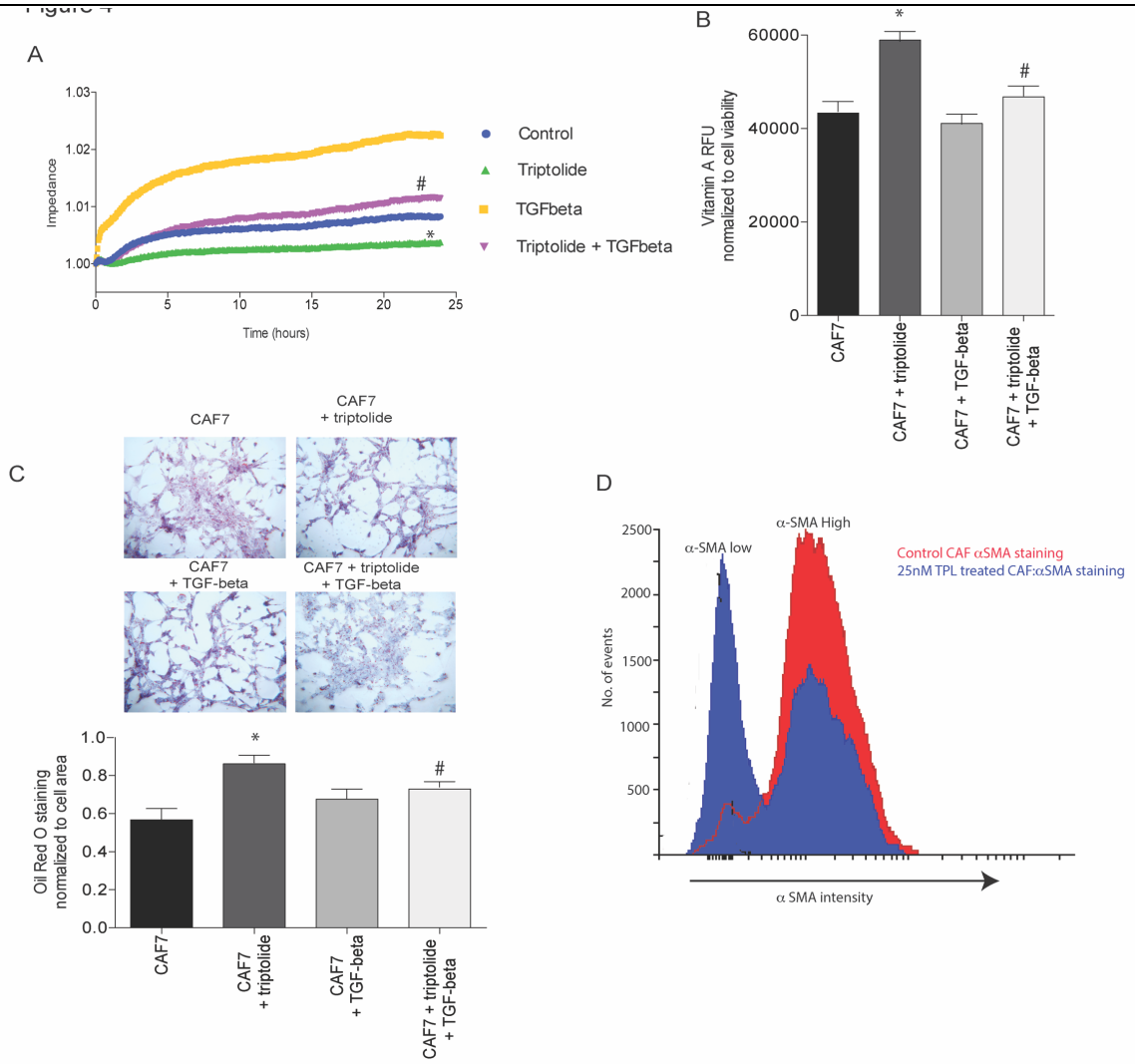

Figure 4.3: Downregulation of TGF-β pathway in CAFs by triptolide reverts them from activated to inactivated state

Treatment of TEC (KPC001) with conditioned media from CAF7 treated with 25 nM triptolide decreased proliferation rate of KPC001 as measured by ECIS (A), resulted in vitamin A accumulation as observed by change of fluorescence at 338 nm (B) and lipid droplet accumulation by oil red staining (C). Further, analysis of α-SMA expression by flow cytometry showed a decrease in the intensity of staining indicating an inactivation of CAF cells in the presence of triptolide (D).

* signifies $p<0.05$ in control vs. triptolide treatment; # signifies $p<0.05$ in triptolide treated vs. TGF-β + triptolide treated samples.

To study if treatment with triptolide is affecting the other functions of CAFs as well, we next analyzed their ECM secretion. Our results showed that treatment with 25 nM triptolide decreased the secretion of fibronectin (Figure 4.4A), periostin (Figure 4.4B),

collagen (Figure 4.4C), hyaluronic acid (Figure 4.4D), MMP2 (Figure 4.4E), and MMP9 (Figure 4.4F). Further, treatment with TGF-β reverted this decreased ECM production (Figure 4.4G-H).

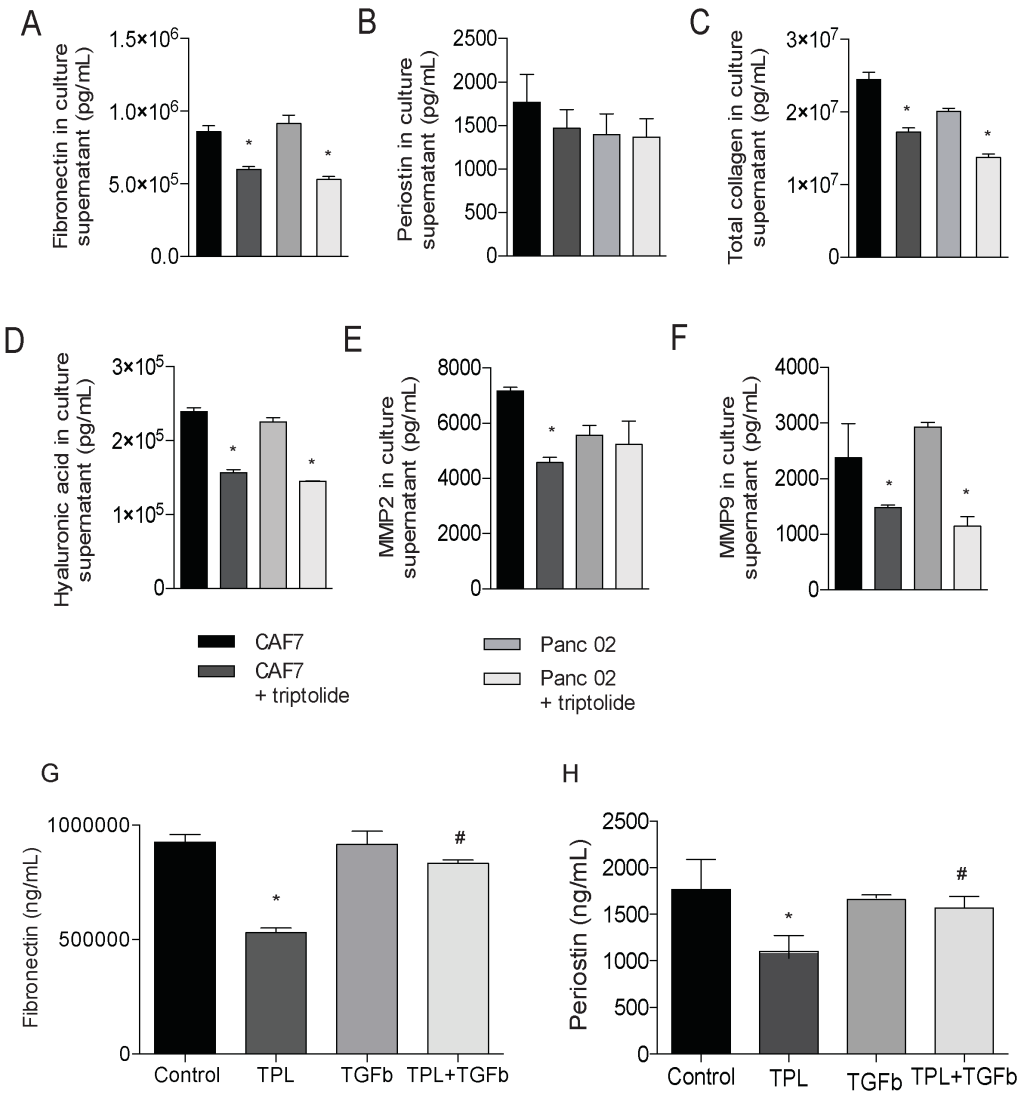

Figure 4.4: Treatment with triptolide decreased ECM secretion by CAFs
Treatment with 25 nM triptolide decreased the secretion of fibronectin (A), periostin (B), collagen (C), hyaluronic acid (D), MMP2 (E), and MMP9 (F). Further, treatment with TGF-β reverted this decreased ECM production (G, H); * signifies $p<0.05$ in control vs. triptolide treatment; # signifies $p<0.05$ in triptolide treated vs. TGF-β + triptolide treated samples.

Decreased TGF-β signaling in CAFs affected oncogenic signaling in tumor epithelial cells

It is well established that the tumor-stroma crosstalk is involved in tumor progression and metastasis. Since our data indicated that triptolide decreased the TGF-β signaling in the CAF cells and also induced inactivation, we next studied the effect of this inactivation on the TEC. Our previously published data showed that SP1 was one of the transcription factors that was overexpressed in pancreatic cancer, and this in turn upregulated the anti-apoptotic pathways and proteins like NF-κB pathway and HSP70. To study if the decreased TGF-β from the "inactivated" CAFs decreased these pathways, we next set used conditioned media from activated PSC cells (+/- triptolide) and added it to MIA PaCa-2 cells. In a parallel set, we added 10 ng/mL TGF-β to the MIA PaCa-2 cells with conditioned media from 25 nM triptolide treated PSC cells.

A dual luciferase reporter assay for SMAD showed that the conditioned media from triptolide treated PSC cells downregulated the SMAD transcriptional activity, which was rescued in the presence of TGF-β (Figure 4.5A). Since SMAD transcriptional activity leads to transcription of SP1[25, 156, 157], we next tested the SP1 gene expression and activity. Our results showed that SP1 mRNA expression was downregulated in the set with conditioned media from 25 nM triptolide. This expression was subsequently rescued upon adding TGF-β to the MIA PaCa-2 cells (Figure 4.5B).

We next studied the effect of CAF inactivation on SP1 DNA binding and transcriptional activity. Our results showed that in the presence of conditioned media from the 25 nM triptolide treated PSC, SP1 binding was significantly decreased (Figure 4.5C), indicating that CAF inactivation led to inhibition of transcriptional activity as well. Treatment with TGF-β reverted the SP1 DNA binding, confirming that this inhibition of DNA binding was mediated via downregulation of TGF-β secretion by the PSCs. Our previously published data show that in the TECs, SP1 downregulation inhibits anti-apoptotic proteins like NF-κB and HSP70.

To study if inactivation of PSCs also led to this phenotype we studied the HSP70 and NF-κB gene expression after treating cancer cells with conditioned media from 25 nM triptolide. Our results showed that MIA PaCa-2 cells treated with conditioned media from PSCs plus triptolide downregulated p50 and p65 expression, and adding TGF-β upregulated expression, when compared to untreated PSC conditioned media (Figure 4.5D).

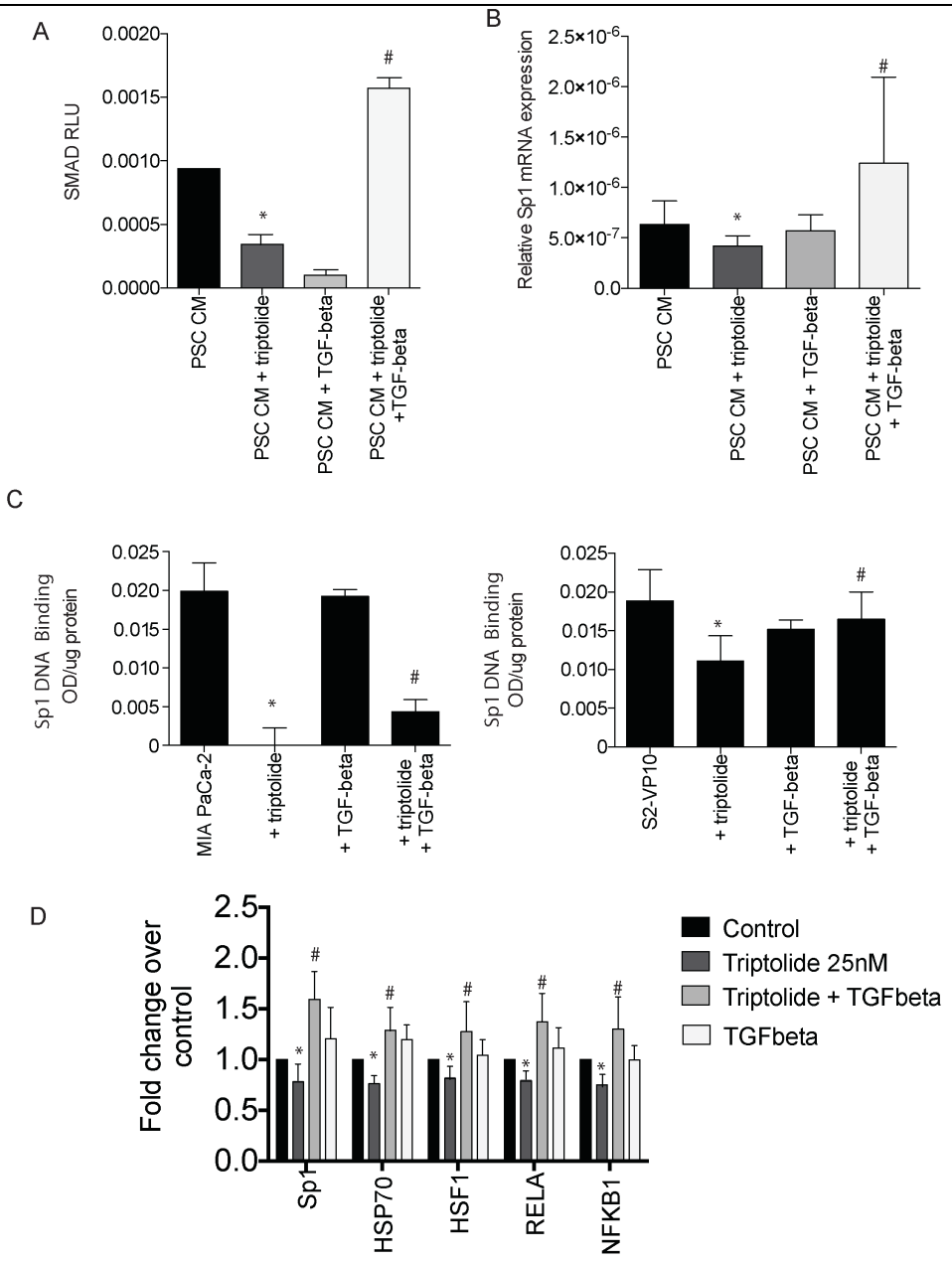

Figure 4.5: Downregulation of TGF-β in CAFs inhibits oncogenic signaling in TECs
Treatment of TEC (MIA PaCa-2 or S2-VP10) with conditioned media from activated PSC treated with 25 nM triptolide decreased SMAD transcriptional activity as seen by dual luciferase assay (A). This resulted in decreased SP1 expression in the TECs (B). Further, DNA binding ability of SP1 was inhibited (C). Expression of genes downstream of SP1 like HSP70, HSF1, and components of NF-kB pathway (RELA and NFKB1) were also downregulated. These were rescued upon addition of recombinant TGF-β (D).
* signifies $p<0.05$ in control vs. triptolide treatment; # signifies $p<0.05$ in triptolide treated vs. TGF-β + triptolide treated samples.

DISCUSSION

Pancreatic tumors are characterized by a robust desmoplastic stroma; a significant part of which is comprised of myo-fibroblast like cells. The origin of these cells remains unclear but a substantial part of these cells are derived from PSCs. These cells are very similar to those found in the liver (hepatic stellate cells, HSC), which have been well studied in context of liver injury. In a normal pancreas, the PSCs are a quiescent population typically characterized by the presence of a large amount of vitamin A droplets or retinol[158-160]. Exposure of PSCs to UV light at 300-338 nm elicits a transient blue-green fluorescence that can be quantitated[147]. Upon inflammatory stimulation from the environment, these cells become activated, "losing" their retinoid containing lipid droplets and become myo-fibroblastic, secreting α-SMA. Even though a number of studies have been focused on the biology of the pancreatic stellate cells and their activation, the mechanism of loss of retinoids has not been studied in PSCs as they have been studied in HSCs. In HSCs, activation leads to the metabolism of retinol to retinoic acid, which acts as a ligand for the RAR/RXR signaling pathway. This pathway is one of the key pathways involved in differentiation and is very tightly regulated. Upon activation, the RAR/RXR bind to their response elements (RARE) in the promoter of specific genes and regulate transcription of genes involved in differentiation, proliferation and survival. One such pathway stimulated by the RAR/RXR is the TGF-β signaling pathway.

It is classically believed that resident fibroblasts in any tissue become activated during wound healing and revert to their inactive state upon resolution[150]. However, when associated with TECs, this activation often become irreversible, leading to formation of CAFs. In the pancreas, an injury or insult leads to activation of the PSCs. During the course of pancreatic tumor progression, the PSCs become activated by the TECs and reach a stage where they presumably become irreversibly activated and drive tumor growth. At this point, they express fibroblast activation protein and fibroblast secretory protein and become cancer associated fibroblasts or CAFs that cannot go back to the quiescent stage. Thus, targeting the CAFs at this stage with molecules that can revert the back to "quiescent" state can be considered an attractive therapeutic strategy, as this will disrupt the tumor-stroma crosstalk and inhibit the tumor growth and progression.

Our transcriptomics data showed that treatment of CAFs (isolated from a mature KPC mouse tumor) with triptolide deregulated the TGF-β pathway (Figure 4.1) and the RAR/RXR signaling pathway. Interestingly, the expression of RBP was increased by this analysis and the expression of RDH was downregulated. This indicated that triptolide was affecting the retinol-metabolizing pathway. Instead of the retinol being metabolized to RA (by RDH), there was more retinol in the CAFs that needed stabilization by RBPs. This was confirmed by both our Oil Red staining and vitamin A accumulation assay (Figure 4.3). We further observed, this could be that the RAR/RXR pathway is a key developmental and differentiation pathway in the cells, it is very tightly regulated. While retinoic acid (ATRA and 9cisRA) can stimulate the RAR/RXR transcriptional activity, an excess of it acts as an inhibitor of RDH and shuts down the conversion of retinol to RA. A number of studies have shown that ATRA can prevent activation of PSCs and this only observed at high doses[161, 162]. Our studies showed that treatment with ATRA at a low dose increased proliferation of CAFs, while at an increased dose of 1 uM, it inhibited proliferation presumably by causing a feedback inhibition of the RAR/RXR pathway[142].

Previous work from our laboratory has shown that Minnelide™, the water-soluble prodrug of triptolide, is an effective anti-tumor and anti-stromal compound[12]. At a dose of 0.4 mg/kg, Minnelide™ depletes the stroma, induces stromal and tumor cell death, and prevents metastasis. However, our recently completed Phase 1 clinical trial shows that the maximum tolerated dose of Minnelide™ in patients in 0.67 mg/m^2, which translates to 0.2 mg/kg in mice. At this dose, Minnelide™ still decreases the ECM in the stroma, but does not have any profound effect on viability of TECs or CAFs. In the current work, we show that while CAFs promoted tumor growth and invasion, treatment with Minnelide™ did not significantly decrease metastasis *in vivo*[142]. However, treatment with Minnelide™ did result in less number of proliferating cells in the tumor as was seen by BrdU uptake[142]. This effect was confirmed *in vitro* as well, where treatment with conditioned media from triptolide treated CAFs decreased proliferation of TECs as well as CAFs (Figure 4.3A).

It is well known that CAFs produce TGF-β, which in turn activates oncogenic signaling in the tumor epithelial cells via the SMAD group of transcription factors[15, 22]. It is also known

that TGF-β signaling leads to induction of SP1 transcriptional activity in tumors[155]. Though SP1 is not present is terminally differentiated tissues, we and others have shown that pancreatic cancer has an increased SP1 activity[163] and its inhibition leads to cancer cell death. Our data suggest that triptolide treatment of CAFs leads to inhibition of TGF-β mRNA levels as well as its secretion (Figure 4.2). Upon treating MIA PaCa-2 cells with conditioned media from 25 nM triptolide treated PSCs, we saw a distinct decrease in the SMAD transcriptional activity, SP1 expression, as well as SP1 activity (Figure 4.5). In addition, other anti-apoptotic pathways that are known to be upregulated in pancreatic cancer (and regulated by SP1 activity) were also found to be downregulated.

In addition to decreased proliferation, treatment with triptolide also decreased ECM secretion by CAFs. Interestingly, all the "inhibitory" effects of triptolide were recovered upon treatment with TGF-β, which indicated that triptolide-induced inactivation of CAFs led to a decreased TGF-β secretion by these cells, which deregulated both the autocrine signaling in the CAFs as well as the paracrine signaling in the TECs.

CONCLUSION

The role of CAFs in promoting tumor growth and invasion has been established in a number of cancers including pancreatic cancer. Several studies in pancreatic cancer have also been focused on depletion of stromal components specifically the ECM. In the current study, we show for the first time that Minnelide™, and its active compound triptolide, is able to revert the presumably “irreversible” CAFs to an inactive state, where they show decreased TGF-β secretion and less ECM production. This in turn affects the TECs, and lowers their proliferation and decreases oncogenic signaling, leading to a tumor regression. This mechanistic insight on the effect of triptolide on CAF inactivation will pave the way for developing viable and attractive therapy for pancreatic cancer, a disease that still lacks efficient chemotherapeutic options.

METHODS

Cell Lines and Cell Culture

Four primary cell lines were isolated from KrasG12D; Trp53R172H; Pdx-1-Cre (KPC) mice. The TECs were isolated according to our previous study[153]. Isolation of CAFs (CAF-1, CAF-5 and CAF-7) from three KPC mice was performed following the protocol described by Sharon *et al*[163]. The purity of fibroblasts was checked by flow-cytometry after staining isolated fibroblasts with fibroblast surface protein (FSP) antibody and CK19 antibody. Population with FSP+CK19-staining was used for downstream experiments. All the established cell lines were used between passages 5 and 18. We also used three pre-established cell lines, the mouse PDAC cell line Panc02 and human PDAC cell lines MIA PaCa-2 (ATCC), S2-VP10 (a gift from Dr. Masato Yamamoto's lab, University of Minnesota), and the human pancreas fibroblasts SC00A5 (Vitro Biopharma). MIA PaCa-2, KPC-1, and CAFs were maintained in DMEM (Gibco, ThermoFisher Scientific) containing 10% fetal bovine serum (FBS) and 1% Pen Strep (Gibco). Panc02 and S2-VP10 were cultured in RPMI 1640 (Gibco) containing 10% FBS and 1% Pen Strep (Gibco). SC00A5 was maintained in MSC-GRO™ Low serum, Complete Media (Vitro Biopharma). All cell lines were routinely tested for mycoplasma and STR profiles (ATCC).

Conditioned media (CM) of tumor cells and CAFs was produced using FBS-free basal media to exclude the effects of growth factors in serum for downstream experiments. In normal conditions, 70% confluent cells were cultured in FBS-free basal media for 48 hours. In experiments designed to analyze the effects of triptolide, 100% confluent cells were cultured in FBS-free basal media containing 25 nM triptolide for 24 hours and then changed to no drug, FBS-free, basal media for 48 hours. The resulting CM were centrifuged for 10 minutes at 1,000 rpm after collection and stored at -80°C for no more than two months before use.

Fluorescence Activated Cell Sorter Analysis

Single-cell suspensions were prepared from fresh cell culture. Cell fixation and permeabilization was performed with the BD Bioscience Cytofix/Cytoperm kit (BD

Biosciences), according to the manufacturer's instructions. Apoptosis and BrDU incorporation for proliferation was done using Apoptosis and Cell Proliferation Kit following manufacturer's instructions (BD Biosciences). Analysis of alpha-SMA, TGF-Beta receptor type 1, and TGFBR2 (Abcam) were conducted by FACS. All samples were analyzed on BD FACSCANTO II flow cytometers (BD Biosciences). Data was acquired and analyzed with FACSDiVa software (BD Biosciences) and FlowJo Software.

Measurement of ECM and TGF-β Secretion

To evaluate the effects of triptolide on ECM secretion of CAFs, we measured concentration of total collagens, fibronectin (FN), periostin, hyaluronic acid (HA), matrix metallopeptidase 2 (MMP2), and MMP9 in CM derived from CAFs. Enzyme-linked immuno sorbent assay (ELISA) was used to quantify FN (BioVision), periostin (Thermo Scientific), HA (TSZELISA), MMP2 (Abcam), and MMP9 (Abcam). Total collagen was quantified by Sircol collagen assay kit (Biocolor Life Science Assays). Meanwhile, autocrine signaling of TGF-Beta 1 (Abcam) and TGF-Beta 2 (R&D Systems) were determined by ELISA in CM. All the experiments were performed according to the manufacturer's protocol.

Quantitative real-time Polymerase Chain Reaction Assay

Messenger RNA (mRNA) expression was analyzed through quantitative real-time polymerase chain reaction (qRT-PCR) using LightCycler 480 System (Roche) and SYBR Green (Qiagen). The 18s ribosomal RNA expression was used to normalize the results obtained in different conditions. Primers SP1, HSP70, HSF1, RELA, NFKB1 were acquired from Qiagen. Other primers used in this article were listed in Supplementary Table 4-1.

Supplementary Table 4-1: Primers used

Primers for human samples	**Forward**	**Reverse**
18SrRNA	GGC CCT GTA ATT GGA ATG AGT C	CCA AGA TCC AAC TAC GAG CTT
TGFB1	GAG CCG TGG AGG GGA AAT TG	CCG GTA GTG AAC CCG TTG AT
TGFB2	CCC TCC GAA ACT GTC TGC C	ATG GCA TCA AGG TAC CCA CAG
TGFB3	ATG ACC CAC GTC CCC TAT CA	TCC GAC TCG GTG TTT TCC TG

SMAD2	GTT CCT GCC TTT GCT GAG AC	TCT CTT TGC CAG GAA TGC TT
SMAD3	CTG TGG ATG GCT TCA CCG AC	GAT GTA GTA GAG CCG CAC GC
SMAD4	GGG GAC CGG ATT ACC CAA GA	AGG TTG TGG GTC TGC AAT CG
PDGFA	TAC TGA ATT TCG CCG CCA CA	GAA CAT GGG CGA GGT ATC CG
PDGFB	TTC CTG TCT CTC TGC TGC TAC C	CAG CAG GCG TTG GAG ATC AT
STAT1	GTT ATG GGA CCG CAC CTT CA	CAG TGA ACT GGA CCC CTG TC
SMAD6	AGA GTG ACT GCG AGA CGG T	CGC TTC GCG ACT CCG C
TFEB	AGG AGC GGC AGA AGA AAG AC	GTC ATT GGC CTT GGG GAT CA
CDKN2B	CGC GGG GAC TAG TGG AGA AG	CCA TCA TCA TGA CCT GGA TCG C

Transcriptome Deep Sequencing and Analysis

Aliquots of RNA were derived from the qRT-PCR samples. CAF-1, CAF-5 and CAF-7 control group, triptolide short-term treatment group, and long-term treatment group were analyzed. The RNA was quality tested using a Bioanalyzer 2100 (Agilent Technologies). cDNA was created by reverse transcription of oligo-dT purified polyadenylated RNA and fragmented, blunt-ended, and then ligated to barcoded adaptors. Then, the library was size selected, and the selection process was validated and quantified by capillary electrophoresis and qPCR, respectively. Samples were load on the HiSeq 2500 (Illumina Inc.) to generate around 25 million paired-end 50bp reads for each sample. Quality control was conducted by FastQC 0.11.2 according to http://www.bioinformatics.babraham.ac.uk/projects/fastqc[164]. TopHat 2.0.5, was used to map the paired reads to the UCSC mm10 assembly of the mouse genome[165]. The mean inner distance was established using the insertion size metrics feature of Picard-tools. The resulting TopHat data served as input to other Cufflinks tools 2.2.0[166]. Transcripts were also assembled using Cufflinks, with stipulating the reference transcriptome Mus_musculus. GRCm38.74. All cufflinks assemblies were merged with Cuffmerge. DEGs were calculated with Cuffdiff and presented the data in terms of fragments per kilobase of transcript per million mapped reads (FPKMs). Visualization of data from Cuffdiff outputs was used CummeRbund v2.0.0[141]. clusterProfiler[167] and Ingenuity Pathway Analysis (Qiagen) were used for pathway enrichment analysis. Gene set enrichment analysis (GSEA)[168] was conducted using app from http://www.broadinstitute.org/gsea/index.jsp. Raw data files and processed expression files are available online in the Gene Expression Omnibus at http://www.ncbi.nlm.nih.gov/geo/ (GenBank Accession Number GSE74490).

Estimation of Active and Total TGF-β

Conditioned media from TECs (MIA PaCa-2 and S2-VP10) and activated pancreatic stellate cells (PSC) were collected after 48 hours of plating. Cell lysates from the TECs and PSCs were prepared by lysing the cells in RIPA buffer. Total and active TGF-β was estimated in the media and cell lysate using LegendMax TGF-b1 ELISA kit and LegendMax Free active TGF-b1 ELISA kit (Biolegends).

Vitamin A Accumulation Assay

5,000 CAF-7 cells were plated in each well of a black 96-well plate with clear bottom. The following day, cells were either left untreated, or treated with 25 nM triptolide for 48 hours. After treatment, 10 ng/mL TGF-β was added for 30 minutes to two untreated rows (12 wells), and two rows treated with triptolide (12 wells). After 30 minutes, cells were washed gently with PBS, and phenol-free media was replaced. Fluorescence was measured with excitation of 300 nm and emission of 338 nm on half of the plate. The other half of the plate was used for determining viability, as previously described.

Oil Red Staining

20,000 CAF-7 cells were plated in each well of a four-well chamber slide. The following day, two wells were treated with 25 nM triptolide for 48 hours. After treatment, 10 ng/mL TGF-β was added for 30 minutes to one untreated well, and one well treated with triptolide. Cells were then washed gently with PBS, and fixed with 2% paraformaldehyde for 30 minutes. Cells were washed with water, and incubated with 60% isopropanol/40% water for 5 minutes. 60% isopropanol was removed, and replaced with Oil Red O working solution (3 parts Oil Red O:2 parts water) for 20 minutes. Cells were again washed with water, and counterstained with hematoxylin for 1 minute. Cells were washed, mounted with permount, and imaged with a light microscope.

SP1 Activity Assay

Human pancreatic stellate cells (hPSC) were seeded in four, 10 cm plates, and cultured until 70-80% confluent, and were then treated with 25 nM triptolide for 48 hours.

Meanwhile, 300,000 MIA PaCa-2 and S2-VP10 cells were seeded in 6 cm plates. After 48 hours, 10 ng/mL TGF-β was added to one untreated hPSC plate and one triptolide treated hPSC plate for 30 minutes. The conditioned media from the hPSCs was collected. Any DMEM on the MIA PaCa-2 cells was removed and the cells were rinsed with PBS. Conditioned media from the hPSCs was added to the MIA PaCa-2 cells for an additional 24 hours as follows: untreated hPSC, hPSC + TGF-β, hPSC + triptolide, and hPSC + triptolide + TGF-β. Cell lysates were collected for each sample and added in duplicate to the SP1 TransAM ELISA plate (Active Motif). The ELISA was performed per the manufacturer's instructions, and the SP1 binding was normalized to protein concentration.

Dual Luciferase Reporter Assay

MIA PaCa-2 and human pancreatic stellate cells (hPSCs) were plated at a density of 80,000 cells per well in a 24 well plate. Cells were treated with triptolide (25 nM for 48 hours) and TGF-β (10ng/ml for 30 minutes). The supernatant from hPSC cells treated with triptolide was plated on top of the MIA PaCa-2 cells. After 48 hours of the hPSC conditioned media on MIA PaCa-2 cells, the cells were lysed with 1X passive lysis buffer. The plate was then kept at -80°C overnight and the luciferase activity was measured the next day using the stop and glow kit from Promega according to the manufacturer's protocol.

ECIS

CAF-7 proliferation was measured by Electric Cell-substrate Impedance Sensing (ECIS). CAF-7 cells were seeded in 8W10E+ PET arrays with or without TGF-β (10ng/ml) and or triptolide (25 nM). Impedance (Z), capacitance (C) and resistance (R) were monitored for 60 hours by an ECIS Model ZΘ instrument (Applied BioPhysics Inc.) and normalized to Z0.

Statistical Analysis

Values are expressed as the mean ± SEM. Two-group data were analyzed using a t-test. Multigroup data were first analyzed using one-way ANOVA, if there are positive

findings; Bonferroni's multiple comparisons test was performed to finish pairwise comparisons. A p-value< 0.05 was considered statistically significant.

DISCUSSION

Summary

Collectively, our studies suggest that the unfolded protein response (UPR) is a complex homeostatic mechanism. Depending on the type of stress (hypoxia, nutritional, pharmacological), the duration of stress, and the functionality of the UPR, the outcomes of endoplasmic reticulum (ER) stress can vary quite significantly.

In Chapter 1 we have shown that chronic ER stress can occur when glucose regulatory protein 78 (GRP78), the master regulator of the UPR is depleted. Our study shows that downregulating specificity protein 1 (SP1), a transcription factor that is overexpressed in pancreatic cancer, activates UPR, and results in chronic ER stress. We have shown that SP1 downregulation is responsible for inadequate UPR signaling, by preventing GRP78 from being transcribed. Further, we show that both inhibition of SP1 and well as inducing chronic ER stress (with known pharmacological agents), lead to lysosome membrane permeabilization (LMP), a sustained accumulation of cytosolic calcium, and eventually cell death in pancreatic cancer.

Using a pharmacological agent to induce ER stress is potentially a useful strategy for killing cancer cells, particularly when used in combination with chemotherapeutics with other targets. The use of bortezomib, a proteasome inhibitor that causes ER stress and proteotoxicity through caspase-4 activation, has been evaluated clinically for cancer treatment [169, 170]. Bortezomib alone has shown to be effective in hematological malignancies; however, in solid tumors it showed minimal effects [170-172]. Bortezomib and gemcitabine combination demonstrated synergistic effects in solid tumors[173]. Pharmacological agents do not always result in cancer cell death, which is why understanding mechanisms of action is incredibly valuable. For example, in breast cancer, some therapies (tamoxifen and faslodex) actually induce acute ER stress, which promotes cell survival and drug resistance[128].

In an acute stress scenario, we and others have shown that cancer cells upregulate

multiple UPR components in order to keep up with the nutrient and biosynthetic demands of tumor cells. In Chapter 2, we have shown that basal levels of SP1, GRP78, nuclear factory, erythroid 2-like 2 (NRF2), and multiple ATP-binding cassette (ABC)-transporters are overexpressed in pancreatic cancer. SP1 and GRP78 are responsible for upregulating pro-survival pathways. NRF2 has been reported to upregulate certain ABC-transporters, as well as decrease the amount of reactive oxygen species (ROS) produced by cells, which are both know mechanism of drug resistance. As a result, we have shown that transiently silencing GRP78 or SP1 pushes the cancer cells towards a chronic ER stress phase. We therefore achieve less efflux activity by ABC-transporters and greater ROS production (a loss of protection), thereby increasing sensitivity to otherwise resistant drugs.

While transient silencing of gene expression is useful in certain mechanistic studies, it can contrast with gene expression that occurs in long-term silencing. Modulation of long-term gene expression (via shRNA, CRISPER, or animal knockouts) can lead to the activation of long-term compensatory signaling and/or secondary modulations. For example, stable cell lines have been generated that have been exposed to long-term oxidative stress, and resistant cells were selected and propagated[174, 175]. Further, it has been shown by Lee *et al.* that the proteome of hypoxic cells is completely different than cells grown in normoxia [176, 177]. Since a transient reduction in a protein may have a completely different effect than the long-term removal of a protein, we next looked at using a stable-sh cell line for GRP78 in Chapter 3. We have concluded that the stable shGRP78 cells have a very different proteomic profile. While the shGRP78 cells are viable, they proliferate at a slower rate. Additionally, these cells have reduced stemness properties (colony formation, invasion).

Pancreatic cancer characteristically has a dense, desmoplastic stroma. The stroma creates hypoxic niches, and results in a pro-inflammatory environment that aids in tumor progression and confers chemoresistance. In Chapter 4, we focused on the tumor epithelial and stroma interactions. By using a pharmacological inhibitor, Minnelide™, we found an inactivation of the cancer-associated fibroblasts (CAFs), which have previously been thought to be terminally-activated. These inactivated CAFs secreted less transforming growth factor-beta (TGF-β) and produced less extracellular matrix (ECM).

This decreases CAF proliferation and oncogenic signaling, leading to tumor regression.

Our studies suggest that SP1 and GRP78 could be potential targets for future therapeutics in PDAC. These mechanistic studies on the effect of triptolide/Minnelide™ ER stress, UPR activation/inactivation, CAF inactivation, and cell death will pave the way for developing a viable and attractive therapy for pancreatic cancer, a disease that still lacks efficient chemotherapeutic options.

Future Directions

The third chapter of this dissertation is an incomplete study at this time, because the preliminary findings suggest that ER stress plays an essential role in cancer stem cell maintenance. There currently are few studies that describe a role of the UPR in stemness, and no current study suggesting a direct link between cancer stem cells and the UPR. One tool that I was working on making, which would be instrumental in answering these questions, is an inducible-GRP78 knockdown system. I have cloned a shGRP78 sequence into a pLKO-Tet-on-neo backbone, packaged them in a Lenti-viral system, and transduced my cell line of choice (S2-VP10). I am currently propagating the clonal populations into stable inducible cells. Eventually, these cells will be able to be used for the same *in vitro* and *in vivo* studies, as well as others. We have multiple follow up questions to the studies which I have presented in this dissertation.

1. Is GRP78 required for stemness, and therefore tumor initiation?
2. Is there a delay in tumor initiation when tetracycline/doxycycline is added to the pLKO-Tet-on-shGRP78 cells?
3. After tumor initiation, does pLKO-Tet-on-shGRP78 still have an effect on tumor reduction, and weight?
3. In advance tumor status, are pLKO-Tet-on-shGRP78 cells more sensitive to traditional therapies used in pancreatic cancer (gemcitabine, 5-FU, paclitaxel)?

Additionally, these cells will be useful in metabolomics studies, since UPR components have been linked with the hexosamine biosynthetic pathway and glucose uptake.

CONCLUSIONS

Endoplasmic reticulum (ER) stress initiates an important mechanism for cell adaptation and survival, named the unfolded protein response (UPR). Severe or chronic/prolonged UPR can breach the threshold for survival and lead to cell death. This dissertation has the central theme of ER stress, and the homeostatic mechanism of the UPR in pancreatic cancer.

My first study focused on how the UPR could be pushed to the chronic stage, and the cell death mechanisms that follow. The current study identified specificity protein 1 (SP1) and glucose regulatory protein 78 (GRP78) as potential targets for future therapeutics in pancreatic ductal adenocarcinoma (PDAC); discovered a protective role of SP1 in cancer; as well as further detailed ER stress response in cell death mechanisms.

The second study in this dissertation addresses acute ER stress in cancer. It has been well documented in cancer that cancer cells utilize the UPR to their growth and survival advantages, which can also aid in drug resistance. This study identifies some of the drug resistance mechanisms utilized by pancreatic cancer cells, and how targeting the UPR directly with siGRP78 or indirectly with siSP1 both result in chemosensitivity.

My third study further explores the roles of the UPR in pancreatic cancer, by utilizing a stable cell line with GRP78 knocked down. The transcriptomic and proteomic studies confirm that GRP78 is an essential protein in maintaining cellular homeostasis. The shGRP78 cells display significantly slower proliferation, lipid dysregulation, and a decrease in stemness and self-renewal properties. Further, GRP78 knock down delays tumor initiation and decreases tumor growth.

The final study included in this dissertation showed for the first time that Minnelide™, and its active compound triptolide, is able to revert the “irreversible” cancer-associate fibroblasts (CAFs) to an inactive state. Inactivated CAFs showed decreased transforming growth factor-beta (TGF-β) secretion and less extracellular matrix (ECM) production. This in turn affects the tumor epithelial cells (TECs), and lowers their proliferation and decreases oncogenic signaling, leading to a tumor regression.

BIBLIOGRAPHY

1. Society AC. Cancer Facts & Figures 2018. American Cancer Society. 2018: 1-71.
2. Longley DB, Johnston PG. Molecular mechanisms of drug resistance. J Pathol. 2005;205: 275-292.
3. Agarwal R, Kaye SB. Ovarian cancer: strategies for overcoming resistance to chemotherapy. Nat Rev Cancer. 2003;3: 502-516.
4. Avril T, Vauleon E, Chevet E. Endoplasmic reticulum stress signaling and chemotherapy resistance in solid cancers. Oncogenesis. 2017;6: e373.
5. Neesse A, Algul H, Tuveson DA, Gress TM. Stromal biology and therapy in pancreatic cancer: a changing paradigm. Gut. 2015;64: 1476-1484.
6. Von Hoff DD, Ervin T, Arena FP, et al. Increased survival in pancreatic cancer with nab-paclitaxel plus gemcitabine. N Engl J Med. 2013;369: 1691-1703.
7. Xu C, Bailly-Maitre B, Reed JC. Endoplasmic reticulum stress: cell life and death decisions. J Clin Invest. 2005;115: 2656-2664.
8. Tabernero J, Elez ME, Herranz M, et al. A pharmacodynamic/pharmacokinetic study of ficlatuzumab in patients with advanced solid tumors and liver metastases. Clin Cancer Res. 2014;20: 2793-2804.
9. Chugh R, Sangwan V, Patil SP, et al. A preclinical evaluation of Minnelide as a therapeutic agent against pancreatic cancer. Sci Transl Med. 2012;4: 156ra139.
10. Nomura A, McGinn O, Dudeja V, Sangwan V, Saluja AK, Banerjee S. Minnelide effectively eliminates CD133(+) side population in pancreatic cancer. Mol Cancer. 2015;14: 200.
11. Alsaied OA, Sangwan V, Banerjee S, et al. Sorafenib and triptolide as combination therapy for hepatocellular carcinoma. Surgery. 2014;156: 270-279.
12. Banerjee S, Modi S, McGinn O, et al. Impaired Synthesis of Stromal Components in Response to Minnelide Improves Vascular Function, Drug Delivery, and Survival in Pancreatic Cancer. Clin Cancer Res. 2016;22: 415-425.
13. Banerjee S, Nomura A, Sangwan V, et al. CD133+ tumor initiating cells in a syngenic murine model of pancreatic cancer respond to Minnelide. Clin Cancer Res. 2014;20: 2388-2399.
14. Banerjee S, Saluja A. Minnelide, a novel drug for pancreatic and liver cancer. Pancreatology. 2015;15: S39-S43.
15. Banerjee S, Sangwan V, McGinn O, et al. Triptolide-induced cell death in pancreatic cancer is mediated by O-GlcNAc modification of transcription factor Sp1. J Biol Chem. 2013;288: 33927-33938.
16. Chen Z, Sangwan V, Banerjee S, et al. Triptolide sensitizes pancreatic cancer cells to TRAIL-induced activation of the death receptor pathway. Cancer Lett. 2014;348: 156-166.
17. Krosch TC, Sangwan V, Banerjee S, et al. Triptolide-mediated cell death in neuroblastoma occurs by both apoptosis and autophagy pathways and results in inhibition of nuclear factor-kappa B activity. Am J Surg. 2013;205: 387-396.
18. Mujumdar N, Banerjee S, Chen Z, et al. Triptolide activates unfolded protein response leading to chronic ER stress in pancreatic cancer cells. Am J Physiol Gastrointest Liver Physiol. 2014;306: G1011-1020.
19. Mujumdar N, Mackenzie TN, Dudeja V, et al. Triptolide Induces Cell Death in Pancreatic Cancer Cells by Apoptotic and Autophagic Pathways. Gastroenterology. 2010;139: 598-608.
20. Phillips PA, Dudeja V, McCarroll JA, et al. Triptolide induces pancreatic cancer cell

death via inhibition of heat shock protein 70. Cancer Res. 2007;67: 9407-9416.
21. Rousalova I, Banerjee S, Sangwan V, et al. Minnelide: a novel therapeutic that promotes apoptosis in non-small cell lung carcinoma in vivo. PLoS One. 2013;8: e77411.
22. Dudeja V, Mujumdar N, Phillips P, et al. Heat shock protein 70 inhibits apoptosis in cancer cells through simultaneous and independent mechanisms. Gastroenterology. 2009;136: 1772-1782.
23. Mujumdar N, Banerjee S, Chen Z, et al. Triptolide activates unfolded protein response leading to chronic ER stress in pancreatic cancer cells. Am J Physiol Gastrointest Liver Physiol. 2014;306: G1011-G1020.
24. Kanai M, Wei D, Li Q, et al. Loss of Kruppel-like factor 4 expression contributes to Sp1 overexpression and human gastric cancer development and progression. Clin Cancer Res. 2006;12: 6395-6402.
25. Pardali K, Kurisaki A, Moren A, ten Dijke P, Kardassis D, Moustakas A. Role of Smad proteins and transcription factor Sp1 in p21(Waf1/Cip1) regulation by transforming growth factor-beta. J Biol Chem. 2000;275: 29244-29256.
26. Beishline K, Azizkhan-Clifford J. Sp1 and the 'hallmarks of cancer'. FEBS J. 2015;282: 224-258.
27. Kelly Donovan, Oleg Alekseev, Xin Qi, William Cho, Azizkhan-Clifford1 J. O-GlcNAc Modification of Transcription Factor Sp1 Mediates Hyperglycemia-Induced VEGF-A Upregulation in Retinal Cells. Investigative Ophthalmology & Visual Science. 2014;55: 7862-7873.
28. Deniaud E, Baguet J, Chalard R, et al. Overexpression of transcription factor Sp1 leads to gene expression perturbations and cell cycle inhibition. PLoS One. 2009;4: e7035.
29. Deniaud A, Sharaf el dein O, Maillier E, et al. Endoplasmic reticulum stress induces calcium-dependent permeability transition, mitochondrial outer membrane permeabilization and apoptosis. Oncogene. 2008;27: 285-299.
30. Wang S, Kaufman RJ. The impact of the unfolded protein response on human disease. J Cell Biol. 2012;197: 857-867.
31. Chambers JE, Marciniak SJ. Cellular mechanisms of endoplasmic reticulum stress signaling in health and disease. 2. Protein misfolding and ER stress. Am J Physiol Cell Physiol. 2014;307: C657-C670.
32. Wang M, Kaufman RJ. The impact of the endoplasmic reticulum protein-folding environment on cancer development. Nat Rev Cancer. 2014;14: 581-597.
33. Chevet E, Hetz C, Samali A. Endoplasmic reticulum stress-activated cell reprogramming in oncogenesis. Cancer Discov. 2015;5: 586-597.
34. Zhang K, Wong HN, Song B, Miller CN, Scheuner D, Kaufman RJ. The unfolded protein response sensor IRE1α is required at 2 distinct steps in B cell lymphopoiesis. Journal of Clinical Investigation. 2005;115: 268-281.
35. Greenman C, Stephens P, Smith R, et al. Patterns of somatic mutation in human cancer genomes. Nature. 2007;446: 153-158.
36. Kakiuchi C, Iwamoto K, Ishiwata M, et al. Impaired feedback regulation of XBP1 as a genetic risk factor for bipolar disorder. Nat Genet. 2003;35: 171-175.
37. Kaser A, Lee AH, Franke A, et al. XBP1 links ER stress to intestinal inflammation and confers genetic risk for human inflammatory bowel disease. Cell. 2008;134: 743-756.
38. Yilmaz E, Akar R, Eker ST, Deda G, Adiguzel Y, Akar N. Relationship between functional promoter polymorphism in the XBP1 gene (-116C/G) and atherosclerosis, ischemic stroke and hyperhomocysteinemia. Mol Biol Rep. 2010;37: 269-272.

39. Kakiuchi C, Ishiwata M, Nanko S, et al. Functional polymorphisms of HSPA5: possible association with bipolar disorder. Biochem Biophys Res Commun. 2005;336: 1136-1143.
40. Luo S, Mao C, Lee B, Lee AS. GRP78/BiP is required for cell proliferation and protecting the inner cell mass from apoptosis during early mouse embryonic development. Mol Cell Biol. 2006;26: 5688-5697.
41. Ye R, Jung DY, Jun JY, et al. Grp78 heterozygosity promotes adaptive unfolded protein response and attenuates diet-induced obesity and insulin resistance. Diabetes. 2010;59: 6-16.
42. Dauer P, Nomura A, Saluja A, Banerjee S. Microenvironment in determining chemo-resistance in pancreatic cancer: Neighborhood matters. Pancreatology. 2017;17: 7-12.
43. McGinn O, Gupta VK, Dauer P, et al. Inhibition of hypoxic response decreases stemness and reduces tumorigenic signaling due to impaired assembly of HIF1 transcription complex in pancreatic cancer. Sci Rep. 2017;7: 7872.
44. Jacobetz MA, Chan DS, Neesse A, et al. Hyaluronan impairs vascular function and drug delivery in a mouse model of pancreatic cancer. Gut. 2013;62: 112-120.
45. Provenzano PP, Cuevas C, Chang AE, Goel VK, Von Hoff DD, Hingorani SR. Enzymatic targeting of the stroma ablates physical barriers to treatment of pancreatic ductal adenocarcinoma. Cancer Cell. 2012;21: 418-429.
46. Kelleher FC. Hedgehog signaling and therapeutics in pancreatic cancer. Carcinogenesis. 2011;32: 445-451.
47. Hingorani SR, Wang L, Multani AS, et al. Trp53R172H and KrasG12D cooperate to promote chromosomal instability and widely metastatic pancreatic ductal adenocarcinoma in mice. Cancer Cell. 2005;7: 469-483.
48. Rhim AD, Oberstein PE, Thomas DH, et al. Stromal elements act to restrain, rather than support, pancreatic ductal adenocarcinoma. Cancer Cell. 2014;25: 735-747.
49. Society AC. Cancer Facts & Figures 2016. Atlanta, GA: American Cancer Society, 2016:1-66.
50. Conroy T, Desseigne F, Ychou M, et al. FOLFIRINOX versus Gemcitabine for Metastatic Pancreatic Cancer. The New England Journal of Medicine. 2011;364: 1817-1825.
51. Orrenius S, Zhivotovsky B, Nicotera P. Regulation of cell death: the calcium-apoptosis link. Nat Rev Mol Cell Biol. 2003;4: 552-565.
52. Huang WC, Lin YS, Chen CL, Wang CY, Chiu WH, Lin CF. Glycogen synthase kinase-3beta mediates endoplasmic reticulum stress-induced lysosomal apoptosis in leukemia. J Pharmacol Exp Ther. 2009;329: 524-531.
53. Fonseca SG, Gromada J, Urano F. Endoplasmic reticulum stress and pancreatic beta-cell death. Trends Endocrinol Metab. 2011;22: 266-274.
54. Hammadi M, Oulidi A, Gackiere F, et al. Modulation of ER stress and apoptosis by endoplasmic reticulum calcium leak via translocon during unfolded protein response: involvement of GRP78. FASEB J. 2013;27: 1600-1609.
55. Schonthal AH. Endoplasmic reticulum stress: its role in disease and novel prospects for therapy. Scientifica (Cairo). 2012;2012: 857516.
56. Hedrick E, Cheng Y, Jin U-H, Kim K, Safe S. Specificity protein (Sp) transcription factors Sp1, Sp3 and Sp4 are non-oncogene addiction genes in cancer cells. Oncotarget. 2016;7: 22245.
57. Jiang NY, Woda BA, Banner BF, Whalen GF, Dresser KA, Lu D. Sp1, a new biomarker that identifies a subset of aggressive pancreatic ductal adenocarcinoma. Cancer Epidemiol Biomarkers Prev. 2008;17: 1648-1652.

58. Hang J, Hu H, Huang J, et al. Sp1 and COX2 expression is positively correlated with a poor prognosis in pancreatic ductal adenocarcinoma. Oncotarget. 2016;7: 28207.
59. Abdelrahim M, Liu S, Safe S. Induction of endoplasmic reticulum-induced stress genes in Panc-1 pancreatic cancer cells is dependent on Sp proteins. J Biol Chem. 2005;280: 16508-16513.
60. Boya P, Kroemer G. Lysosomal membrane permeabilization in cell death. Oncogene. 2008;27: 6434-6451.
61. Aits S, Jaattela M. Lysosomal cell death at a glance. J Cell Sci. 2013;126: 1905-1912.
62. Sano R, Reed JC. ER stress-induced cell death mechanisms. Biochimica et Biophysica Acta. 2013;1833: 3460-3470.
63. Flores-Peredo L, Rodriguez G, Zarain-Herzberg A. Induction of cell differentiation activates transcription of the Sarco/Endoplasmic Reticulum calcium-ATPase 3 gene (ATP2A3) in gastric and colon cancer cells. Mol Carcinog. 2016;9999: 1-16.
64. Williams JA, Hou Y, Ni HM, Ding WX. Role of intracellular calcium in proteasome inhibitor-induced endoplasmic reticulum stress, autophagy, and cell death. Pharm Res. 2013;30: 2279-2289.
65. Suh DH, Kim M-K, Kim HS, Chung HH, Song YS. Unfolded protein response to autophagy as a promising druggable target for anticancer therapy. Annals of the New York Academy of Sciences. 2012;1271: 20-32.
66. Park H-R, Tomida A, Sato S, et al. Effect of Tumor Cells of Blocking Survival Response to Glucose Deprivation. Journal of the National Cancer Institute. 2004;96: 1300-1310.
67. Yeung BH, Huang DC, Sinicrope FA. PS-341 (bortezomib) induces lysosomal cathepsin B release and a caspase-2-dependent mitochondrial permeabilization and apoptosis in human pancreatic cancer cells. J Biol Chem. 2006;281: 11923-11932.
68. Harr MW, Distelhorst CW. Apoptosis and autophagy: decoding calcium signals that mediate life or death. Cold Spring Harb Perspect Biol. 2010;2: a005579.
69. McDonald JK, Ellis S. On the substrate specificity of cathepsins B1 and B2 including a new fluorogenic substrate for cathepsin B1. Life Sci. 1975;17: 1269-1276.
70. Society AC. Cancer Facts & Figures 20172017: 1-71.
71. Hessmann E, Patzak MS, Klein L, et al. Fibroblast drug scavenging increases intratumoural gemcitabine accumulation in murine pancreas cancer. Gut. 2017;0: 1-11.
72. Lee AS. GRP78 induction in cancer: therapeutic and prognostic implications. Cancer Res. 2007;67: 3496-3499.
73. Ma Y, Hendershot LM. The role of the unfolded protein response in tumour development: friend or foe? Nat Rev Cancer. 2004;4: 966-977.
74. Lee AS. Glucose-regulated proteins in cancer: molecular mechanisms and therapeutic potential. Nat Rev Cancer. 2014;14: 263-276.
75. Roller C, Maddalo D. The Molecular Chaperone GRP78/BiP in the Development of Chemoresistance: Mechanism and Possible Treatment. Front Pharmacol. 2013;4: 10.
76. Shen J, Ha DP, Zhu G, et al. GRP78 haploinsufficiency suppresses acinar-to-ductal metaplasia, signaling, and mutant Kras-driven pancreatic tumorigenesis in mice. Proc Natl Acad Sci U S A. 2017;114: E4020-E4029.
77. Fernandez PM, Tabbara SO, Jacobs LK, et al. Overexpression of the glucose-regulated stress gene GRP78 in malignant but not benign human breast lesions. Breast Cancer Research and Treatment. 2000;59: 15-26.

78. Niu Z, Wang M, Zhou L, Yao L, Liao Q, Zhao Y. Elevated GRP78 expression is associated with poor prognosis in patients with pancreatic cancer. Sci Rep. 2015;5: 16067.
79. Gifford JB, Huang W, Zeleniak AE, et al. Expression of GRP78, Master Regulator of the Unfolded Protein Response, Increases Chemoresistance in Pancreatic Ductal Adenocarcinoma. Mol Cancer Ther. 2016;15: 1043-1052.
80. Kim KM, Yu TK, Chu HH, et al. Expression of ER stress and autophagy-related molecules in human non-small cell lung cancer and premalignant lesions. Int J Cancer. 2012;131: E362-370.
81. Scriven P, Coulson S, Haines R, Balasubramanian S, Cross S, Wyld L. Activation and clinical significance of the unfolded protein response in breast cancer. Br J Cancer. 2009;101: 1692-1698.
82. RASK K, THO˙RN M, PONTE´N F, et al. INCREASED EXPRESSION OF THE TRANSCRIPTION FACTORS CCAAT-ENHANCER BINDING PROTEIN-. Int J Cancer. 2000;86: 337-343.
83. Xing X, Lai M, Wang Y, Xu E, Huang Q. Overexpression of glucose-regulated protein 78 in colon cancer. Clin Chim Acta. 2006;364: 308-315.
84. Zheng HC, Takahashi H, Li XH, et al. Overexpression of GRP78 and GRP94 are markers for aggressive behavior and poor prognosis in gastric carcinomas. Hum Pathol. 2008;39: 1042-1049.
85. Langer R, Feith M, Siewert JR, Wester HJ, Hoefler H. Expression and clinical significance of glucose regulated proteins GRP78 (BiP) and GRP94 (GP96) in human adenocarcinomas of the esophagus. BMC Cancer. 2008;8: 70.
86. Shuda M, Kondoh N, Imazeki N, et al. Activation of the ATF6, XBP1 and grp78 genes in human hepatocellular carcinoma: a possible involvement of the ER stress pathway in hepatocarcinogenesis. Journal of Hepatology. 2003;38: 605-614.
87. Luk JM, Lam CT, Siu AF, et al. Proteomic profiling of hepatocellular carcinoma in Chinese cohort reveals heat-shock proteins (Hsp27, Hsp70, GRP78) up-regulation and their associated prognostic values. Proteomics. 2006;6: 1049-1057.
88. Tang J, Guo YS, Zhang Y, et al. CD147 induces UPR to inhibit apoptosis and chemosensitivity by increasing the transcription of Bip in hepatocellular carcinoma. Cell Death Differ. 2012;19: 1779-1790.
89. Pootrakul L, Datar RH, Shi SR, et al. Expression of stress response protein Grp78 is associated with the development of castration-resistant prostate cancer. Clin Cancer Res. 2006;12: 5987-5993.
90. Tan SS, Ahmad I, Bennett HL, et al. GRP78 up-regulation is associated with androgen receptor status, Hsp70-Hsp90 client proteins and castrate-resistant prostate cancer. J Pathol. 2011;223: 81-87.
91. Fu W, Wu X, Li J, et al. Upregulation of GRP78 in renal cell carcinoma and its significance. Urology. 2010;75: 603-607.
92. Kuroda K, Horiguchi A, Asano T, et al. Glucose-Regulated Protein 78 Positivity as a Predictor of Poor Survival in Patients with Renal Cell Carcinoma. Urologia Internationalis. 2011;87: 450-456.
93. Zhuang L, Scolyer RA, Lee CS, et al. Expression of glucose-regulated stress protein GRP78 is related to progression of melanoma. Histopathology. 2009;54: 462-470.
94. Huang L, Lin C, Lee C, Liu T, Jeng C. Overexpression of GRP78 Is Associated With Malignant Transformation in Epithelial Ovarian Tumors. Appl Immunohistochem Mol Morphol. 2012;20: 381-385.
95. Balague O, Mozos A, Martinez D, et al. Activation of the endoplasmic reticulum stress-associated transcription factor x box-binding protein-1 occurs in a subset of

normal germinal-center B cells and in aggressive B-cell lymphomas with prognostic implications. Am J Pathol. 2009;174: 2337-2346.
96. Mozos A, Roue G, Lopez-Guillermo A, et al. The expression of the endoplasmic reticulum stress sensor BiP/GRP78 predicts response to chemotherapy and determines the efficacy of proteasome inhibitors in diffuse large b-cell lymphoma. Am J Pathol. 2011;179: 2601-2610.
97. Boelens J, Jais JP, Vanhoecke B, et al. ER stress in diffuse large B cell lymphoma: GRP94 is a possible biomarker in germinal center versus activated B-cell type. Leuk Res. 2013;37: 3-8.
98. Chio IIC, Jafarnejad SM, Ponz-Sarvise M, et al. NRF2 Promotes Tumor Maintenance by Modulating mRNA Translation in Pancreatic Cancer. Cell. 2016;166: 963-976.
99. DeNicola GM, Karreth FA, Humpton TJ, et al. Oncogene-induced Nrf2 transcription promotes ROS detoxification and tumorigenesis. Nature. 2011;475: 106-109.
100. Chartoumpekis DV, Wakabayashi N, Kensler TW. Keap1/Nrf2 pathway in the frontiers of cancer and non-cancer cell metabolism. Biochem Soc Trans. 2015;43: 639-644.
101. Menegon S, Columbano A, Giordano S. The Dual Roles of NRF2 in Cancer. Trends Mol Med. 2016;22: 578-593.
102. Palam LR, Gore J, Craven KE, Wilson JL, Korc M. Integrated stress response is critical for gemcitabine resistance in pancreatic ductal adenocarcinoma. Cell Death Dis. 2015;6: e1913.
103. Zalatnai A, Molnár J. Molecular Background of Chemoresistance in Pancreatic Cancer. in vivo. 2007;21: 339-348.
104. Zhao L, Zhao Y, Schwarz B, et al. Verapamil inhibits tumor progression of chemotherapy-resistant pancreatic cancer side population cells. Int J Oncol. 2016;49: 99-110.
105. Pang L, Word B, Xu J, et al. ATP-Binding Cassette Genes Genotype and Expression: A Potential Association with Pancreatic Cancer Development and Chemoresistance? Gastroenterol Res Pract. 2014;2014: 414931.
106. Choudhuri S, Klaassen CD. Structure, function, expression, genomic organization, and single nucleotide polymorphisms of human ABCB1 (MDR1), ABCC (MRP), and ABCG2 (BCRP) efflux transporters. Int J Toxicol. 2006;25: 231-259.
107. Krishna RM, LD. Multidrug resistance (MDR) in cancer: Mechanisms, reversal using modulators of MDR and the role of MDR modulators in influencing the pharmacokinetics of anticancer drugs. European Journal of Pharmaceutical Sciences. 2000;11: 265-283.
108. Konig J, Hartel M, Nies AT, et al. Expression and localization of human multidrug resistance protein (ABCC) family members in pancreatic carcinoma. Int J Cancer. 2005;115: 359-367.
109. Dauer P, Gupta VK, McGinn O, et al. Inhibition of Sp1 prevents ER homeostasis and causes cell death by lysosomal membrane permeabilization in pancreatic cancer. Sci Rep. 2017;7: 1564.
110. Martinon F. Targeting endoplasmic reticulum signaling pathways in cancer. Acta Oncol. 2012;51: 822-830.
111. Healy SJ, Gorman AM, Mousavi-Shafaei P, Gupta S, Samali A. Targeting the endoplasmic reticulum-stress response as an anticancer strategy. Eur J Pharmacol. 2009;625: 234-246.
112. Donmez Y, Akhmetova L, Iseri OD, Kars MD, Gunduz U. Effect of MDR modulators verapamil and promethazine on gene expression levels of MDR1 and MRP1 in doxorubicin-resistant MCF-7 cells. Cancer Chemother Pharmacol. 2011;67: 823-

828.
113. Bisi A, Gobbi S, Merolle L, et al. Design, synthesis and biological profile of new inhibitors of multidrug resistance associated proteins carrying a polycyclic scaffold. Eur J Med Chem. 2015;92: 471-480.
114. Hedrick E, Cheng Y, Jin UH, Kim K, Safe S. Specificity protein (Sp) transcription factors Sp1, Sp3 and Sp4 are non-oncogene addiction genes in cancer cells. Oncotarget. 2016;7: 22245-22256.
115. Kitamura H, Onodera Y, Murakami S, Suzuki T, Motohashi H. IL-11 contribution to tumorigenesis in an NRF2 addiction cancer model. Oncogene. 2017;36: 6315-6324.
116. Capussotti L, Massucco P, Ribero D, Vigano` L, Muratore A, Calgaro M. Extended Lymphadenectomy and Vein Resection for Pancreatic Head Cancer. ARCH SURG. 2003;138: 1316-1322.
117. Bachmann J, Michalski CW, Martignoni ME, Buchler MW, Friess H. Pancreatic resection for pancreatic cancer. HPB (Oxford). 2006;8: 346-351.
118. Carpelan-Holmstrom M, Nordling S, Pukkala E, et al. Does anyone survive pancreatic ductal adenocarcinoma? A nationwide study re-evaluating the data of the Finnish Cancer Registry. Gut. 2005;54: 385-387.
119. Neoptolemos JP, Stocken DD, Friess H, et al. A Randomized Trial of Chemoradiotherapy and Chemotherapy after Resection of Pancreatic Cancer. N Engl J Med. 2004;350: 1200-1210.
120. Richter A, Niedergethmann M, Sturm JW, Lorenz D, Post S, Trede M. Long-term results of partial pancreaticoduodenectomy for ductal adenocarcinoma of the pancreatic head: 25-year experience. World J Surg. 2003;27: 324-329.
121. Schmidt CM, Powell ES, Yiannoutsos CT, et al. Pancreaticoduodenectomy: A 20-Year Experience in 516 Patients. ARCH SURG. 2004;139: 718-727.
122. Tran KTC, Smeenk HG, van Eijck CHJ, et al. Pylorus Preserving Pancreaticoduodenectomy Versus Standard Whipple Procedure. Annals of Surgery. 2004;240: 738-745.
123. Wagner M, Redaelli C, Lietz M, Seiler CA, Friess H, Buechler MW. Curative resection is the single most important factor determining outcomes in patients with pancreatic adenocarcinoma. British Journal of Surgery. 2004;91: 586-594.
124. Riha R, Gupta-Saraf P, Bhanja P, Badkul S, Saha S. Stressed Out - Therapeutic Implications of ER Stress Related Cancer Research. Oncomedicine. 2017;2: 156-167.
125. Basseri S, Austin RC. Endoplasmic reticulum stress and lipid metabolism: mechanisms and therapeutic potential. Biochem Res Int. 2012;2012: 841362.
126. Ackerman D, Simon MC. Hypoxia, lipids, and cancer: surviving the harsh tumor microenvironment. Trends Cell Biol. 2014;24: 472-478.
127. Baenke F, Peck B, Miess H, Schulze A. Hooked on fat: the role of lipid synthesis in cancer metabolism and tumour development. Dis Model Mech. 2013;6: 1353-1363.
128. Cook KL, Soto-Pantoja DR, Clarke PA, et al. Endoplasmic Reticulum Stress Protein GRP78 Modulates Lipid Metabolism to Control Drug Sensitivity and Antitumor Immunity in Breast Cancer. Cancer Res. 2016;76: 5657-5670.
129. Wu MJ, Jan CI, Tsay YG, et al. Elimination of head and neck cancer initiating cells through targeting glucose regulated protein78 signaling. Mol Cancer. 2010;9: 283.
130. Wey S, Luo B, Lee AS. Acute inducible ablation of GRP78 reveals its role in hematopoietic stem cell survival, lymphogenesis and regulation of stress signaling. PLoS One. 2012;7: e39047.
131. Matsumoto T, Uchiumi T, Monji K, et al. Doxycycline induces apoptosis via ER stress selectively to cells with a cancer stem cell-like properties: importance of stem

cell plasticity. Oncogenesis. 2017;6: 397.
132. Nomura A., Banerjee S., Chugh R., et al. CD133 inititates tumors, induces epithelial-mesenchymal transition and increases metastasis in pancreatic cancer. Oncotarget. 2015;6: 8313-8322.
133. Nomura A, Dauer P, Gupta V, et al. Microenvironment mediated alterations to metabolic pathways confer increased chemo-resistance in CD133+ tumor initiating cells. Oncotarget. 2016;7: 56324-56337.
134. Baumann M, Krause M, Hill R. Exploring the role of cancer stem cells in radioresistance. Nat Rev Cancer. 2008;8: 545-554.
135. Yanzhou Yang HHC, JiaJie Tu, Kai Kei Miu, Wai Yee Chan. New insights into the unfolded protein response in stem cells. Oncotarget. 2016;7: 54010-54027.
136. Miharada K, Karlsson G, Rehn M, et al. Cripto regulates hematopoietic stem cells as a hypoxic-niche-related factor through cell surface receptor GRP78. Cell Stem Cell. 2011;9: 330-344.
137. Bartkowiak K, Effenberger KE, Harder S, et al. Discovery of a Novel Unfolded Protein Response Phenotype of Cancer Stem/Progenitor Cells from the Bone Marrow of Breast Cancer Patients. Journal of proteome research. 2010;9: 3158-3168.
138. Li XX, Zhang HS, Xu YM, et al. Knockdown of IRE1alpha inhibits colonic tumorigenesis through decreasing beta-catenin and IRE1alpha targeting suppresses colon cancer cells. Oncogene. 2017;36: 6738-6746.
139. Nomura A, Gupta VK, Dauer P, et al. NFkappaB-Mediated Invasiveness in CD133(+) Pancreatic TICs Is Regulated by Autocrine and Paracrine Activation of IL1 Signaling. Mol Cancer Res. 2018;16: 162-172.
140. Tadros S, Shukla SK, King RJ, et al. De Novo Lipid Synthesis Facilitates Gemcitabine Resistance through Endoplasmic Reticulum Stress in Pancreatic Cancer. Cancer Res. 2017;77: 5503-5517.
141. Goff LA, Trapnell C, Kelley DR. CummeRbund: analysis, exploration,manipulation, and visualization of Cufflinks high-throughput sequencing data 2.10.0: R package2013.
142. Dauer P, Zhao X, Gupta VK, et al. Inactivation of cancer-associated-fibroblasts (CAF) disrupts oncogenic signaling in pancreatic cancer cells and promotes its regression. Cancer Res. 2017.
143. Jemal A, Bray F, Center MM, Ferlay J, Ward E, Forman D. Global cancer statistics. CA Cancer J Clin. 2011;61: 69-90.
144. Hamada S, Masamune A, Shimosegawa T. Novel therapeutic strategies targeting tumor-stromal interactions in pancreatic cancer. Front Physiol. 2013;4: 331.
145. Khan S, Ebeling MC, Chauhan N, et al. Ormeloxifene suppresses desmoplasia and enhances sensitivity of gemcitabine in pancreatic cancer. Cancer Res. 2015;75: 2292-2304.
146. Neesse A, Michl P, Frese KK, et al. Stromal biology and therapy in pancreatic cancer. Gut. 2011;60: 861-868.
147. Apte MV, Xu Z, Pothula S, Goldstein D, Pirola RC, Wilson JS. Pancreatic cancer: The microenvironment needs attention too! Pancreatology. 2015;15: 6.
148. Heinemann V, Reni M, Ychou M, Richel DJ, Macarulla T, Ducreux M. Tumour-stroma interactions in pancreatic ductal adenocarcinoma: rationale and current evidence for new therapeutic strategies. Cancer Treat Rev. 2014;40: 118-128.
149. Lunardi S MR, Brunner TB. The stromal compartments in pancreatic cancer: are there any therapeutic targets? Cancer Lett. 2014;343.
150. Kalluri R. The biology and function of fibroblasts in cancer. Nat Rev Cancer.

2016;16: 582-598.
151. Sherman MH, Yu RT, Engle DD, et al. Vitamin D receptor-mediated stromal reprogramming suppresses pancreatitis and enhances pancreatic cancer therapy. Cell. 2014;159: 80-93.
152. Banerjee S, Thayanithy V, Sangwan V, Mackenzie TN, Saluja AK, Subramanian S. Minnelide reduces tumor burden in preclinical models of osteosarcoma. Cancer Lett. 2013;335: 412-420.
153. Sangwan V, Banerjee S, Jensen KM, et al. Primary and liver metastasis-derived cell lines from KrasG12D; Trp53R172H; Pdx-1 Cre animals undergo apoptosis in response to triptolide. Pancreas. 2015;44: 583-589.
154. Antonoff MB, Chugh R, Borja-Cacho D, et al. Triptolide therapy for neuroblastoma decreases cell viability in vitro and inhibits tumor growth in vivo. Surgery. 2009;146: 282-290.
155. Greeno E BE, Gockerman J, Korn R, Saluja A, Von Hoff D. Phase I dose escalation and pharmacokinetic study of 14-O-phosphonooxymethyltriptolide2015.
156. Jungert K, Buck A, von Wichert G, et al. Sp1 is required for transforming growth factor-beta-induced mesenchymal transition and migration in pancreatic cancer cells. Cancer Res. 2007;67: 1563-1570.
157. Koo BH, Kim Y, Cho YJ, Kim DS. Distinct roles of transforming growth factor-beta signaling and transforming growth factor-beta receptor inhibitor SB431542 in the regulation of p21 expression. Eur J Pharmacol. 2015;764: 413-423.
158. Apte MV, Pirola RC, Wilson JS. Pancreatic stellate cells: a starring role in normal and diseased pancreas. Front Physiol. 2012;3: 344.
159. Apte MV, Wilson JS. Dangerous liaisons: pancreatic stellate cells and pancreatic cancer cells. J Gastroenterol Hepatol. 2012;27 Suppl 2: 69-74.
160. McCarroll JA, Naim S, Sharbeen G, et al. Role of pancreatic stellate cells in chemoresistance in pancreatic cancer. Front Physiol. 2014;5: 9.
161. Chronopoulos A, Robinson B, Sarper M, et al. ATRA mechanically reprograms pancreatic stellate cells to suppress matrix remodelling and inhibit cancer cell invasion. Nat Commun. 2016;7: 12630.
162. Sarper M, Cortes E, Lieberthal TJ, Del Rio Hernandez A. ATRA modulates mechanical activation of TGF-beta by pancreatic stellate cells. Sci Rep. 2016;6: 27639.
163. Sharon Y, Alon L, Glanz S, Servais C, Erez N. Isolation of normal and cancer-associated fibroblasts from fresh tissues by Fluorescence Activated Cell Sorting (FACS). J Vis Exp. 2013: 6.
164. Andrews S. FastQC: a quality control tool for high throughput sequence data2010.
165. Trapnell C, Pachter L, Salzberg SL. TopHat: discovering splice junctions with RNA-Seq. Bioinformatics. 2009;25: 1105-1111.
166. Trapnell C, Roberts A, Goff L, et al. Differential gene and transcript expression analysis of RNA-seq experiments with TopHat and Cufflinks. Nat Protoc. 2012;7: 562-578.
167. Yu G, Wang LG, Han Y, He QY. clusterProfiler: an R package for comparing biological themes among gene clusters. OMICS. 2012;16: 284-287.
168. Subramanian A, Tamayo P, Mootha VK, et al. Gene set enrichment analysis: a knowledge-based approach for interpreting genome-wide expression profiles. Proc Nat Acad Sci. 2005;102: 15545-15550.
169. Nawrocki ST, Carew JS, Dunner K, Jr., et al. Bortezomib inhibits PKR-like endoplasmic reticulum (ER) kinase and induces apoptosis via ER stress in human

pancreatic cancer cells. Cancer Res. 2005;65: 11510-11519.
170. Chen D, Frezza M, Schmitt S, Kanwar J, Dou QP. Bortezomib as the First Proteasome Inhibitor Anticancer Drug: Current Status and Future Perspectives. curr Cancer Drug Targets. 2011;11: 239-253.
171. Kane RC, Farrell AT, Sridhara R, Pazdur R. United States Food and Drug Administration approval summary: bortezomib for the treatment of progressive multiple myeloma after one prior therapy. Clin Cancer Res. 2006;12: 2955-2960.
172. Kapoor P, Ramakrishnan V, Rajkumar SV. Bortezomib combination therapy in multiple myeloma. Semin Hematol. 2012;49: 228-242.
173. Luu T, Chow W, Lim D, et al. Phase I trial of fixed-dose rate gemcitabine in combination with bortezomib in advanced solid tumors. Anticancer Res. 2010;30: 167-174.
174. Peak MJ, Jones CA, Sedita BA, Dudek EJ, Spitz DR, Peak JG. Evidence that hydrogen peroxide generated by 365-nm UVA radiation is not important in mammalian cell killing. Radiat Res. 1990;123: 220-227.
175. Spitz DR, Li GC, McCormick ML, Y. S, Oberley LW. Stable H2O2-resistant variants of Chinese hamster fibroblasts demonstrate increases in catalase activity. Radiat Res. 1988;114: 10.
176. Ho JJD, Wang M, Audas TE, et al. Systemic Reprogramming of Translation Efficiencies on Oxygen Stimulus. Cell Rep. 2016;14: 1293-1300.
177. Uniacke J, Holterman CE, Lachance G, et al. An oxygen-regulated switch in the protein synthesis machinery. Nature. 2012;486: 126-130.

Appendices

Author Contributions

This dissertation was written by Patricia Dauer. However, some of these chapters contain data collected by multiple individuals, whom should be acknowledged for their contribution.

Chapter One

Patricia Dauer designed, performed, and analyzed most experiments. Vineet K. Gupta performed the Western blot analyses (thanks, Vineet!). Nivi Arora helped complete the animal study. Patricia Dauer, Sulagna Banerjee, and Ashok Saluja conceived of the study. All authors read and approved of the final manuscript.

Chapter Two

Patricia Dauer designed, performed, and analyzed experiments. Patricia Dauer and Sulagna Banerjee conceived of the study and interpreted the data. Sulagna Banerjee and Ashok Saluja supervised the project. All authors read and approved of the final manuscript.

Chapter Three

Patricia Dauer designed, performed, and analyzed experiments. Patricia Dauer and Sulagna Banerjee conceived of the study and interpreted the data. Sulagna Banerjee and Ashok Saluja supervised the project. All authors read and approved of the final manuscript.

Chapter Four

Xianda Zhao designed, performed, and analyzed the *in vivo* experiments and transcriptomic data analysis. Patricia Dauer, Vineet K. Gupta, and Nikita Sharma designed and performed *in vitro* cell signaling experiments. Sulagna Banerjee and Ashok Saluja conceived of the study, helped interpret the data, and supervised the project. All authors read and approved of the final manuscript.